VALUE-ADDED CARBON FIBER REINFORCED COMPOSITES FROM POST-CONSUMER POLY (ETHYLENE TEREPHTHALATE) BOTTLES AND THERMOFORM

By

Aparajith Venkataramanan

A THESIS

Submitted to
Michigan State University
in partial fulfillment of the requirements
for the degree of

Packaging – Master of Science

2025

ABSTRACT

Poly(ethylene terephthalate) (PET) constitutes a substantial fraction of packaging plastics in the U.S., facing recycling challenges such as contamination from thermoformed PET (PET-T) and the necessity for purification for food-contact reuse. This research focuses on developing value-added, non-food composite materials by blending postconsumer PET bottles (PET-B) and thermoforms (PET-T), with the objective of improving the PET circular economy. The study developed carbon fiber-reinforced composites with PET-B/PET-T blends (80/20 wt.%) combined with carbon fibers of three lengths (0.5, 1, and 2 inches) and two loadings (1 and 3 wt.%), incorporating both epoxy-based chain extenders and without them. The evaluated mechanical qualities include tensile strength, modulus of elasticity, impact strength, elongation at break, alongside thermal properties including glass transition temperature, melting point, degree of crystallinity, and thermal degradation. SEM examination offered insights into fiber distribution and polymer-fiber adhesion. The results demonstrated significant mechanical enhancements at a 3 wt.% carbon fiber loading: tensile strength increased by 20%, modulus of elasticity by 50%, and impact strength by 18% compared to unreinforced PET-B/PET-T. These reinforced composites exceeded virgin polypropylene (PP) carbon fiber composites in mechanical strength, though they had reduced elongation at break. Moreover, thermal resistance specifically heat deflection temperature has enhanced, signifying suitability for automotive and other structural applications. The study finds that recycled PET-B/PET-T composites reinforced with carbon fiber offer an exciting potential for high-performance, non-food applications. Future investigations should examine elevated fiber loadings and surface-modified fibers. The utilization of such materials can substantially enhance sustainability by diminishing dependence on virgin plastics and decreasing carbon emissions.

ACKNOWLEDGEMENTS

I wish to convey my sincere appreciation to my mentor, Prof. Muhammad Rabnawaz, for his exceptional guidance and the opportunity to conduct research within his Sustainable Materials Group, which has significantly augmented my understanding of polymers and plastics. He has provided unwavering support and encouragement during this process.

I am also grateful to my research committee members, Dr. Shiwang Cheng and Dr. Mohammad Mohiuddin, for their invaluable guidance and constructive feedback. I also thank Dr. Mohammed Abdelwahab for his time and guidance during this research.

I want to thank other Sustainable Research Group members for helping me with their timely advice and favors.

Aaron Walworth, Ranjith Weerasiri Rankothge, and the School of Packaging have always been helpful with their timely training and for letting me use their state-of-the-art machines for my research.

I would finally like to thank my family, who have always stood by my side. Their constant support has always encouraged me to finish my research and academic studies. They have always motivated me throughout this journey and would be indebted to them.

TABLE OF CONTENTS

LIST OF ABBREVATIONS...v

CHAPTER1: INTRODUCTION..1

CHAPTER 2: LITERATURE REVIEW...6

CHAPTER 3: MATERIALS AND METHODS..................................16

CHAPTER 4: RESULTS AND DISCUSSIONS................................23

CHAPTER 5: CONCLUSION AND FUTURE WORK....................................47

REFERENCES……………………………………………………………....49

APPENDIX…………………………………………………………….........54

LIST OF ABBREVATIONS

PET	Polyethylene terephthalate
PET-B	Polyethylene terephthalate- Bottle
PET-T	Polyethylene terephthalate- Thermoform.
CE	Chain Extenders
CF	Carbon Fiber
rPET	Recycled Polyethylene Terephthalate
APET	Amorphous Polyethylene Terephthalate
BPET	Biaxially Oriented Polyethylene Terephthalate
CPET	Crystalline Polyethylene Terephthalate
OPET	Oriented Polyethylene Terephthalate
DSC	Differential Scanning Calorimetry
TGA	Thermogravimetric Analysis
T_g	Glass transition temperature
T_m	Melting temperature.
B*	Base sample
SEM	Scanning Electron Microscopy
PP	Polypropylene
HDT	Heat deflection temperature
EPR	Extender Production Responsibility
PETG	Polyethylene Terephthalate Glycol
EG	Ethylene glycol
TPA	Terephthalic acid

SSP	Solid State Polymerization

CHAPTER 1: INTRODUCTION

1.1 Introduction:

In the U.S. alone, poly (ethylene terephthalate) (PET) consumption was 5.23 million tons in 2018.[1] Due to its desirable characteristics such as good moisture and oxygen barrier properties, optical clarity and strength, PET is widely used for food and beverage packaging.[2] Consequently, PET is found in bottles, caps, cups, containers, thermoformed clamshells, and other packaging applications. For all these reasons, PET accounts for 26% of all plastic used in the packaging sector in the U.S.[3]

The demand for PET packaging is growing rapidly, but recycling rates remain low overall.[4] PET recycling rates have been steady at 29% in the US.[5] In the EU, PET bottles are recycled at a rate of 58% due to the EPR system.[6] PET bottle recycling has gradually increased over time as part of efforts to promote a plastic circular economy, reduce waste, and keep materials in the loop for future use. With the new EPR regulations in the US, if adopted nationwide, one may expect a rapid increase in bottle PET recycling in this country.

Chemical recycling of PET, which involves converting PET into its feedstock monomers, is an attractive method as it produces virgin-like PET, rendering it appropriate for food and medical packaging.

This method is also effective for contaminated PET. Nonetheless, because to the substantial capital investment and energy-intensive nature of the process, the chemical recycling of PET into monomers and subsequent re-polymerization is predominantly constrained to a limited scale. The primary factor influencing cost and energy usage is the purification of monomers following the depolymerization of PET and the subsequent re-polymerization into virgin PET.[7,8]

Recycling PET can save fossil fuels and cut carbon emissions by as much as 50%. The production of virgin PET is an energy-intensive process. Consequently, recycled PET might conserve energy utilized in the polymerization process of PET. "Drop-in" PET produced from renewable monomers has been documented; still, it has resulted in a carbon footprint that is twice that of petrochemical-derived PET.[9] PET is vulnerable to hydrolysis because of its ester bonds, particularly at elevated temperatures, such as during sterilization, the transformation of PET sheets into thermoforms, melt-treatment for packaging, hot filling, or even in environmental conditions.

This degradation results in reduced molecular weight, leading to a deterioration of PET characteristics. Historically, multiple procedures have been employed to recover the mechanical qualities of PET, including chain extenders, solid-state polymerization, and blending with virgin PET.[10] Blending with virgin PET often uses large amounts, such as 70-80 wt.% virgin PET.

The fact that mechanical recycling is a popular and affordable method of recycling PET is clear. Nonetheless, a novel problem emerges from the presence of thermoform-grade PET (PET-T) within PET bottle-grade bales.

Approximately 7% of PET-T has been documented in bottle-grade PET. PET-T and PET-B are distinguished by their differing intrinsic viscosities.[11] Currently, recyclers need to remove PET-T from PET-B, which leads to material losses and increases the cost of recycled PET. Recently, Rabnawaz et al. reported an approach for recycling PET-B and PET-T into bottle-grade PET using glycidol-free chain extenders.[12] This novel method will facilitate the increased utilization of PET thermoforms, which are presently discarded and directed to landfills.

The purpose of this study was to examine thermoform blends and carbon fiber-reinforced PET bottles and compare their characteristics to those of virgin PP and carbon fiber-reinforced PET. Contamination concerns, prevalent in post-consumer plastics used for food contact applications, were a primary rationale for emphasizing composites.[13] Secondly, the value-added pricing of composites for automotive applications enables low-cost recycled PET to be transformed into value-added upcycled composites, which incentivizes recyclers to put more effort into this sector and explains why PET collecting and recycling is important.

1.2 Objectives:

The overarching goal of this thesis was to create value-added composite materials from PET bottles (PET-B) and PET thermoform (PET-T) by incorporating carbon fiber and analyzing its performance against carbon fiber reinforced - virgin polypropylene and PET composites.

Sub-Objective 1: Investigate the effect of a chain extender on the PET-T and PET-B blend and its impact on the rheological, thermal, and mechanical properties.

Sub-Objective 2: Create carbon fiber-reinforced PET-B and PET-T composites and assess their thermal, mechanical, and rheological properties, comparing them to carbon fiber reinforced virgin PET and virgin polypropylene as a control.

1.3 Thesis Work Scope:

- Investigate carbon fiber reinforced composites from postconsumer PET-T and PET-B blends.
- Investigate the thermal and mechanical properties of these carbon fiber reinforced PET-B and PET-T composites.
- Investigate the effect of chain extenders on the carbon-fiber reinforced recycled PET-B and PET-T composites.

- Comparative study of carbon fiber reinforced recycled PET-B and PET-T composites versus carbon fiber reinforced virgin PET composites versus carbon fiber reinforced virgin PP composites.

1.4 Hypothesis:

We hypothesize that carbon fiber reinforced PET-T and PET-B composites are likely to have good mechanical and thermal properties comparable to that of virgin poly (ethylene terephthalate) and polypropylene composites because carbon fiber composites are expected to have better adhesion with the polar PET matrix, compared to non-polar polypropylene.

Furthermore, the chain extenders will increase the adhesion between fiber and matrix and thus further improve the mechanical properties of these composites.

1.5 Rational for this work:

The main motivation for this work is to enhance the plastic circular economy, promote reuse, and develop value-added materials for packaging plastic waste. The resulting composite materials can be used for various applications, such as automotive parts, battery casings, etc.

Choosing non-food applications, such as automotive, in this case, will also help overcome the challenges posed by stringent regulations of postconsumer plastics for food contact applications.

1.6 Novelty:

While recycled PET has been extensively studied for packaging and fiber applications, its potential in high-performance composite materials remains largely unexplored. This research represents the first systematic examination of the mechanical, thermal, and structural characteristics of carbon fiber-reinforced composites produced from PET waste streams, addressing issues such fiber-matrix compatibility, crystallization behavior, and performance.

This research seeks to improve the mechanical strength, thermal stability, and durability of recycled PET-based composites by utilization of carbon fiber as reinforcing agent, thus potentially creating value added applications in the automotive, aerospace, and structural sectors. The results enhance circular economic efforts and promote the development of environmentally sustainable, high-performance polymer composites, representing a crucial advancement in sustainable material developments.

1.7 Structure of the Thesis:

Chapter 1: Introduction

Chapter 2: Literature Review

Chapter 3: Materials and Methods

Chapter 4: Results and Discussion

Chapter 5: Conclusions and Outlook

CHAPTER 2: LITERATURE REVIEW

2.1 Polyethylene terephthalate:

Polyethylene terephthalate (PET) is among the most extensively utilized polymers globally. Global polyester production is projected to increase from 63.3 million tons to 67 million tons, predominantly for synthetic fibers, packaging bottles, and thermoforms, as per the materials market research report.[14]

Approximately ,30% of PET produced is used in packaging, such as bottles and clamshells, with demand rising. PET bottles are popular due to their strength, barrier, and clarity. In 2019, 650 billion plastic bottles were sold.[15]

Disposable plastic bottles, however, constitute a substantial amount of garbage. Researchers estimate that between 1- 8 million tons of plastic enter the waters each year.[16]

Figure 1: The figure is derived from data in Textile Exchange's yearly Materials Market Report. The picture displays the projected polymer manufacturing data for 2024.[17]

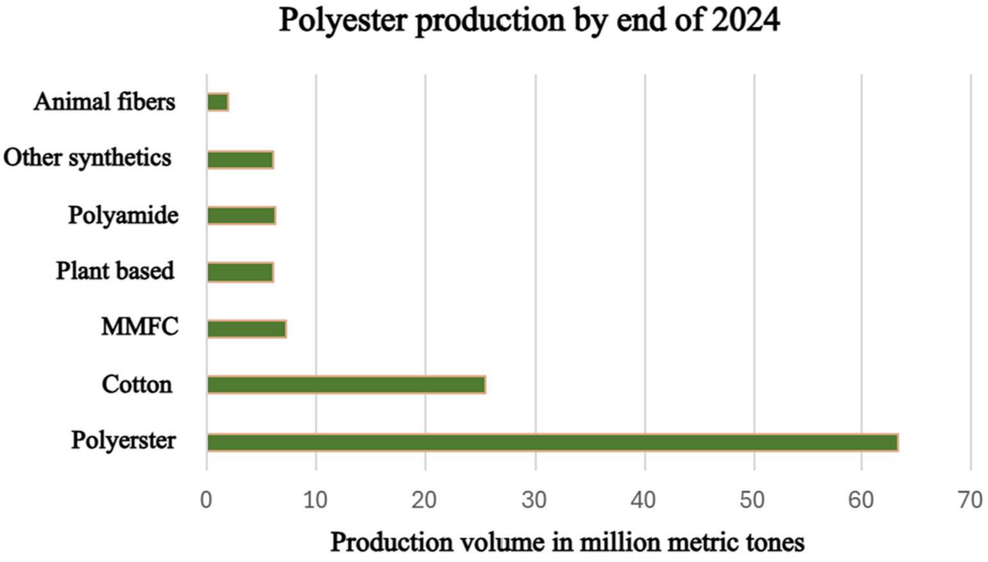

PET was patented in 1941 by John Rex Whinfield and James Tennant Dickson, working under the Calico Printers' Association, which was developed in Manchester, England.[18]

In the beginning, PET was exclusively utilized for synthetic fiber because of the fiber's durability, strength, and resistance to water. As a result, PET was recognized and utilized as a material for engineering purposes.

In 1973, Nathaniel Wyeth patented the first PET bottle, and in 1978, Coca-Cola introduced carbonated beverages in PET bottles.[19,20] In the 1970s, there is fierce competition between acrylonitrile/styrene copolymers (ANS) for carbonated beverage bottles.

Eventually, PET won this market despite ANS having better CO_2 retention; perhaps acrylonitrile was perceived as a bad monomer. Since then, PET has become the most widely used bottle in the packaging industry.

2.1.1 PET property and its structure:

Figure 2: PET chemical structure.[19]

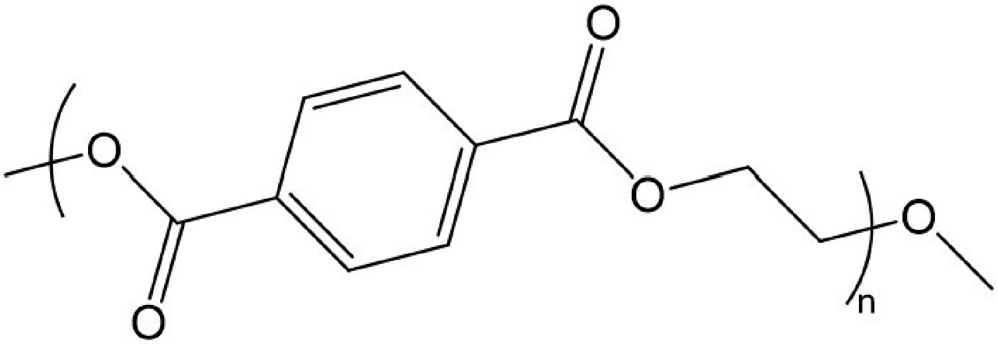

PET is synthesized from dimethyl terephthalate (DMT) or terephthalic acid (TPA) through polycondensation with ethylene glycol (EG) to form PET. Methanol must be distilled from DMT and water from TPA during the polymerization process.[20] If methanol or water is not eliminated during polymerization, a high molecular weight will not be obtained, and as a result, it will not be suitable for PET bottle applications.

Making bottle-grade PET typically involves four steps: i) transesterification, ii) pre-polymerization, iii) polymerization, and iv) SSP. BHET bis(hydroxyethyl) terephthalate is produced by esterifying EG and TPA (or DMT) at 180°C. After that, BHET undergoes further polymerization under vacuum at 220 °C. After that, the polymer melts condensation at 150–220°C until a degree of polymerization of ~ 100.[21]

PET has a melting point ranging from 250 to 260 degrees Celsius and contains ester linkages in its backbone structure. PET has a T_g of 70°C.[22] The density of PET fluctuates based on its crystallinity; amorphous PET possesses a density of 1.333 g/cm³, whereas crystalline PET has a density of 1.455 g/cm³.

2.1.2 PET Types:

PET is extensively used in different forms: Polyethylene terephthalate (PETE), oriented polyethylene terephthalate (OPET), and amorphous PET.

PETE or PET is a semicrystalline homopolymer of PET. It may be semi-rigid or rigid. PET has many complex applications, such as electrical circuit elements, automotive parts, pharmaceutical and medical device components, and industrial components.

Oriented PET: Due to its high tensile strength and stability, oriented PET is utilized in high-end applications. OPET is used in films, carbonated bottles, and fibers. PET films or fiber are heated above T_g and below T_m to become soft and stretched; this leads to OPET. This enhances PET's clarity and barrier qualities.

A continuous biaxial orienting method is frequently employed in PET films to produce OPET. A tenter-frame biaxial stretching is a method for producing biaxially oriented films with a tenter frame, which allows the cast film to be elongated in both the machine and cross-machine directions.

For oriented bottles, vertical stretching is often achieved with a rod, whereas horizontal stretching is accomplished using blow molding for PET drinking bottles. This orientation in PET enhances gas and moisture barrier qualities and enhances strength, making it prevalent in carbonated beverage applications due to its superior barrier performance. [23]

Amorphous PET is a type of PET resin created by copolymerization, which keeps the polymer amorphous. Amorphous PET comes in two varieties, namely Polyethylene Terephthalate Glycol (PETG) and Polycyclohexylene Dimethylene Terephthalate Glycol (PCTG). A copolymer, PETG, is created by reacting ethylene glycol and terephthalic acid with diethylene glycol and isophthalic acid.[24] The modifier ensures that the polymer's melting point and crystallization rate are decreased.

Furthermore, they guarantee that crystals remain unaligned. A variant of PETG, termed PCTG, is synthesized through the copolymerization of TPA and EG, including a minor quantity of cyclohexane di-methanol into the PET framework. PETG and PCTG exhibit excellent chemical resistance and transparency. PCTG is predominantly utilized in the cosmetic sector and is distinguished for its remarkable impact resistance. PETG's exceptional clarity renders it suitable for usage in the food industry for trays and in the medical sector for thermoforming applications.[25]

2.1.3 PET Applications:

PET is widely used in food and beverage, pharmaceuticals and medical fields, automotive manufacturing, electronics, power tools, clothing, and textiles due to its versatile nature and advantageous physical and chemical properties.[26]

PET has exceptional optical clarity and durability and is lightweight, thus making it a popular material for producing water, soft drinks, juice, and other beverage bottles.

The physio- mechanical properties satisfy the manufacturing requirements. Polyester fabrics, used in apparel, upholstery, and other textiles, are created by spinning PET into fibers, which is the function of PET in the textile sector, highlighting its robustness and adaptability in the creation of fabrics.[27] PET is utilized to make items that need to be durable and heat-resistant, such as fuse boxes and engine covers.

For ready-to-eat food trays that must resist heating in the oven or microwave, CPET is frequently utilized. CPET trays offer the required heat stability for these kinds of applications.

Due to its convenience of use, and capacity for producing prints of excellent quality, PETG (glycol-modified PET) is frequently used in 3D printing. PETG's superior printability and material attributes make it a preferred choice for 3D printing prototypes and functional parts.[28] PET films have good dielectric qualities and mechanical robustness, making them applicable for insulation and protective casings for electronic equipment. PET films are essential to electronics because of their strength and insulation qualities.[29]

2.2 PET Recycling:

As mentioned earlier, PET recycling helps preserve oil resources, lowers carbon emissions, and fosters circularity within the plastic circular economy. Two primary approaches are employed: mechanical recycling and chemical recycling, each possessing distinct advantages and disadvantages.

2.2.1 Chemical Recycling of PET:

PET chemical recycling has been the most explored avenue compared to the chemical recycling of any other plastics. This is because chemical recycling of PET enables even contaminated PET feedstock to become suitable for food-grade applications.

Three common types of PET chemical recycling include **methanolysis,** where methanol is used as a solvent to depolymerize PET; **glycolysis,** where glycol is used to depolymerize PET; and **hydrolysis**, where water is used to depolymerize PET. The resulting acid or ester can be repurposed for the synthesis of virgin PET in all these instances.

Regarding catalysis, organometallic catalysts, organic catalysts, and biocatalysts-like enzymes have all been successfully tested to depolymerize PET.

The challenge in PET chemical recycling is not the depolymerization of PET itself, but the necessity of catalysts for depolymerization, followed by the removal of the catalyst and the recovery of pure monomers. This process results in an increase in energy consumption and costs associated with chemical recycling. Over the past few decades, there have been numerous studies published in this field, with a significant number of publications occurring in recent years.[30]

However, the recycling of PET chemicals continues to encounter obstacles, such as the high costs, the high energy input, and the purification procedures that necessitate a substantial amount of effort and expense. The development of more energy-efficient and cost-effective chemical recycling methods for PET is warranted by future research.

2.2.2 Mechanical Recycling:

Mechanical recycling is also known as secondary recycling. This process converts post-consumer plastics (in this case PET) into new products without significantly altering the polymer chemical structure. PET mechanical recycling involves multiple steps, beginning with collecting post-consumer plastics and sorting PET from other materials in plastic bales. PET is sorted from the PET bales and then thoroughly cleaned to remove labels, adhesives, and other residues.

In order to make sure that the PET is clear of contaminants, particularly the adhesives from labels, it is usually cleaned with caustic soda and rinsed with water. Subsequently, clean PET is pulverized into little flakes.

The flakes are subsequently dried prior to the creation of pellets or granules. Improper drying will result in degrading moisture-degrading PET when subjected to heat during pelletization.

After drying, PET flakes are subjected to high temperatures (260-280°C) for melting and subsequently extruded through a die to produce filaments, which are then severed into pellets.

Recycled PET pellets or granules are prepared for the manufacture of new products. They can be liquefied and shaped into many products, including containers, bottles, textile fibers, and other plastic items.

The primary advantage of mechanical recycling of PET is its lower energy consumption compared to the production of PET from raw materials, hence diminishing greenhouse gas emissions and lessening environmental effects.

The limitations of PET mechanical recycling encompass the necessity for high-quality post-consumer PET bottles to guarantee their appropriateness for food-grade uses. Moreover, the existence of contaminants necessitates comprehensive sanitation and FDA no-objection letters (NOL) for utilization in food contact applications.

2.3 Restoring r-PET properties:

As mentioned earlier, post-consumer PET experiences hydrolytic degradation, leading to diminished molecular weight and inferior qualities, including reduced mechanical characteristics, lower intrinsic viscosity, and elevated melt flow indices. Consequently, further measures are required to reinstate their properties.

Methods such as blending with virgin PET, solid state polycondensation (SSP) treatment, chain extenders, or combining these approaches are commonly employed to enhance their quality.

SSP treatment involves heating pelletized recycled PET at a temperature slightly below its melting point. Throughout this process, the polymer chains interconnect, liberating tiny molecules that are persistently extracted via nitrogen recirculation or under vacuum conditions.

This produces high molecular weight and high intrinsic viscosity PET, appropriate for diverse packaging applications.This technique also effectively eliminates volatile components or impurities, given that they possess an appropriate boiling point or vapor pressure for removal at this temperature. The downside of SSP treatment is its high energy consumption, as it typically requires 8 to 24 hours.

Using chain extenders to enhance the performance of recycled PET is a common tactic used. Chain extenders are low molecular weight molecules, oligomers, or polymers with two or more functional groups that can react with the terminal functional groups of PET, thus connecting the PET chains.

This linkage improves molecular weight and inherent viscosity, aiding in the restoration of PET performance (rheological and mechanical). A variety of chain extenders have been investigated, with epoxy-based variants being commercialized and currently utilized.[31]

Chain extension technologies provide benefits including rapid processing, attainable within minutes without disrupting production. It is cost-effective and demands less energy. However, a drawback is that it may sporadically lead to branching structures or gel formation, thereby affecting the quality of the film or container.

In some cases, particular chain extenders may provide safety concerns due to migration issues in food applications. Rabnawaz's group and other researchers have tackled this topic.[32]

Mechanical recycling is a cost-effective and pragmatic method for recycling PET. A new difficulty emerges from the presence of thermoform-grade PET (PET-T) in bales designated for bottle-grade PET. Approximately 7% of PET-T has been documented in bottle-grade PET.

PET-T and PET-B are distinguished by their differing intrinsic viscosities. In certain instances, PET thermoforms may exhibit lower viscosity than PET bottle grade, whilst in other cases, they may demonstrate higher viscosity, contingent upon the specific applications for which the thermoforms are utilized. Now, recyclers must separate PET-T from PET-B, resulting in material losses and elevated costs for recovered PET.

This innovative method of combining PET-B and PET-T with enhancers such as chain extenders and carbon fiber additions would undoubtedly facilitate the increased utilization of PET thermoform, which is presently discarded and directed to landfills.

2.4 PET composites:

Figure 3: shows the outline of the materials added to make the carbon fiber composites. The recycled individual PET bottle and thermoform polymers are combined with Joncryl ADR 4468 making them base sample and carbon fiber is reinforced as additive.

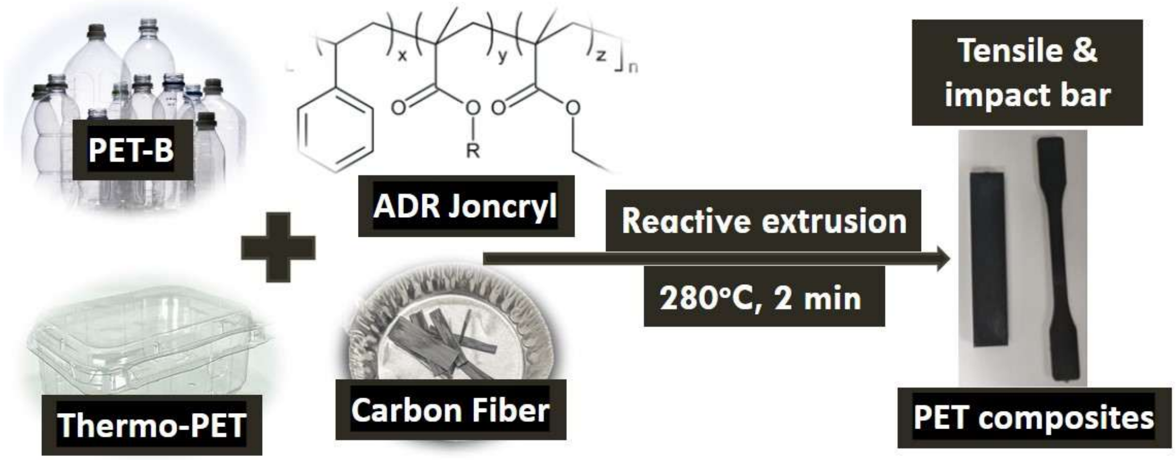

Concerns over food safety for post-consumer PET have prompted the investigation of alternative applications for recycled PET, including automotive composites. The benefit of automotive composites in this situation is that PET bottles are less expensive than virgin PET, offering a more economical material alternative without hygienic constraints.[33,34]

Previous research has established the successful production of fiber-reinforced PET composites, encompassing glass fiber, carbon fiber, and natural fiber variants. Natural fiber-based PET composites exhibit significant degradation at elevated temperatures due to incompatible functional groups with PET plastic.

Carbon fiber-reinforced PET composites are utilized in the automotive and aerospace industries due to their lightweight properties, exceptional strength, and outstanding mechanical characteristics. PET, due to its stiffness, elevated glass transition temperature, and enhanced mechanical qualities relative to polypropylene, has been regarded as a viable alternative to polypropylene-based composites.

Research has investigated the mechanical properties of carbon fiber-reinforced PET composites, specifically examining the influence of crystallinity during the cooling process in injection-molded specimens.[35]

Now, thermoform PET is frequently excluded from PET bottle bales, presenting an opportunity to explore composites of PET-T and PET-B with carbon fiber. This is the first study to compare the performance of carbon fiber-reinforced composites made of PET-B and PET-T. We were also interested in the effects of carbon fiber reinforcing on the mechanical, chemical, and thermal properties of the generated composites.

CHAPTER 3: MATERIALS AND METHODS

3.1 Materials:

Carbon fiber 2433 – TZOO series of different lengths (0.5, 1, and 2 inches) were purchased from Composite Emissions, USA. Joncryl ADR 4468 (denoted with 'J') was purchased from BASF (molecular weight of 7.25 Kg/mol).

All the other reagents and chemicals were purchased from Sigma Aldrich, USA. The post-consumer PET bottles and PET thermoforms were sourced from the Michigan State University Surplus Store.

3.1.1 PET – Thermoform (PET-T) and PET- Bottle (PET-B) samples:

First, PET beverage bottles (PET-B) and the PET thermoform (PET-T) containers were manually separated into PET-T and PET-B. Next, the labels were removed from the containers and bottles. Then these bottles and containers were washed using a detergent solution to ensure no residual adhesive/glue was left from the labels. Afterward, the containers/bottles were dried in a vacuum oven at 80°C for a day to remove the moisture.

The moisture content was 0.034 wt.% after the drying step. The PET-T and PET-B samples were then shredded into tiny powder (sized 2-3 mm) with the help of B.T.P Granulator (CT, USA). These shredded samples were placed in the oven for 24 hours to ensure they are well-dried before the pelletization process.

Note: If the moisture level is high, significant degradation will occur.

3.1.2 Pelletizing of PET-Bottle and PET-Thermoform:

The PET-B and PET-T dry powder were separately processed into pellets using a co-rotating twin–screw extruder (Leistritz, USA) having a screw diameter of 27mm and L/D ratio of 48 with temperatures ranging from 190° C to peaking at 245° C across all the three zones feeding, compression and metering zone was used.

The extruder operated at a speed of 100 rpm, maintaining a melt temperature of 230°C and a torque of 40 Nm.

3.1.3 PET-B and PET-T Blends Formation:

PET-B and PET-T were dried well at 80° C for 24 h in an oven to get rid of moisture. Then, PET-B and PET-T were melt-blended in a micro compounder DSM extrusion machine (Xplore Instruments BV) at 280°C. Two minutes of residing time and 100 rpm were employed.

The melt was then transferred to an injection molding. The mold temperature was set at 32°C. All samples were aged 48 hours before further evaluation.

3.2 Chain Extender Joncryl ADR 4468:

The commercial chain extender Joncryl ADR 4468 was acquired from the BASF to increase the melt strength and the molecular weight of the PET sample.[36] ADR was physically blended at 0.5 and 1 phr with pelletized samples, it was dried in a vacuum oven at 80°C for 24h prior to processing to avoid moisture content and reactions occurring in the Xplore DSM extruder.

Once dried, the sample is then mixed with a chain extender and extruded in the Xplore DSM extruder at 280°C with a screw speed of 100 rpm (rotations per minute) with a residing time of 2 minutes at a torque of 40 Nm. The molten sample is then transferred to type 4 molds to make test samples for tensile and Izod impact tests.

3.3 Carbon fiber reinforced composites:

The blends were added with carbon fiber of different lengths—0.5, 1, and 2 inches. Each fiber length was added at 1 wt.% and 3 wt.% separately to analyze the impact of fiber length. The sample was extruded using the Xplore DSM extruder, with the sample and carbon fiber of varying lengths dried separately at 80°C for 24 hours prior to extrusion.

Upon drying, the samples were extruded with the Xplore DSM extruder, and the molten blend of the sample and carbon fiber was subsequently transferred to a type 4 mold for mechanical investigation.

3.4 Characterization:

3.4.1 Mechanical Properties:

3.4.1.1 Tensile Properties:

For each sample, seven to eight specimens of T bone shape were prepared and tested where the samples were nearly 6 mm in width (narrow) with the overall length of the sample was 115 mm and the thickness of the sample was 1.5 mm.

Following the injection molding procedure, each specimen was stored for 48 hours under standard laboratory conditions of 23°C and 50% relative humidity. A load cell and an Instron model 5565 (Massachusetts, USA) with tensile grips were utilized, along with a testing speed parameter of 30 mm/min, to measure the tensile strength.

The test was conducted in accordance with ASTM Standard D638-14 (Type V). The specimens' gauge length was 10 mm, and the gap between the grips was 25 mm. The machine loads the specimen between the grips, and the force needed for the specimen to stretch, and break is measured.

The formula below is to calculate the tensile stress and the elongation ratio:

a) Tensile Stress

$$\sigma = \frac{F}{A_0}$$

σ = Tensile stress (Pa or N/m^2)

F = Applied tensile force (N)

A_0 = Initial cross-sectional area of the sample (m^2)

b) Elongation ratio

$$\lambda = \frac{L}{L_0}$$

λ = Elongation ratio (dimensionless)

L = Stretched or current length of the sample (m)

L_0 = Initial length of the sample (m)

3.4.1.2 Izod Impact Test:

Six rectangular bars were processed for each sample using the extrusion-injection molding process. Each bar was 63.5 mm long and 3.5 mm thick and the specimens were bar shaped and were notched on the side parallel to the direction of injection.

Then, the Izod impact samples were notched using the notch cutter (TMI 22-05, USA) where the depth of the plastic material remaining under the notch was 10.58±0.04 mm and then they were checked with the tapered blade fit at the end of the notch machine (notched prior keeping 48 h at room temperature).

The notched samples were subjected to Izod impact tests using a Ray-Ran Universal Pendulum Impact system according to the ASTM – D256. The ASTM-D256 standards for notched sample testing produced a value of 5.417 J for the hammer impact energy.

The specimen was vertically positioned within the grips of the Ray-Ray impact tester, using the ASTM-D256 methodology. A single swing of the hammer pendulum impacted the specimen, and the energy absorbed was quantified. The five specimens' average was calculated and reported in KJ/m^2.

3.4.2 Thermal Properties (DSC and TGA):

DSC measurements were performed with nitrogen gas at 70 mL/min flow rate. Individual samples (~10 g) were heated at 280°C, then were cooled at -20°C, and then reheated again to 280C. The heating and cooling rates were 10°C/min.

The calculations are done according to the formula where we get the degree of crystallinity.

$$X_c = \Delta Hm / \Delta H° mPET * 100$$

The enthalpy of 100% crystalline PET (Δ H°m) is reported to be **140J/g** where X_c denotes degree of crystallinity of the sample.A TGA Q50 thermogravimetric analyzer was used to assess each sample using thermogravimetric analysis (TGA). A sample of approximately 10 milligrams was subjected to heating at 600° C under a nitrogen flow rate of 40 mL/min, with a temperature increase of 10° C/min. All experiments were performed in triplicates.

3.4.3 Melt Flow Index:

The melt flow index of each sample was determined according to the ASTM D1238, where the samples were dried at 80°C for 24 h (moisture content before processing 0.034 wt. %). The temperature was set at 280°C with 12g of the sample inside the melt chamber at a residing time of 6 minutes, whereafter the flow of the polymer was determined using the following formula:

MFI = Weight (gram) of Melted samples / 10 minutes

3.5 Heat deflection temperature (HDT):

The calibration for conducting heat deflection was done according to the ASTM D648, where the rectangular bars were made similar to the Izod impact samples; the tests were conducted using the DMA Q800 (TA Instruments), where the samples were preconditioned for more than 40h under standard temperature condition before testing.[37]

The formula given below can be employed to establish the necessary load for the test, contingent upon the specimen dimensions.

$$\mathbf{F = 2/3\ (\sigma\ (b\ d^2)\ /\ L}$$

Strain of the ASTM Sample

$$\mathbf{Strain\ \varepsilon = 6\ d_{ASTM}\ T_{ASTM} / L_{ASTM}}$$

F represents the load in Newtons (N).

σ represents the stress in megapascals (often 0.455 MPa or 1.82 MPa).

b represents the width of the specimen in millimeters.

d denotes the depth (thickness) of the specimen in millimeters.

L is the distance between the supports in millimeters, generally 101.6 mm or 100 mm.

3.6 Morphological Section:

3.6.1 Digital Microscopy:

In this analysis, Digital Microscope (Keyence VHX-600; VHX-S15) on 200 x zoom where 250μm was the reference length. The samples were prepared by taking 8 mg of each sample and utilizing thermogravimetric analysis to break it down at 600°C. The remaining sample was examined using a digital microscope, capturing photos of each sample with a reference measurement of 250μm. Subsequently, the mean length of the carbon fiber samples was assessed.

Figure 4: Digital Microscope image of 0.5-inch carbon fiber reinforced PET-B/PET-B matrix.

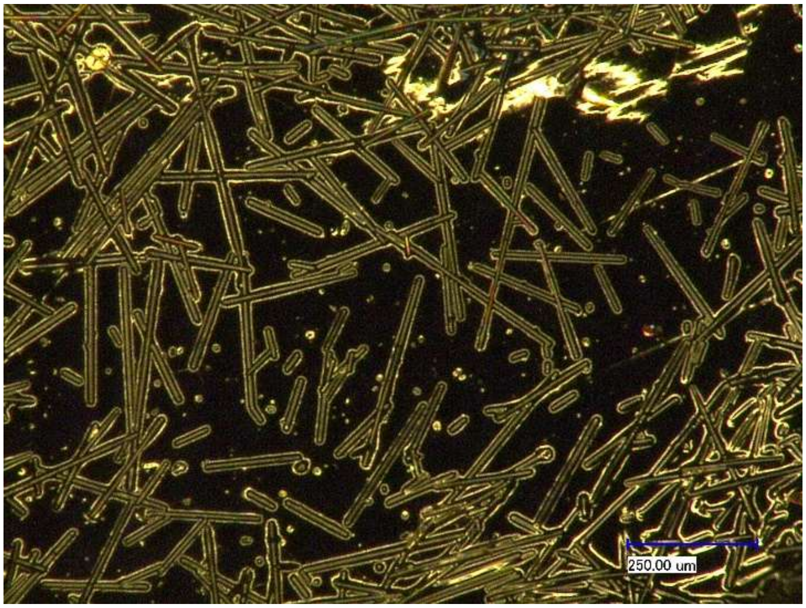

3.6.2 Scanning Electron Microscopy analysis:

The Izod impact samples were used for the electron microscopy where unnotched samples of each of the blend samples, base sample B*, and the carbon fiber samples of each of the 3 wt. % samples of different lengths (0.5,1,2 inch) were scanned, where the samples were notched cryogenically as samples were submerged in liquid nitrogen for approximately 1 minute, then were fractured with the help of a chisel and hammer. The fractured samples were affixed to aluminum stubs using high vacuum carbon tabs and subsequently coated with approximately 30 nm of gold in an Emscope Sputter Coater model SC 500. The mounted samples were put inside the vacuum chamber and examined in JOEL 6610LV (tungsten harpin emitter) scanning electron microscope (JEOL Ltd., Tokyo, Japan). Observations were made in 50x, 100x, 200x and 1000x.

CHAPTER 4: RESULTS AND DISCUSSION

4.1 MFI, mechanical and thermal properties of PET-T and PET-B Blends with and without Chain extender

4.1.1 Melt-flow index (MFI) analysis: Table.1 lists MFI values for Neat PET-B, Neat PET-T, PET-B/10% PET-T, Neat PET-B, PET-B/20% PET-T, PET-T + 0.5 phr Joncryl (B*), PET-B/20% PET-T + 0.5 phr Joncryl (B*) and PET-B/20% PET-T + 1 phr Joncryl (B*). Reflecting on this data, one can clearly see that Neat PET-B has a lower MFI of 61.87g/10 min. relative to Neat PET-T, which has a very high MFI of 134.4 g/10 min.

The markedly elevated MFI of PET-T relative to PET-B suggests that PET-T possesses a lower molecular weight. Polymers with lower molecular weight possess shorter chains, facilitating easier flow under pressure and, therefore, a higher MFI. The results demonstrate that PET-T possesses a lower molecular weight than PET-B, as evidenced by its higher MFI, which signifies enhanced flow resulting from shorter polymer chains.

For PET-B with 10% PET-T, the MFI increased to 104 g/10 min. from 61.87 g/10 min., and it further increased to 113 g/10 min. with 20% PET-T. The incorporation of PET-T essentially acts as plasticizers, resulted in an increased MFI, as shorter chains exhibit enhanced flow under pressure. This trend agrees with expectations, as the addition of PET-T, with its higher MFI, influences the overall MFI of the blend.[38]

Table 1: Mechanical and thermal properties of the samples prepared in this study.

S.NO.	Samples	MFI (g/10 min)	Tensile Strength (MPa)	Young's modulus (MPa)	%Elongation (At Break)	Impact Strength (KJ/m^2)
1	Neat PET-B	61.9 ± 0.1	64.0± 0.9	2170 ±22	444.0 ± 46.8	2.8± 0.6
2	Neat PET-T	134.4± 0.1	63.9 ± 3.9	2130±15	313.8±19.9	1.1 ± 0.2
3	PET-B /10% PET-T	104.2 ± 7.0	62.1 ± 4.82	2190 ± 48	457.5 ± 32.7	2.7± 1.1
4	PET-B /20%PET-T	113 ± 20	60.1 ± 3.5	2010 ± 16	448.4 ± 27.8	2.6 ± 1.2
5	PET-B/20% PET-T + 0.5 phr Joncryl (B*)	66.8±1.4	64.2±0.9	2030±46	406.9±6.5	2.9 ± 0.3
6	PET-B/20% PET-T + 1 phr Joncryl	46.3 ± 1.9	64.2±0.7	2040±70	414.0± 0.8	2.1± 0.7

Furthermore, an enhancement in MFI is achieved using an epoxy chain extender, significantly lowering the MFI at 0.5 phr to 66.8 ± 1.4 g/cm³, matching that of neat PET-B.

At 1 phr Joncryl led to a significant MFI decrease to 46.26 g/10min. This clearly shows that chain extenders effectively coupled different PET chains, leading to increased molecular weight, reduced melt flow, and increased viscosity, suggesting successful chain extension as illustrated in **Scheme A.**

Scheme A. Illustration of Chain extension of PET, which chain extenders clavinet body PET chains together.

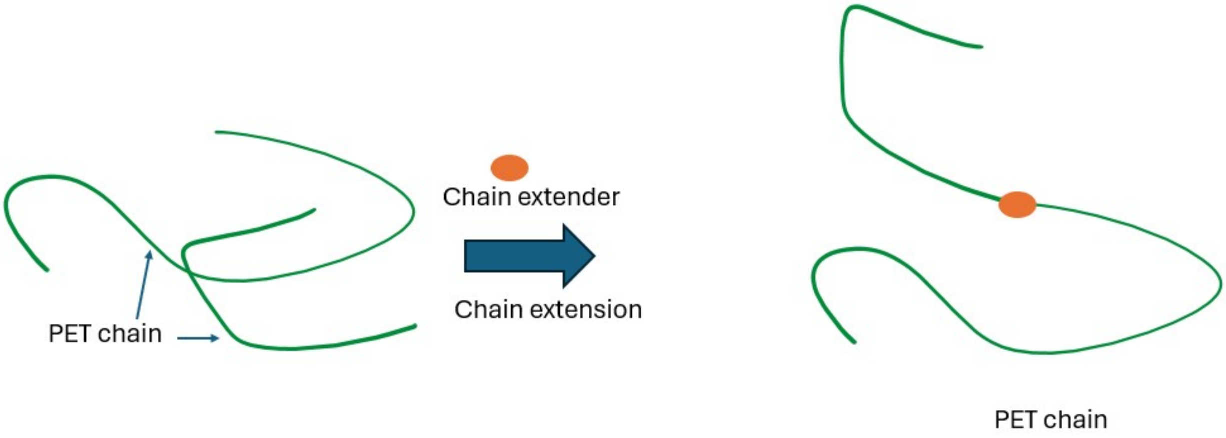

4.1.2 Tensile Properties:

a) Tensile Strength: Table 1 presents a comparison of tensile strength, elastic modulus, and percentage elongation at break. for Neat PET-B, Neat PET-T, PET-B/10% PET-T, Neat PET-B, PET-B/20% PET-T, PET-T + 0.5 phr Joncryl (B*), PET-B/20% PET-T + 0.5 phr Joncryl (B*) and PET-B/20% PET-T + 1 phr Joncryl (B*). Tensile tests were conducted at 100 mm/min. We observed a downward trend for 10% and 20% PET-T in PET-B blends. However, this was within the standard deviation range, so there was no significant change in tensile strength.[39]

Compared to the 10% and 20% blends without a chain extender, the samples with a chain extender showed some increase in tensile strength. For example, PET-B/20% PET-T + 1 phr Joncryl had a tensile strength of 64.2 MPa compared to 60.1 MPa for PET-B/20% PET-T without the chain extender. Tensile strength is influenced by chain entanglement and intermolecular forces. As shown in Table 1, there is little to no significant change in tensile strength, which is presumably attributed to the fact that PET-B and PET-T share similar chemical structures, resulting in identical intermolecular forces and comparable chain rigidity.

b) Elastic modulus: For the elastic modulus, neat PET-B had a value of 2170 MPa, and a similar value was observed for PET-T at 2130 MPa. For the 10% PET-T sample, an elastic modulus of 2190 MPa, while PET-B had an elastic modulus of 2010 MPa. With the addition of the chain extender (at 0.5 PHR and 1 PHR), the modulus mostly remained around 2030 and 2040 MPa, respectively. Considering the standard deviations of the data, we found that these variations are not statistically significant.[40]

Elastic modulus corresponds to the ratio of stress and strain in the elastic region. Elastic modulus is influenced by chain entanglement, polymer chain rigidity, crystallinity, and intermolecular forces between polymer chains. No significant changes were observed in the elastic modulus, as shown in Table 1, which corresponds to the fact that PET-B and PET-T share similar chemical structures, resulting in identical intermolecular forces and comparable chain rigidity.

c) Percentage Elongation (at break): For the neat PET-B, we observed an elongation at a break of 444%. However, for PET-T, the % elongation (at break) was 313%. This is due to the higher molecular weight in PET-B leading to more chain entanglement due to longer chains, this leads to higher chain damage before break comparatively.

The elongation for 10% and 20% blends with PET thermoform were 457 and 448, respectively. The addition of chain extenders caused a decrease in the elongation. Chain extenders can crosslink polymer chains in addition to the increase in the polymer chain length. These crosslinks limit the mobility of polymer chains, reducing the ductility of materials and, hence, a reduction in % elongation.[41] For example, with the 20% thermoform blend at 0.5 phr Joncryl, the % elongation at break was around 406.9%, while without a chain extender, it showed an elongation of 457.5%.

d) Izod Impact test: The purpose of the Izod Impact test is to determine how samples respond to sudden impacts. In this regard, impact tests were conducted. PET-B exhibited a significantly higher impact strength of 2.8 KJ/m^2 compared to Neat PET-T, which had an impact strength of 1.1 KJ/m^2. The more amorphous nature of PET-B contributes to its considerable absorption impact than the more crystalline PET-T. The impact strength decreased for the 10% and 20% blends with the addition of PET-T. The incorporation of PET-T, due to a greater degree of crystallinity, leads to an overall reduction in the impact strength of the blend. The impact strength, if other parameters are constant, is inversely related to the degree of crystallinity of a polymer sample. Increased crystallinity results in a reduction of amorphous regions. These amorphous regions in polymers play a crucial role in absorbing impact and shock..[42] This is consistent with our findings, as reduced crystallinity frequently results in comparatively enhanced impact strength.

Figure 5: The graphs presented tell us about the mechanical results wherein (I) Melt Flow Index (II) Impact strength (III) Tensile Strength (IV) Young's Modulus

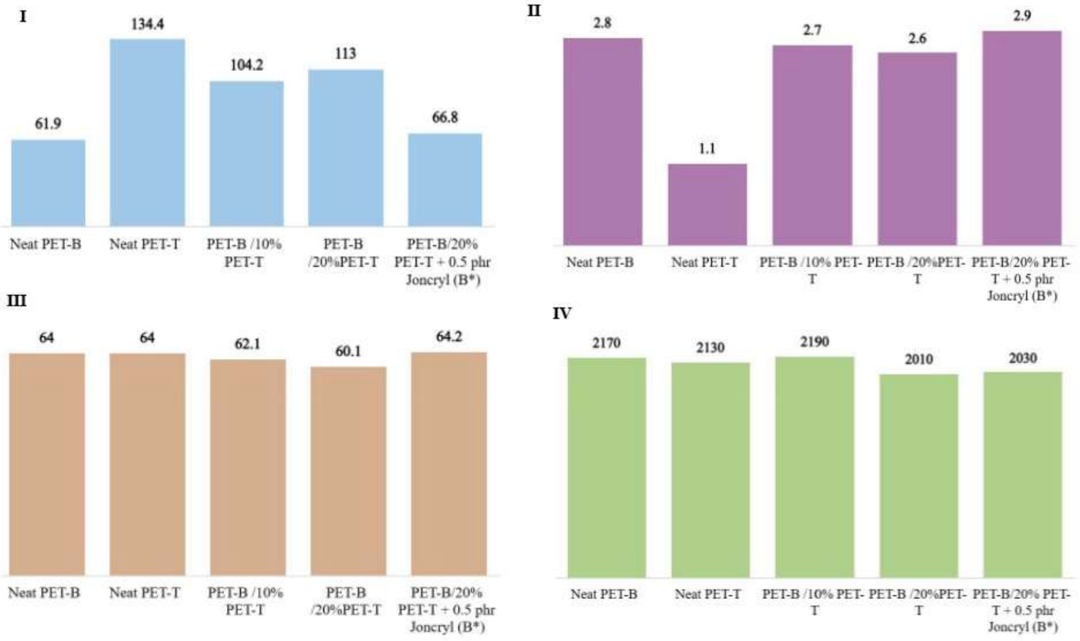

4.1.3 Thermal Properties:

We analyzed the thermal properties of these samples, including the glass transition temperature (Tg), melting temperature (Tm), crystallization temperature (Tc), and degradation temperature, as detailed in **Table 2**. Tg of a polymer is influenced by various factors, including its molecular structure, intermolecular forces, crystallinity, and molecular weight. Additionally, such as the presence of plasticizers, crosslinking, copolymerization, and environmental exposure also play a significant role. In this study, the chemical structure of PET-T and PET-B is the same, so, their Tg values are essentially very close. However, factors such as crystallinity and molecular weights affect their Tg values.

During the 2nd heating cycle, the neat PET-B and neat PET-T had T_g values of 80.8 °C and 87.2 °C, respectively. This increase in Tg corresponds to an increase in the degree of crystallinity the PET-T compared to that of PET-B. For PET-B /20%PET-T, the T_g was 72.18 °C, this could be attributed to the fact that PET-T, due to its low molecular weight, may act as a plasticizer, increasing the flexibility of polymer chains in the PET-B/PET-T blends. With the addition of the chain extender Joncryl (J), the T_g increased to 79.92 °C for PET-B/20% PET-T + 0.5 phr Joncryl (B*).

This corresponds to the potential crosslinking in the sample, increased that limits the chain mobility and the caused an increase in the Tg of PET-B/20% PET-T + 0.5 phr Joncryl (B*).Tm corresponds to the melting temperature of a polymer sample. In this study, we observed two melting temperature peaks (Tm_1 and Tm_2).

The presence of two melting peaks (Tm_1 and Tm_2) in PET samples is due to the complex melting characteristics of semicrystalline polymers. Tm1 is typically linked to the melting of less perfect crystals and corresponds to lower temperature, whereas Tm_2 corresponds to melting of more perfect crystals.

Generally, the first, Tm_1, was approximately 10 °C lower than the second melting temperature (Tm_2). For neat PET-B, Tm_1 was 241.4 °C, while PET thermoform has Tm_1 of 241.8 °C.

For 10% and 20% PET, no significant change was observed in Tm_1 as the value remained around 241.8 °C. However, by adding the chain extender, we observed a slight decrease in melting temperature.[43] For Tm_1, it was 236.8 °C, while Tm_2 around 250 ± 1 °C, with the exception 0.5 PHR Joncryl added sample that showed a Tm_2 of 247.7 °C, approximately 2 degrees lower than the neat PET sample.

Overall, the changes in Tm were not significant for the PET-T/PET-B blends and this is because both PET-T and PET-B have the same chemistry with similar interactions.

Table 2: Thermal Analysis DSC and TGA

DSC							TGA
Description	**2nd Cycle**	**3rd Cycle**					
Name	**T_c (°C)**	**T_g(°C)**	**Tm_1 (°C)**	**Tm_2(°C)**	**ΔHm (J/g)**	**%Xc**	**Temp at 10%**
Neat PET-B	204.5	80.8±0.32	241.4±0.2	249.3±0.0	35.4±1.7	25.3	412.2±1.1
Neat PET-T	211.8±0.4	87.2±0.34	241.8±1.0	250.5±0.5	41.6±3.2	29.7	402.5±0.3
PET-B /10% PET-T	201.9	81.7±3.04	241.7±1.4	249.1±0.5	36.2±2.1	25.8	410.7±1.7
PET-B /20%PET-T	208.2	76.4±0.62	241.7±0.22	249.2±0.6	37.2	26.6	410.2±0.9
PET-B/20% PET-T + 0.5 phr Joncryl (B*)	204.3±3.2	79.9±0.21	236.8±2.5	247.7±0.8	38.1±8.4	27.2	409.3±0.2

Thermogravimetric analysis (TGA) was conducted to determine the thermal degradation temperatures of the samples. The data is presented in Table 2. All samples were analyzed under the same conditions, and temperatures corresponding to a 10 wt.% weight loss were recorded. Overall, the degradation temperature for all samples ranged from 402 °C (for a PET thermoform) and 412 °C (for the PET bottle grade). Technically, crystalline PET-T should be more stable than the less crystalline PET-B. However, in this case, the lower molecular weight (Mw) of PET-T suggests large number of COOH groups per unit sample, which can lead to rapid degradation, particularly in the presence of moisture.

With a 10% and 20% PET thermoform addition to the PET-B, the degradation temperatures were 410.7 °C and 400.2 °C, respectively. Adding Joncryl at 0.5 PHR did not significantly change the degradation temperature, which remained at 409.2 °C. Overall, there is less than a 1% change for PET-B/20% PET-T + 0.5 phr Joncryl (B*) compared to neat PET bottle grade.

Overall, the PET-B and PET-T blends are thermally stable in the absence and presence of the chain extender.[44] The addition of Joncryl somewhat reduced the melting temperature, but it does not significantly affect their thermal stability.

a) Degree of crystallinity: The degree of crystallinity (X_c) is shown in **Table 2.** Neat PET-B has the lowest degree of crystallinity at 25.29%. PET thermoform had an Xc value of 29.7%, ET-B /10%, PET-T was 25.8%, and PET-B /20%PET-T was 26.59%. This increase in crystallinity of the blends corresponds to the addition of crystalline PET-T. PET-B typically possesses a larger molecular weight, hence decreasing chain mobility and restricting crystallization.

Conversely, PET-T has a low molecular weight, with improved chain mobility, facilitating more efficient and rapid crystallization during the cooling after melt-processing. PET-B/20% PET-T + 0.5 phr Joncryl (B*), the crystallinity was 27.2%. No real impact of the J on crystallinity is observed. This could correspond to opposing effects: crosslinking, which reduces crystallinity, and the plasticizing effect of J molecules, which increases crystallinity.

4.2 Mechanical Properties Carbon Fiber-Reinforced Composites of PET-B and PET-T Blends Without Chain Extenders:

Carbon fibers are known for their excellent mechanical properties, such as tensile strength 4900 MPa, and modulus of elasticity of 230,000 MPA, as shown in **Table 3.** Therefore, we decided to use carbon fiber as reinforcing agent for PET-B and PET-T blends to improve the mechanical properties of these blends. We explored two unique systems, 1) incorporating carbon fiber without a chain extender and 2) with chain extenders. Furthermore, carbon fiber of 0.5 inches, 1 inch, and 2 inches in length at two different concentrations (1% and 3% carbon fiber loading) were explored.

a) Tensile strength: For PET-B /20%PET-T, the tensile strength was 60.1 MPa. For carbon fiber-reinforced samples, at 1% carbon fiber loading, we observed that as the fiber length increased from 0.5 inches to 1 inch, the tensile strength increased from 65.9 MPa to 71.6 MPa but then decreased significantly to 61.9 MPa for 2 in fiber. The enhancement of tensile strength with fiber length up to 1 inch is due to the improved stress transfer from the matrix to the carbon fiber in the matrix. Longer fibers offer better load bearing. But when the fiber length goes beyond 1 inch, a diminished load transfers happen. The loading issue may be attributed to inadequate mixing of longer fibers within the matrix, particularly at a low loading level of 1%. This could have resulted in the formation of weak spots in the samples.

For 3% carbon fiber loading, the tensile strength was 71.5 MPa for 0.5-inch fibers, 72.1 MPa for 1-inch fibers, and 74.7 MPa for 2-inch fibers, showing a continuous upward trend in tensile strength with increasing fiber length. This improvement is attributed to the higher carbon fiber content, which provides sufficient reinforcement to resist tensile stress and deformation.

b) Young's modulus: PET-B /20%PET-T had a young’s modulus of 2010 MPa. With 1% carbon fiber (0.5 inches), it increased to 2400 MPa, and with 3% loading, it reached 3100 MPa. For 1-inch fibers, Young's modulus was 2330 MPa at 1% loading and 3240 MPa at 3% loading. Similarly, for 2-inch fibers, Young's modulus increased from 2620 MPa at 1% loading to 3430 MPa at 3% loading. Well-aligned longer fibers can enhance the overall stiffness of the composite more efficiently, reducing the material's tendency to deform and requiring greater force to achieve deformation, thus increasing the modulus of elasticity.

When the loading is higher (3%), stiffer fibers take up space in the composite, which makes further increase in Young's modulus.

These results suggest a significant improvement in Young's modulus with carbon fiber reinforcement, as expected due to the higher strength and stiffness of carbon fiber relative to the plastic matrix.

Table 3: Tensile and impact performance of carbon-reinforced PET-B/PET-T blends

S.NO.	Name	Tensile Strength (MPa)	Young's modulus (MPa)	%Elongation	Impact Strength (KJ/m^2)
Reference	Carbon fiber[45]	4900	230,000	1.75[46]	
Control	PET-B /20%PET-T	60.1 ± 3.5	2010 ± 156	448.4 ± 27.8	2.6 ± 1.2
1	PET-B/20% PET-T/1%CF (0.5 in)	65.9±1.5	2400±23	15.3±2.9	2.4±0.2
2	PET-B/20% PET-T/1%CF (1 in)	71.6±0.7	2330±131	15.9±7.6	2.5±0.3
3	PET-B/20% PET-T/1%CF (2 in)	61.9±0.6	2620±28	5.7±1.0	2.1±0.7
4	PET-B/20% PET-T/3%CF (0.5 in)	71.5±0.4	3100±126	4.5±0.8	3.4±0.2
5	PET-B/20% PET-T/3%CF (1 in)	72.4±0.7	3240±137	4.8±1.0	3.5±0.7
6	PET-B/20% PET-T/3%CF (2 in)	74.7±0.4	3430±77	6.7±2.1	3.4±0.3

c) Percentage Elongation (at break): The percentage elongation for the control PET-B /20%PET-T was 448.4%, significantly reduced with carbon fiber addition. For instance, with 1% carbon fiber loading and 0.5-inch fibers, elongation decreased to 15.3%, and for 3% loading, it was only 4.8%. For 1-inch fibers at 1% loading, elongation was 15.9%, decreasing further to 4.8% at 3% loading. For 2-inch fibers at 1% loading, elongation was 5.7%, and at 3% loading, it reached 6.7%. Overall, the trend indicates a significant reduction in elongation as more carbon fiber is added because carbon fibers are stiff and non-stretchable materials that tend to break under large force rather than stretching.

d) Impact strength: The control PET-B /20 wt.% PET-T had an impact strength of 2.6 KJ/m^2. For all samples with 1wt% carbon fiber loading, impact strength remained around 2.4, 2.5, and 2.5 KJ/m^2 for 0.5, 1, and 2-inch fiber-loaded samples. At 3 wt.% carbon fiber loading, impact strength significantly improved, reaching 3.5 KJ/m^2 for 1-inch fiber samples. This enhancement suggests good adhesion between the PET-T/PET-B matrix and carbon fiber, allowing effective stress transfer from matrix to fiber and dissipation along the fiber network, which improves impact strength. Overall, all samples with 3 wt.% carbon fiber loading, regardless of fiber length, showed a significant enhancement in impact strength.

Figure 6: The graphs presented show us the mechanical tests results for the carbon fiber reinforced samples without chain extender Joncryl ADR. They represent (I) Young's Modulus (II) % Elongation (III) Tensile Strength (IV) Impact Strength.

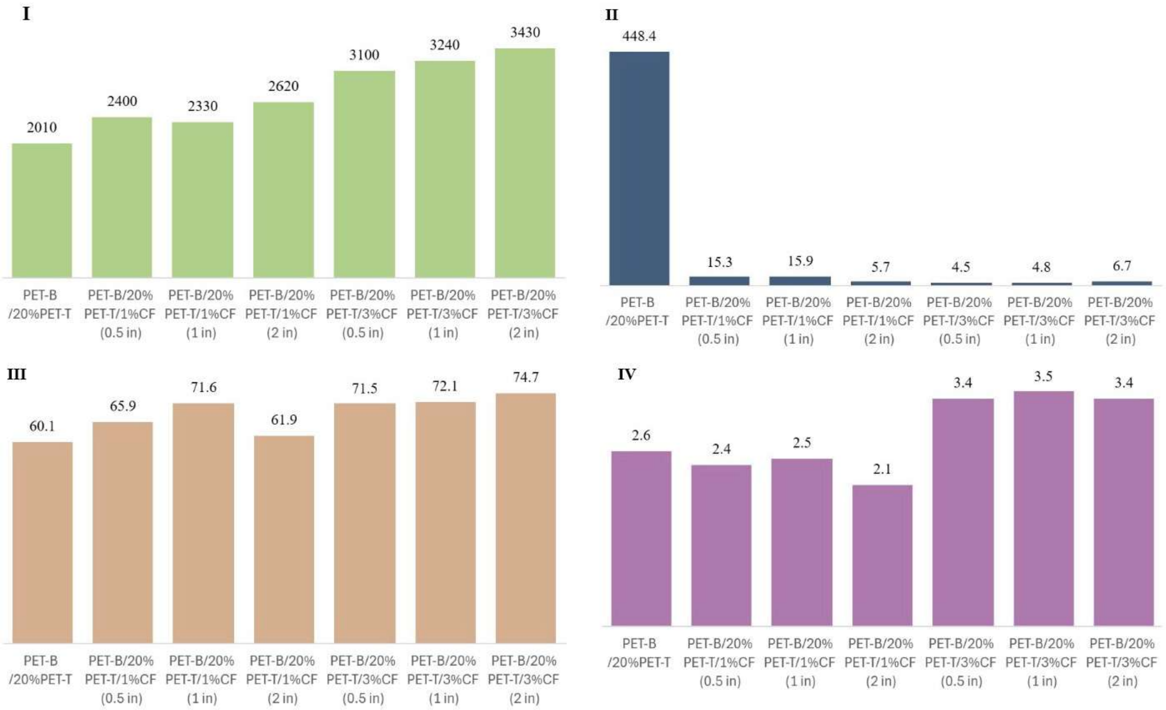

4.3 Mechanical and thermal properties Carbon Fiber-Reinforced Composites of PET-B and PET-T blends with Chain extenders:

Mechanical properties for the carbon fiber reinforced PET-T/PET-B samples were also measured in the presence of 0.5 phr of Joncryl ADR chain extender.

a) Tensile strength: PET-B/20% PET-T + 0.5 phr Joncryl (B*) matrix had the tensile strength was 64.2 MPa. After 1 wt.% carbon fiber loading with 0.5-inch carbon fiber, the tensile strength was 65.9 MPa; at 1 wt.% loading for 1 inch, it was 71.6 MPa; and at 1 wt.% for 2 inches, it was 72.4 MPa. For the 3 wt. % carbon fiber loading, tensile strength was 71.5 MPa, 72.1 MPa, and 74.7 MPa, for 0.5, 1 and 2 inch fibers, respectively. This suggest that increasing the carbon fiber length increased the tensile strength, and a significant increase was observed when going from 1 wt.% carbon fiber loading to 3 wt.% carbon fiber loading, thanks to the very large tensile strength of the carbon fiber itself.

b) Modulus of elasticity: PET-B/20% PET-T + 0.5 phr Joncryl (B*) had a modulus of elasticity value of 2030 MPa, which increased to 2400 MPa for 1 wt.% carbon fiber lading with 0.5-inch fibers. For 2-inch carbon fiber at 1 wt.% loading, it was 2620 MPa. For 3 wt.% carbon fiber loading: 3100 MPa for 0.5-inch fiber, 3240 MPa for 1-inch fibers, and 3430 MPa for 2-inch fibers. This is due to the fact that carbon fibers are remarkably rigid materials rendering the composites rigid with substantial increase in the modulus of elasticity.

c) Percentage Elongation at Break*:* The percent elongation PET-B/20% PET-T + 0.5 phr Joncryl (B*) was 406.9 %, and at 1 wt.% carbon fiber loading, it decreased to 15.3% for 0.5-inch fibers, 15.9% for 1-inch fibers, and 5.7% for 2-inch fibers. It was further reduced by increasing the wt. % of carbon fiber in the sample.

For example, at 3 wt.% carbon fiber loading stood elongation at break was 4.5 % for 0.5-inch fibers, 4.8 % for 1-inch fibers, and 6.7 % for 2-inch fibers. This occurred due to the increase in carbon fiber making the sample stiffer in nature and leading to the loss of flexibility in the matrix.

Table 4: Mechanical analysis with addition of carbon fiber.

Description	**Tensile Strength (MPa)**	**Modulus of Elasticity (MPa)**	**%Elongation**	**Impact Strength (KJ/m^2)**
Carbon fiber[47]	4900	230,000	1.75[48]	-
PET-B/20% PET-T + 0.5 phr Joncryl (B*)	64.2±0.9	2030±46	406.9±6.5	2.94±0.25
B*-1%CF (0.5 in)	65.9±1.5	2400±23	15.3±2.9	2.38±0.24
B*- 1%CF (1 in)	71.6±0.7	2330±131	15.9±7.6	2.46±0.29
B*- 1%CF (2 in)	72.4±0.6	2620±29	5.7±1.0	2.13±0.67
B*- 3%CF (0.5 in)	71.5±0.4	3100±126	4.5±0.8	3.44±0.19
B*- 3%CF (1 in)	72.1±0.7	3240±137	4.8±1.0	3.45±0.73
B*- 3%CF (2 in)	74.7±0.427	3430±77.9	6.70±2.138	3.46±0.33

d) Impact strength: PET-B/20% PET-T + 0.5 phr Joncryl (B*) had an impact strength of 2.94 KJ/m^2. At 1 wt. % carbon fiber loading, it was 2.37 KJ/m^2 for 0.5-inch fibers. 2.46 KJ/m^2 for 1-inch fibers, and 2.13 KJ/m^2 for 2-inch fibers. For 3 wt.% carbon fiber loading, those values were 3.44 KJ/m^2 for 0.5-inch fibers, 3.45 KJ/m^2 for 1-inch fibers, and 3.46 KJ/m^2 for 2-inch fibers. The change in the impact strength as portrayed above is when less concentration fibers (1 wt.%) are there, the matrix is weakened, and the impact strength is lesser.

But with addition of 3 wt.% carbon fibers in the sample enhanced toughness resulting from enough fibers facilitating energy dissipation through fiber fracture, pull-out, and crack bridging. In summary, increasing carbon fiber loading can improve qualities like stiffness and strength, but reduces ductility.

Moreover, excessive fiber loadings can complicate the processing of the composite and perhaps elevate costs. Consequently, the ideal fiber loading amount will be dependent upon the need of end-use.

Figure 7: The graphs representing the mechanical reading of the carbon fiber composites consisting of the chain extenders where (I) Young's Modulus (II) % Elongation (III) Tensile Strength (IV) Impact Strength. B* is the PET-B-80%/PET-T-20% with 0.5 Phr Joncryl which is the base sample

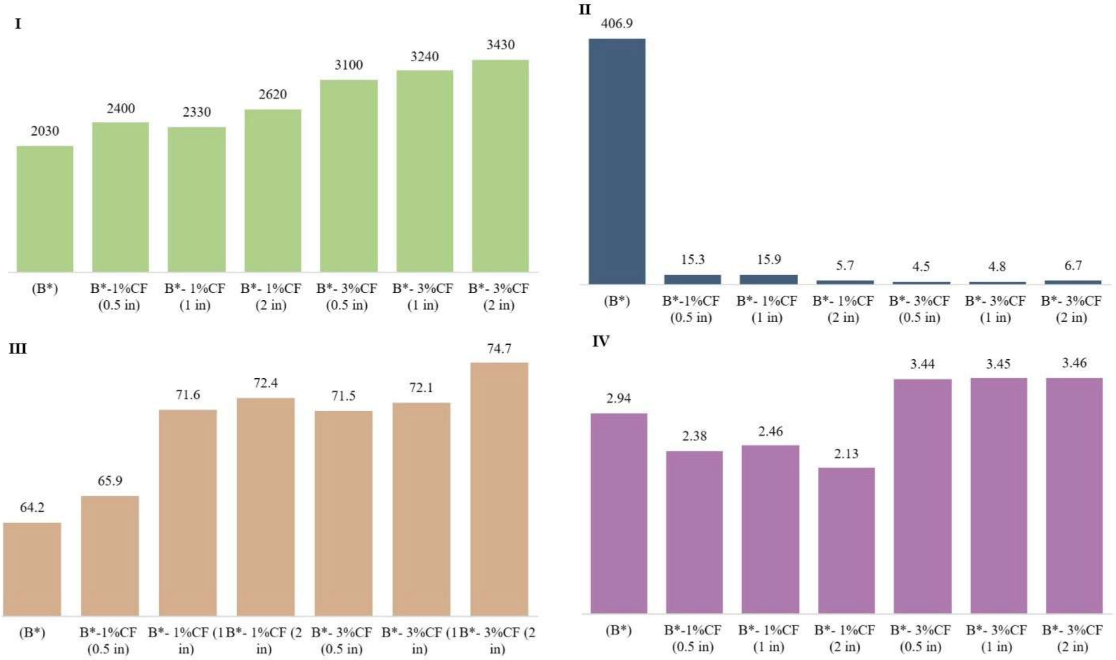

4.3.1 Thermal properties:

The Tg of PET-B/20% PET-T + 0.5 phr Joncryl (B*) was 79.9°C. For the 1 wt.% carbon fiber loading, the T_g values were 76, 77.7, and 73.2°C for 0.5-inch, 1-inch, and 2-inch lengths, respectively. At 3 wt.% carbon fiber loading, the Tg values were 28.4, 28 and 33.9 respectively. The Tg initially decreases with the introduction of a minor quantity of (CF due to enhanced free volume and weak matrix-fiber interaction, particularly with longer fibers. At 3 wt.% CF, a networked structure starts formation, diminishing chain mobility and aligning Tg values more closely with those of the unmodified matrix (B*).

This pattern highlights the complex interactions among fiber dispersion, interfacial adhesion and chain mobility in influencing temperature transitions. PET-B/20% PET-T + 0.5 phr Joncryl (B*) showed Tm_1 of 236.75 °C, and T_{m2} value of 247.69°C. For all 1 wt.% carbon fiber loadings, T_{m1} was in the range of 240°C, and for 3 wt.% carbon fiber loading, it remained around 240°C. T_{m2} values for all samples were around 248°C, with a minimal increase compared to the PET-B/20% PET-T + 0.5 phr Joncryl (B*), indicating that Tm values were not significantly affected by carbon fiber loading.

a) Degradation temperature:

PET-B/20% PET-T + 0.5 phr Joncryl (B*) showed $T_{10\%}$ (10 wt. % loss) at 409.2°C. For 1wt. % carbon fiber loading, it was 408.2°C for 0.5-inch fiber, at 409.6°C for 1-inch fiber, and again at 409.7°C for 2-inch fiber.

With higher carbon fiber loading (at 3 wt.%), we observed a slight decrease to 405°C for 2-inch. Overall, the degradation temperature did not change significantly, thus suggesting the thermal stability of the polymer remains intact for these samples. This may correspond to the fact that carbon fibers are inert and do not interfere with the chemistry or degradation of the polymer matrix.

Table 5: This table shows the DSC and the TGA results portraying the thermal properties.

DSC							TGA
	2nd Cycle	**3rd Cycle**					
Sample Name	**T_c (°C)**	**T_g(°C)**	**Tm_1 (°C)**	**Tm_2(°C)**	**ΔHm (J/g)**	**%Xc**	**Temp at 10%**
PET-B/20% PET-T + 0.5 phr Joncryl (B*)	204.3±3.2	79.9	236.8±2.5	247.7±0.8	38.1±8.4	27.2	409.3±0.2
B*-1%CF (0.5 in)	205.1	76	240.3	248.7	41.3	29.5	408.2±3.6
B*- 1%CF (1 in)	208.6±1.3	77.7±0.3	240.5±0.3	248.9±0.2	39.3±0.3	27.9	409.6
B*- 1%CF (2 in)	209.3±0.6	73.3±3.5	240.3±0.9	248.8±0.1	40.1±1.4	31.4	409.7
B*- 3%CF (0.5 in)	209.3±0.8	74.7±3.9	240.7±2.2	248.5±0.3	39.8±1.6	28.4	410.3
B*- 3%CF (1 in)	209.1	81.2	240.3	249	39.2	28.0	407.2±0.9
B*- 3%CF (2 in)	209.8	70.2	239.3	248.7	38.9	33.9	405.9±0.2
B*= PET-B/20% PET-T + 0.5 phr Joncryl							

b) ***Degree of crystallinity:*** The percent crystallinity for PET-B/20% PET-T + 0.5 phr Joncryl (B*) was 27.2%. With 1wt.% carbon fiber loading, it was 29.5% for 0.5-inch fibers, 27.9% for 1-inch fibers, and 31.4% for 2-inch fibers.For 3 wt.% carbon fiber loading, the degree of crystallinity was 28.4%, 28.0%, 33.9% for 0.5-inch, 1-inch, and 2-inch fibers, respectively.

The trend shows a significant increase in crystallinity as the carbon fiber loading increased, which is presumably due to fiber acting as nucleating agents, where the polymer chains surround the fibers and form crystalline regions, this increasing sample overall crystallinity.

4.4 SEM analysis and Digital microscopy analysis:

SEM and digital microscopy images for B*- 3%CF (0.5 in), B*- 3%CF (1 in), and B*- 3%CF (2 in) are shown in **Table 6**. Here, B* denotes PET-B/20% PET-T + 0.5 phr Joncryl.

SEM images recorded from the fracture samples show a reasonable adhesion between the fiber and the matrix, as some fibers are broken, and some are pulled out. The fibers pulled out from the matrix without having residual resin around it indicate low adhesion between the fiber and the matrix, while in other cases, fibers are broken, suggesting that instead of pulling out, they broke, indicating better adhesion.

Additionally, digital microscopic images were recorded to quantify the fiber length and dispersity in the fiber in the matrix. As shown, fibers, especially the 0.5-inch ones, are well-dispersed in the system. For the 1-inch and 2-inch fibers, we observed a clustering suggesting that longer fibers are more challenging to disperse.

Table 6: SEM and Digital Microscopy images of the B*- 3%CF with different fiber types.

Sample	SEM image (at the same resolution)	Digital Microscopy images
B*- 3%CF (0.5 in)	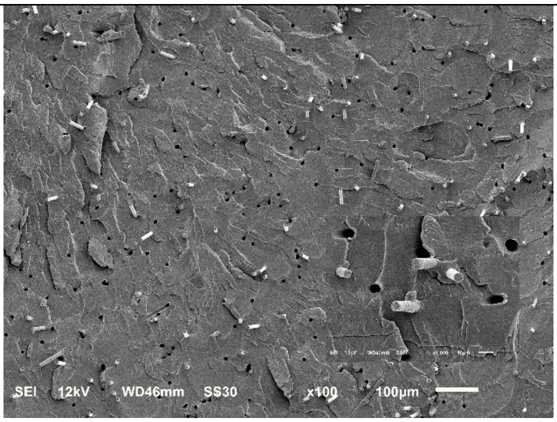	
B*- 3%CF (1 in)	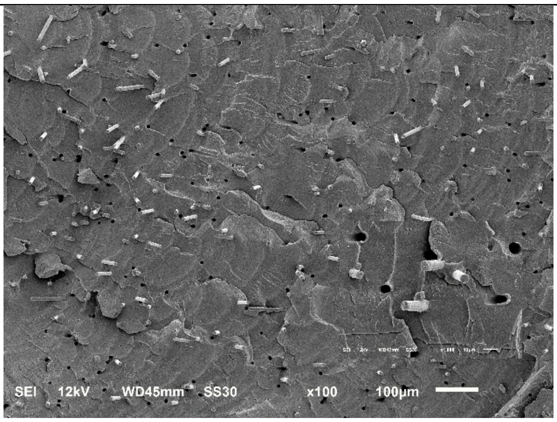	
B*- 3%CF (2 in)	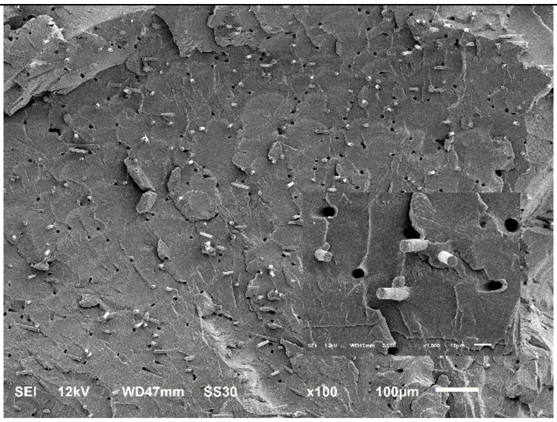	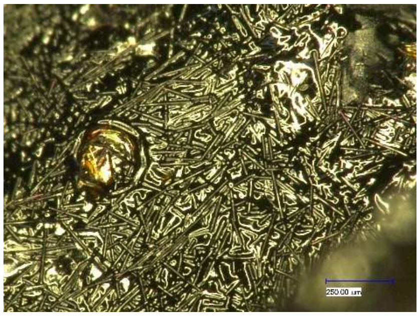

4.5 Mechanical Properties of recycled PET-T/PET-B vs virgin PET vs virgin PP Carbon Reinforced composites:

For comparative analysis, we also tested virgin PET, virgin polypropylene, and compared that with recycled PET-B/20% PET-T + 0.5 phr Joncryl composites, then determined their tensile properties, including tensile strength, modulus of elasticity, percent elongation, and impact strength.

a) Tensile Strength: For virgin PET, the tensile strength was 50.2 MPa, and increased with 3% CF loading reaching 65.0, 65.9, and 67.9 MPa for 0.5-inch and 2-inch fibers, respectively.

Neat virgin polypropylene (PP) had a tensile strength of 39.9 MPa, which increased to 42.6 MPa with 3% carbon fiber loading at 0.5-inch, 43.1 MPa at 1 inch, and 41.9 MPa at 2- inches. The PET-B/20% PET-T + 0.5 phr Joncryl (B*) showed a tensile strength of 64.2 MPa, while the addition of 3wt% carbon fiber resulted in tensile strengths of 71.5, 72.1, and 74.7 MPa for 0.5-inch, 1-inch, and 2-inch fibers, respectively.

Overall, the fiber composites of recycled PET-B/PET-T showed maximum tensile strength compared to virgin PET and virgin polypropylene. The difference between PP and recycled PET-T/PET-B composites is likely due to variations in matrix properties, as the PP matrix has lower tensile strength compared to recycled PET-T/PET-B. In the case of virgin PET versus recycled PET-T/PET-B, the effect may be attributed to the fact that recycled PET-T/PET-B undergoes some oxidation during use, leading to improved adhesion between fiber and the matrix.

b) Elastic Modulus: Virgin PET showed modulus of 2030 MPa, and with 3% carbon fiber, it was 3080, 3150, and 3200 MPa for 0.5-inch, 1-inch, and 2-inch fibers. Neat polypropylene showed an elastic modulus of 1470 MPa and were 1900, 1850, and 1800 MPa with 3% carbon fiber loading for 0.5-inch, 1-inch, and 2-inch fibers, respectively. PET-B/20% PET-T + 0.5 phr Joncryl (B*) had a modulus of 2030 MPa, which increased to 3100, 3240, and 3430 MPa with 3% carbon fiber loading for 0.5-inch, 1-inch, and 2-inch fibers, respectively.

The composites of recycled PET-B/PET-T exhibited a greater modulus of elasticity. An increase of 30-40% in elastic modulus was observed, which is due to the very high elastic modulus (230,000 MPa) of carbon fiber.

c) Percentage Elongation (at break): the PET-B/20% PET-T + 0.5 phr Joncryl (B*) was 406.9%, which decreased to 4.5%, 4.8%, and 6.7% for 3% carbon fiber loading with 0.5-inch, 1-inch, and 2-inch fibers, respectively. For virgin PET, percent elongation at break was 391.5%, and with 3% carbon fiber loading, it was 17.8, 5.7, and 4.8% for 0.5-inch, 1-inch, and 2-inch fibers, respectively. Neat polypropylene had an elongation of 183.5%, which decreased to 30.8, 37.4, and 35.3% with 3% carbon fiber for 0.5-inch, 1-inch, and 2-inch fibers, respectively.

Overall, the addition of carbon fiber led to a severe reduction in the elongation because carbon fiber has only 1.5% elongation itself, and their effects are manifested in the fiber-reinforced samples. Carbon fibers are intrinsically brittle and demonstrate minimal elongation. When incorporated into a polymer matrix, they markedly diminish the overall elongation of the composite.

Table 7: Comparison of the recycled PET composited reinforced with carbon fiber comparison with virgin polymers PP and virgin PET reinforced with carbon fiber.

Description	Tensile Strength (MPa)	Modulus of Elasticity (MPa)	%Elongation (At Break)	Impact Strength (KJ/m^2)
Recycled PET-T/PET-B as matrix				
PET-B/20% PET-T + 0.5 phr Joncryl (B*)	64.2±0.8	2030±45	406.9±6.5	2.93±0.25
B*- 3%CF (0.5 in)	71.5±0.4	3100±126	4.5±0.8	3.44±0.194
B*- 3%CF (1 in)	72.1±0.7	3240±137	4.8±1.0	3.45±0.73
B*- 3%CF (2 in)	74.7±0.4	3430±77.9	6.7±2.1	3.46±0.33
Virgin PET as matrix				
Neat PET (Virgin)	50.2±0.8	2030±25	391.5±6.4	2.43±0.30
PET-3%CF (0.5 in)	65.0±1.3	3082±126	17.8±16.5	3.34±0.52
PET-3%CF (1 in)	65.9±3.7	3150±211	5.7±1.7	3.15±0.00
PET-3%CF (2 in)	67.9 ± 6.9	3200±573	4.8±2.4	3.93±1.73
Virgin PP as matrix				
Neat PP	39.9±1.3	1470±102	183.5±9.8	4.44±0.96
PP-3%CF (0.5 in)	42.6±0.5	1900±74.5	30.8±1.8	3.23±0.72
PP-3%CF (1 in)	43.1±0.4	1850±172	37.5±7.5	3.30±0.42
PP-3%CF (2 in)	41.9 ± 0.7	1800±113	35.3±5.1	3.30±0.18

For impact strength, PET-B/20% PET-T + 0.5 phr Joncryl (B*) had an impact strength of 2.93 kJ/m^2. With 3% carbon fiber loading, it increased to 3.44kJ/m^2, 3.45kJ/m^2, and 3.46 kJ/m^2 for 0.5-inch, 1-inch, and 2-inch fibers, respectively.

Virgin PET had an impact strength of 2.43 kJ/m^2, which increased to 3.34kJ/m^2, 3.15kJ/m^2, and 3.93 kJ/m^2 with 3% carbon fiber loading for 0.5-inch, 1-inch, and 2-inch fibers, respectively.

For polypropylene, the impact strength was 4.44 kJ/m^2, which decreased to 3.23kJ/m^2, 3.30kJ/m^2, and 3.30 kJ/m^2 for 0.5-inch, 1-inch, and 2-inch fibers with 3% carbon fiber. Overall, carbon fiber reinforcement improved impact strength for all polymers except PP samples.

This is due to the strong adhesion between the fiber and the high surface energy PET matrix, facilitating effective impact transfer from the matrix to the fiber. In contrast, the low adhesion observed in PP composites due to low adhesion between the fiber and the non-polar PP matrix, ultimately diminishing the performance of PP composites when compared to those utilizing the PET matrix.

4.6 Heat Deflection Temperatures:

Heat deflection temperatures were determined for Neat PET-B, PET-B-80/20 + 0.5 Phr J (B*), B*-CF-0.5-3 wt.%, B*-CF-1-3 wt.%, and B*-CF-2-3 wt.%. Neat PET-B has a heat deflection temperature of 64.62°C, which PET-B-80/20 + 0.5 Phr J (B*) showed a heat deflection temperature of 76.32°C.

The addition of a chain extender potentially creates crosslinks across polymer chains, so limiting chain mobility thus increasing rigidity of the polymer matrix. As a result, elevated HDT was observed after chain extension. With 3wt.% carbon fiber loading (0.5, 1, and 2 inches), we observed heat deflection temperatures of approximately 84.19°C, 99.39°C, and 120.82, respectively. These increases in HDT correspond to a greater stiffness caused by stronger interaction of the carbon fiber with the PET matrix, which increases the overall resistance to change in temperature, thus leading to an increase in the deflection temperatures.[49]

Table 8: Heat deflection temperatures of carbon fiber composites and a neat blend of PET-B and PET-T.

SAMPLE	HDT (°C)
Neat PET-B	64.62±0.35
PET-B-80/20 + 0.5 Phr J (B*)	76.32±0.43
B*-CF-0.5-3 wt.%	84.19±0.25
B*-CF-1-3 wt.%	99.39±0.86
B*-CF-2-3 wt.%	120.82±0.13

CHAPTER 5: CONCLUSION AND FUTURE WORK

5.1 Conclusion:

We successfully developed carbon fiber-reinforced composites from recycled PET-T and PET-B. Our finding suggests that tensile properties were significantly improved, especially the modulus of elasticity, which increased by 30-40% with a 3 wt.% carbon fiber loading. Similarly, there was a 10-20% increase in tensile strength with the addition of 3wt.% carbon fiber. The impact strength increased by 10-18% for the reinforced carbon matrix.

SEM analysis confirmed a reasonable adhesion between fiber and plastic matrix. No drastic changes in T_g, T_m, and T_c were observed. Similarly, the TGA analysis confirmed the different combination blends are as thermally stable as their polymer matrix.

Heat deflection temperatures were increased with 3 wt.% carbon fiber loading, particularly with longer carbon fiber chains, reaching 120.82°C for the sample with 2-inch carbon fiber compared to 76.2°C for the unreinforced sample.

Carbon fiber-reinforced composites of recycled PET performed better than carbon-reinforced virgin PET and virgin PP composites. For each sample, significant increase in modulus of elasticity and tensile strength, though a notable decrease in elongation at break were observed.

In contrast, impact strength decreased for polypropylene-reinforced composites, while it increased for both virgin and recycled PET matrices in reinforced composites.

5.2 Future Outlook:

A detailed SEM analysis is required to assess the distribution of fibers within the matrix and to gain a better understanding of the fracture mechanisms in these composites. Furthermore, it is essential to explore ways to enhance the interaction between the matrix and the fibers by utilizing functional carbon fibers and/or treating carbon fibers with plasma prior to their incorporation into the polymer matrix.

Another area of interest could be investigating the effects of larger fiber loading, such as 10% and 30% carbon fiber in the system. Exploring these parameters and processes will further enhance the understanding that can be employed to further increase the performance of the composite.

REFERENCES

(1) Environmental Protection Agency, U.; of Land, O.; Management, E.; of Resource Conservation, O. *Advancing Sustainable Materials Management: 2018 Tables and Figures Assessing Trends in Materials Generation and Management in the United States*; 2021.

(2) Nisticò, R. Polyethylene Terephthalate (PET) in the Packaging Industry. *Polym Test* **2020**, *90*, 106707. https://doi.org/10.1016/j.polymertesting.2020.106707.

(3) Rabnawaz, M.; Wyman, I.; Auras, R.; Cheng, S. A Roadmap towards Green Packaging: The Current Status and Future Outlook for Polyesters in the Packaging Industry. *Green Chem.* **2017**, *19* (20), 4737–4753. https://doi.org/10.1039/C7GC02521A.

(4) Environmental Protection Agency, U.; of Land, O.; Management, E.; of Resource Conservation, O. *Advancing Sustainable Materials Management: 2018 Tables and Figures Assessing Trends in Materials Generation and Management in the United States*; 2021.

(5) NAPCOR. *2022-Pet-Recycling-Report*; Middleton, Wisconsin, 2023.

(6) Jared Paben. *European PET Bottle Recycling Hits 58 Percent*; 2019.

(7) Aayanifard, Z.; Khan, A.; Naveed, M.; Schager, J.; Rabnawaz, M. Rapid Depolymerization of PET by Employing an Integrated Melt-Treatment and Diols. *Polymer (Guildf)* **2023**, *265*, 125585. https://doi.org/10.1016/j.polymer.2022.125585.

(8) Khan, A.; Naveed, M.; Aayanifard, Z.; Rabnawaz, M. Efficient Chemical Recycling of Waste Polyethylene Terephthalate. *Resour Conserv Recycl* **2022**, *187*, 106639. https://doi.org/10.1016/j.resconrec.2022.106639.

(9) Rabnawaz, M.; Wyman, I.; Auras, R.; Cheng, S. A Roadmap towards Green Packaging: The Current Status and Future Outlook for Polyesters in the Packaging Industry. *Green Chem.* **2017**, *19* (20), 4737–4753. https://doi.org/10.1039/C7GC02521A.

(10) Mestry, J.; Abdelwahab, M. A.; Elkholy, H. M.; Rabnawaz, M. Mechanical Recycling of a Bottle-Grade and Thermoform-Grade PET Mixture Enabled by Glycidol-Free Chain Extenders. *Ind Eng Chem Res* **2024**, *63* (42), 18067–18074. https://doi.org/10.1021/acs.iecr.4c02562.

(11) Ganapathi, A.; Abdelwahab, M. A.; Rabnawaz, M. Achieving Bottle-grade Poly(Ethylene Terephthalate)-like Properties from Blends of Bottle-grade and Thermoform-grade Poly(Ethylene Terephthalate). *Polym Int* **2024**, *73* (8), 625–630. https://doi.org/10.1002/pi.6633.

(12) Bin, Y.; Oishi, K.; Yoshida, K.; Matsuo, M. Mechanical Properties of Poly(Ethylene Terephthalate) Estimated in Terms of Orientation Distribution of Crystallites and

Amorphous Chain Segments under Simultaneous Biaxially Stretching. *Polym J* **2004**, *36* (11), 888–898. https://doi.org/10.1295/polymj.36.888.

(13) Cecon, V. S.; Da Silva, P. F.; Curtzwiler, G. W.; Vorst, K. L. The Challenges in Recycling Post-Consumer Polyolefins for Food Contact Applications: A Review. *Resour Conserv Recycl* **2021**, *167*, 105422. https://doi.org/10.1016/J.RESCONREC.2021.105422.

(14) Claire Bergkamp. *Textile Exchange's Annual Materials Market Report Shows Further Growth in the Overall Production of New Materials, Including Fossil-Based Synthetic Fibers*; 2024.

(15) Williams, A. T.; Rangel-Buitrago, N. The Past, Present, and Future of Plastic Pollution. *Mar Pollut Bull* **2022**, *176*, 113429. https://doi.org/10.1016/j.marpolbul.2022.113429.

(16) Jambeck, J. R.; Geyer, R.; Wilcox, C.; Siegler, T. R.; Perryman, M.; Andrady, A.; Narayan, R.; Law, K. L. Plastic Waste Inputs from Land into the Ocean. *Science (1979)* **2015**, *347* (6223), 768–771. https://doi.org/10.1126/science.1260352.

(17) *Https://Textileexchange.Org/Knowledge-Center/Reports/Materials-Market-Report-2024/*; 2024.

(18) Veit, D. Polyester. In *Fibers*; Springer International Publishing: Cham, 2022; pp 625–648. https://doi.org/10.1007/978-3-031-15309-9_30.

(19) Wyeth, N. C. INVENTING THE PET BOTTLE. *Research Technology Management* **1988**, *31* (3), 12–14.

(20) Aayanifard, Z.; Khan, A.; Naveed, M.; Schager, J.; Rabnawaz, M. Rapid Depolymerization of PET by Employing an Integrated Melt-Treatment and Diols. *Polymer (Guildf)* **2023**, *265*, 125585. https://doi.org/10.1016/j.polymer.2022.125585.

(21) Mendiburu-Valor, E.; Mondragon, G.; González, N.; Kortaberria, G.; Eceiza, A.; Peña-Rodriguez, C. Improving the Efficiency for the Production of Bis-(2-Hydroxyethyl) Terephtalate (BHET) from the Glycolysis Reaction of Poly(Ethylene Terephtalate) (PET) in a Pressure Reactor. *Polymers (Basel)* **2021**, *13* (9), 1461. https://doi.org/10.3390/polym13091461.

(22) Berg, D.; Schaefer, K.; Moeller, M. Impact of the Chain Extension of Poly(Ethylene Terephthalate) with 1,3-phenylene-bis-oxazoline and *N* , *N* ′-carbonylbiscaprolactam by Reactive Extrusion on Its Properties. *Polym Eng Sci* **2019**, *59* (2), 284–294. https://doi.org/10.1002/pen.24903.

(23) Comprehensive Guide on Polyethylene Terephthalate (PET). *omnexus.specialchem.com*.

(24) Guessasma, S.; Belhabib, S.; Nouri, H. Printability and Tensile Performance of 3D Printed Polyethylene Terephthalate Glycol Using Fused Deposition Modelling. *Polymers (Basel)* **2019**, *11* (7), 1220. https://doi.org/10.3390/polym11071220.

(25) Nisticò, R. Polyethylene Terephthalate (PET) in the Packaging Industry. *Polym Test* **2020**, *90*, 106707. https://doi.org/10.1016/j.polymertesting.2020.106707.

(26) A New Textiles Economy: Redesigning Fashion's Future. *https://www.ellenmacarthurfoundation.org/a-new-textiles-economy*. August 27, 2017.

(27) Paci, M.; La Mantia, F. P. Influence of Small Amounts of Polyvinylchloride on the Recycling of Polyethyleneterephthalate. *Polym Degrad Stab* **1999**, *63* (1), 11–14. https://doi.org/10.1016/S0141-3910(98)00053-6.

(28) Karsli, N. G.; Aytac, A. Tensile and Thermomechanical Properties of Short Carbon Fiber Reinforced Polyamide 6 Composites. *Compos B Eng* **2013**, *51*, 270–275. https://doi.org/10.1016/j.compositesb.2013.03.023.

(29) Shojaei, B.; Abtahi, M.; Najafi, M. Chemical Recycling of <scp>PET</Scp> : A Stepping-stone toward Sustainability. *Polym Adv Technol* **2020**, *31* (12), 2912–2938. https://doi.org/10.1002/pat.5023.

(30) Elkholy, H. M.; Abdelwahab, M. A.; Naveed, M.; Abdelaziz, K.; Rabnawaz, M. Food-Safe Glycidyl-Free Chain Extenders for Polylactides. *Green Chemistry* **2024**, *26* (7), 3968–3978. https://doi.org/10.1039/D3GC04200F.

(31) Owen, M. Characterization of Recycled and Virgin Polyethylene Terephthalate Composites Reinforced with Modified Kenaf Fibers for Automotive Application. *Polym Compos* **2022**.

(32) Torres, N.; Robin, J. J.; Boutevin, B. Study of Thermal and Mechanical Properties of Virgin and Recycled Poly(Ethylene Terephthalate) before and after Injection Molding. *Eur Polym J* **2000**, *36* (10), 2075–2080. https://doi.org/10.1016/S0014-3057(99)00301-8.

(33) Um, H.-J.; Hwang, Y.-T.; Choi, K.-H.; Kim, H.-S. Effect of Crystallinity on the Mechanical Behavior of Carbon Fiber Reinforced Polyethylene-Terephthalate (CF/PET) Composites Considering Temperature Conditions. *Compos Sci Technol* **2021**, *207*, 108745. https://doi.org/10.1016/j.compscitech.2021.108745.

(34) Torres, N.; Robin, J. J.; Boutevin, B. Study of Thermal and Mechanical Properties of Virgin and Recycled Poly(Ethylene Terephthalate) before and after Injection Molding. *Eur Polym J* **2000**, *36* (10), 2075–2080. https://doi.org/10.1016/S0014-3057(99)00301-8.

(35) Torres, N.; Robin, J. J.; Boutevin, B. Study of Thermal and Mechanical Properties of Virgin and Recycled Poly(Ethylene Terephthalate) before and after Injection Molding. *Eur Polym J* **2000**, *36* (10), 2075–2080. https://doi.org/10.1016/S0014-3057(99)00301-8.

(36) Guclu, M.; Alkan Göksu, Y.; Özdemir, B.; Ghanbari, A.; Nofar, M. Thermal Stabilization of Recycled PET Through Chain Extension and Blending with PBT. *J Polym Environ* **2022**, *30* (2), 719–727. https://doi.org/10.1007/s10924-021-02238-8.

(37) Moody, L.; Marchant, D.; Grabow, W.; Lee, A.; Mabry, J. Determination of Mechanical and Surface Properties of Semicrystalline Poss Nanocomposites. *International SAMPE Technical Conference* **2005**, *2005*.

(38) Singh, R.; Fraternali, F.; Farina, I.; Hashmi, M. S. J. Experimental Investigations for Development of Hybrid Feed Stock Filament of Fused Deposition Modeling. In *Reference Module in Materials Science and Materials Engineering*; Elsevier, 2018. https://doi.org/10.1016/B978-0-12-803581-8.10392-3.

(39) Yao, S.; Hu, D.; Xi, Z.; Liu, T.; Xu, Z.; Zhao, L. Effect of Crystallization on Tensile Mechanical Properties of PET Foam: Experiment and Model Prediction. *Polym Test* **2020**, *90*, 106649. https://doi.org/10.1016/j.polymertesting.2020.106649.

(40) Schyns, Z. O. G.; Shaver, M. P. Mechanical Recycling of Packaging Plastics: A Review. *Macromol Rapid Commun* **2021**, *42* (3). https://doi.org/10.1002/marc.202000415.

(41) Bin, Y.; Oishi, K.; Yoshida, K.; Matsuo, M. Mechanical Properties of Poly(Ethylene Terephthalate) Estimated in Terms of Orientation Distribution of Crystallites and Amorphous Chain Segments under Simultaneous Biaxially Stretching. *Polym J* **2004**, *36* (11), 888–898. https://doi.org/10.1295/polymj.36.888.

(42) Schyns, Z. O. G.; Shaver, M. P. Mechanical Recycling of Packaging Plastics: A Review. *Macromol Rapid Commun* **2021**, *42* (3). https://doi.org/10.1002/marc.202000415.

(43) Novello, M. V.; Carreira, L. G.; Canto, L. B. Post-Consumer Polyethylene Terephthalate and Polyamide 66 Blends and Corresponding Short Glass Fiber Reinforced Composites. *Materials Research* **2014**, *17* (5), 1285–1294. https://doi.org/10.1590/1516-1439.281914.

(44) Rashwan, O.; Koroneos, Z.; Townsend, T. G.; Caputo, M. P.; Bylone, R. J.; Wodrig, B.; Cantor, K. Extrusion and Characterization of Recycled Polyethylene Terephthalate (RPET) Filaments Compounded with Chain Extender and Impact Modifiers for Material-Extrusion Additive Manufacturing. *Sci Rep* **2023**, *13* (1), 16041. https://doi.org/10.1038/s41598-023-41744-8.

(45) Santos, R. M.; Costa, A. R. M.; Almeida, Y. M. B.; Carvalho, L. H.; Delgado, J. M. P. Q.; Lima, E. S.; Magalhães, H. L. F.; Gomez, R. S.; Leite, B. E.; Rolim, F. D.; Figueiredo, M. J.; Lima, A. G. B. Thermal and Rheological Characterization of Recycled PET/Virgin HDPE Blend Compatibilized with PE-g-MA and an Epoxy Chain Extender. *Polymers (Basel)* **2022**, *14* (6). https://doi.org/10.3390/polym14061144.

(46) Rezaei, F.; Yunus, R.; Ibrahim, N. A. Effect of Fiber Length on Thermomechanical Properties of Short Carbon Fiber Reinforced Polypropylene Composites. *Mater Des* **2009**, *30* (2), 260–263. https://doi.org/10.1016/j.matdes.2008.05.005.

(47) Hexel. *carbon-fiber-properties*. Gernitex.

(48) Rezaei, F.; Yunus, R.; Ibrahim, N. A. Effect of Fiber Length on Thermomechanical Properties of Short Carbon Fiber Reinforced Polypropylene Composites. *Mater Des* **2009**, *30* (2), 260–263. https://doi.org/10.1016/J.MATDES.2008.05.005.

(49) Andrzejewski, J.; Mohanty, A. K.; Misra, M. Development of Hybrid Composites Reinforced with Biocarbon/Carbon Fiber System. The Comparative Study for PC, ABS and PC/ABS Based Materials. *Compos B Eng* **2020**, *200*, 108319. https://doi.org/10.1016/j.compositesb.2020.108319.

APPENDIX

Mechanical Raw Data:

Figure A.1: PET – NEAT

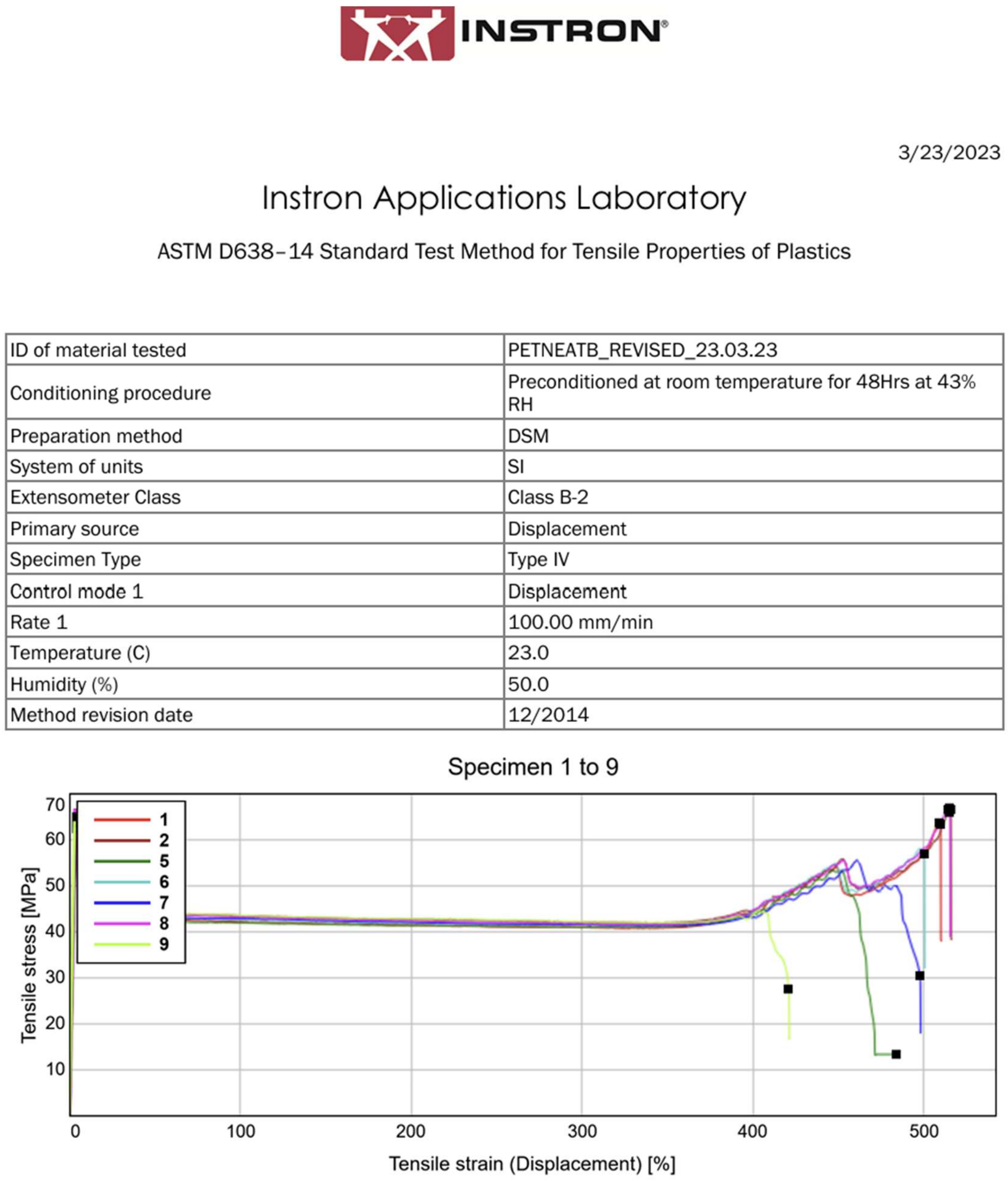

3/23/2023

Instron Applications Laboratory

ASTM D638–14 Standard Test Method for Tensile Properties of Plastics

ID of material tested	PETNEATB_REVISED_23.03.23
Conditioning procedure	Preconditioned at room temperature for 48Hrs at 43% RH
Preparation method	DSM
System of units	SI
Extensometer Class	Class B-2
Primary source	Displacement
Specimen Type	Type IV
Control mode 1	Displacement
Rate 1	100.00 mm/min
Temperature (C)	23.0
Humidity (%)	50.0
Method revision date	12/2014

Specimen 1 to 9

Figure A.1:(cont'd)

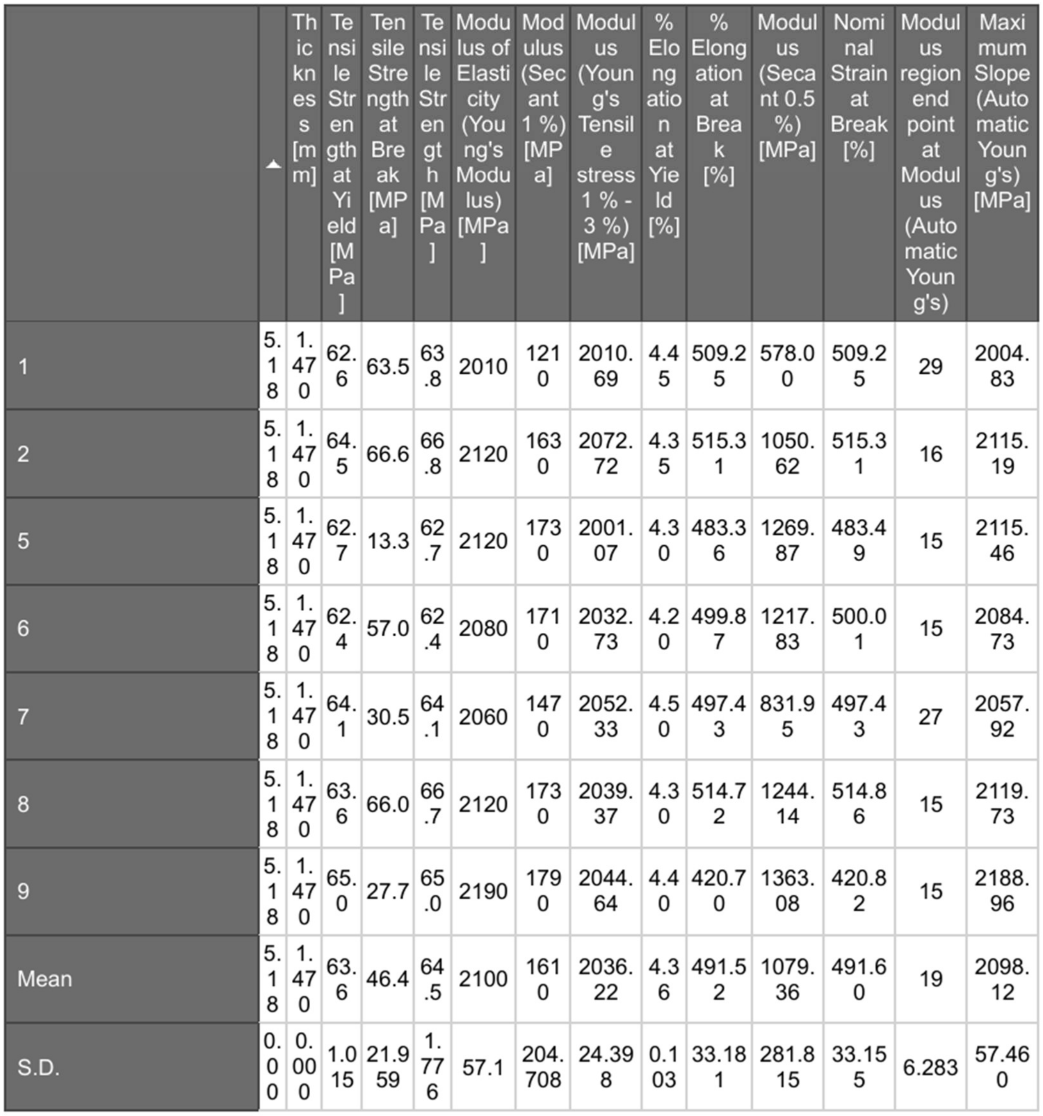

	▲	Thickness [mm]	Tensile Strength at Yield [MPa]	Tensile Strength at Break [MPa]	Tensile Strength [MPa]	Modulus of Elasticity (Young's Modulus) [MPa]	Modulus (Secant 1 %) [MPa]	Modulus (Young's Tensile stress 1 % - 3 %) [MPa]	% Elongation at Yield [%]	% Elongation at Break [%]	Modulus (Secant 0.5 %) [MPa]	Nominal Strain at Break [%]	Modulus region end point at Modulus (Automatic Young's)	Maximum Slope (Automatic Young's) [MPa]
1	5.18	1.470	62.6	63.5	63.8	2010	1210	2010.69	4.45	509.25	578.00	509.25	29	2004.83
2	5.18	1.470	64.5	66.6	66.8	2120	1630	2072.72	4.35	515.31	1050.62	515.31	16	2115.19
5	5.18	1.470	62.7	13.3	62.7	2120	1730	2001.07	4.30	483.36	1269.87	483.49	15	2115.46
6	5.18	1.470	62.4	57.0	62.4	2080	1710	2032.73	4.20	499.87	1217.83	500.01	15	2084.73
7	5.18	1.470	64.1	30.5	64.1	2060	1470	2052.33	4.50	497.43	831.95	497.43	27	2057.92
8	5.18	1.470	63.6	66.0	66.7	2120	1730	2039.37	4.30	514.72	1244.14	514.86	15	2119.73
9	5.18	1.470	65.0	27.7	65.0	2190	1790	2044.64	4.40	420.70	1363.08	420.82	15	2188.96
Mean	5.18	1.470	63.6	46.4	64.5	2100	1610	2036.22	4.36	491.52	1079.36	491.60	19	2098.12
S.D.	0.000	0.000	1.015	21.959	1.776	57.1	204.708	24.398	0.103	33.181	281.815	33.155	6.283	57.460

Figure A.2: PET Thermoform

Instron Applications Laboratory

ASTM D638–14 Standard Test Method for Tensile Properties of Plastics

ID of material tested	PET-Th-3.27.23
Conditioning procedure	
Preparation method	DSM
System of units	SI
Extensometer Class	Class B-2
Primary source	Displacement
Specimen Type	Type IV
Control mode 1	Displacement
Rate 1	100.00 mm/min
Temperature (C)	23.0
Humidity (%)	50.0
Method revision date	12/2014

Specimen 1 to 7

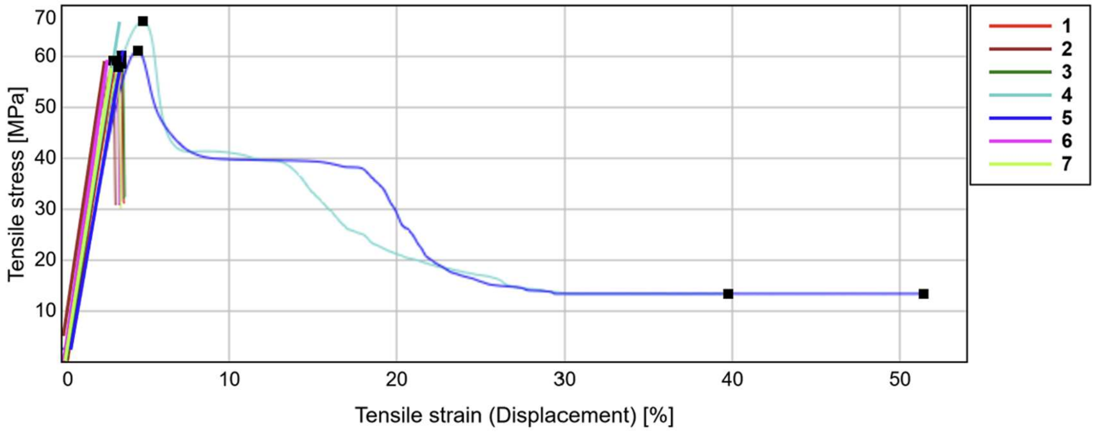

Figure A.2: (cont'd)

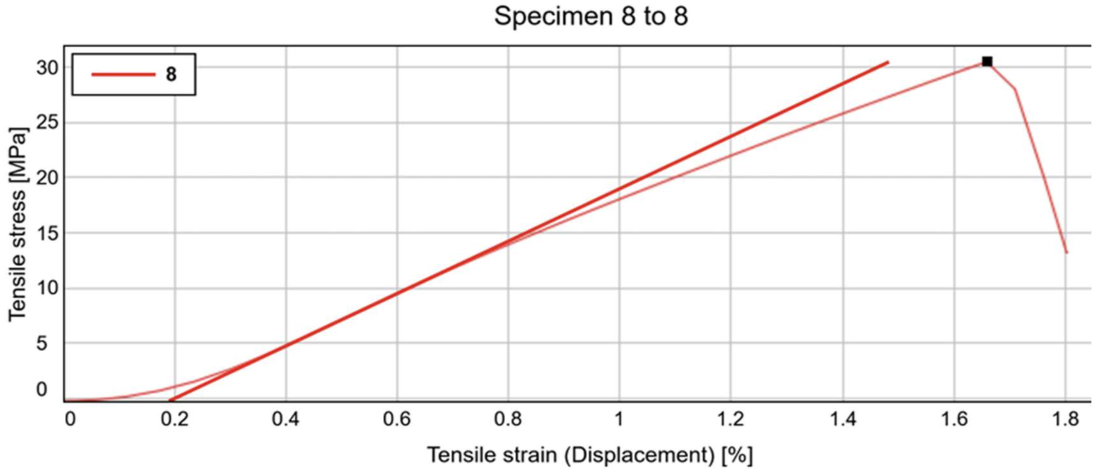

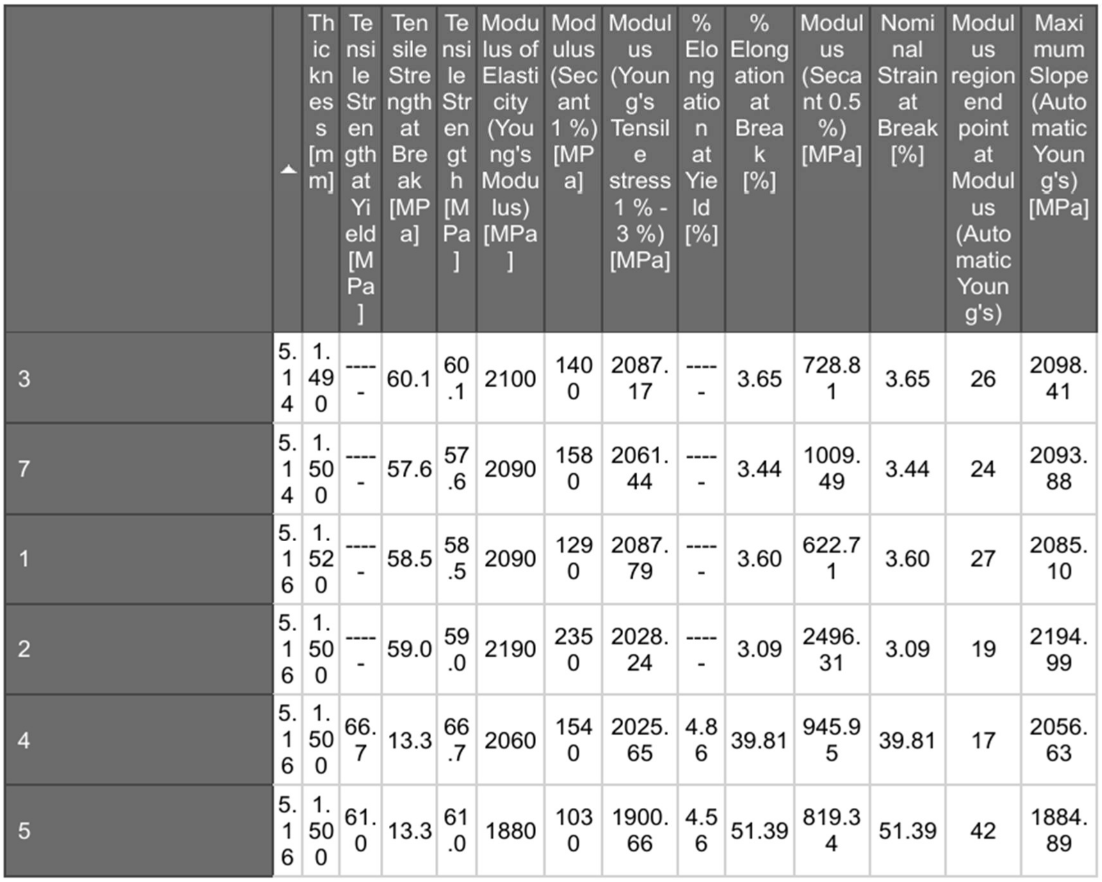

	▲	Thickness [mm]	Tensile Strength at Yield [MPa]	Tensile Strength at Break [MPa]	Tensile Strength [MPa]	Modulus of Elasticity (Young's Modulus) [MPa]	Modulus (Secant 1 %) [MPa]	Modulus (Young's Tensile stress 1 % - 3 %) [MPa]	% Elongation at Yield [%]	% Elongation at Break [%]	Modulus (Secant 0.5 %) [MPa]	Nominal Strain at Break [%]	Modulus region end point at Modulus (Automatic Young's)	Maximum Slope (Automatic Young's) [MPa]
3	5.14	1.490	-----	60.1	60.1	2100	1400	2087.17	-----	3.65	728.81	3.65	26	2098.41
7	5.14	1.500	-----	57.6	57.6	2090	1580	2061.44	-----	3.44	1009.49	3.44	24	2093.88
1	5.16	1.520	-----	58.5	58.5	2090	1290	2087.79	-----	3.60	622.71	3.60	27	2085.10
2	5.16	1.500	-----	59.0	59.0	2190	2350	2028.24	-----	3.09	2496.31	3.09	19	2194.99
4	5.16	1.500	66.7	13.3	66.7	2060	1540	2025.65	4.86	39.81	945.95	39.81	17	2056.63
5	5.16	1.500	61.0	13.3	61.0	1880	1030	1900.66	4.56	51.39	819.34	51.39	42	1884.89

Figure A.2: (cont'd)

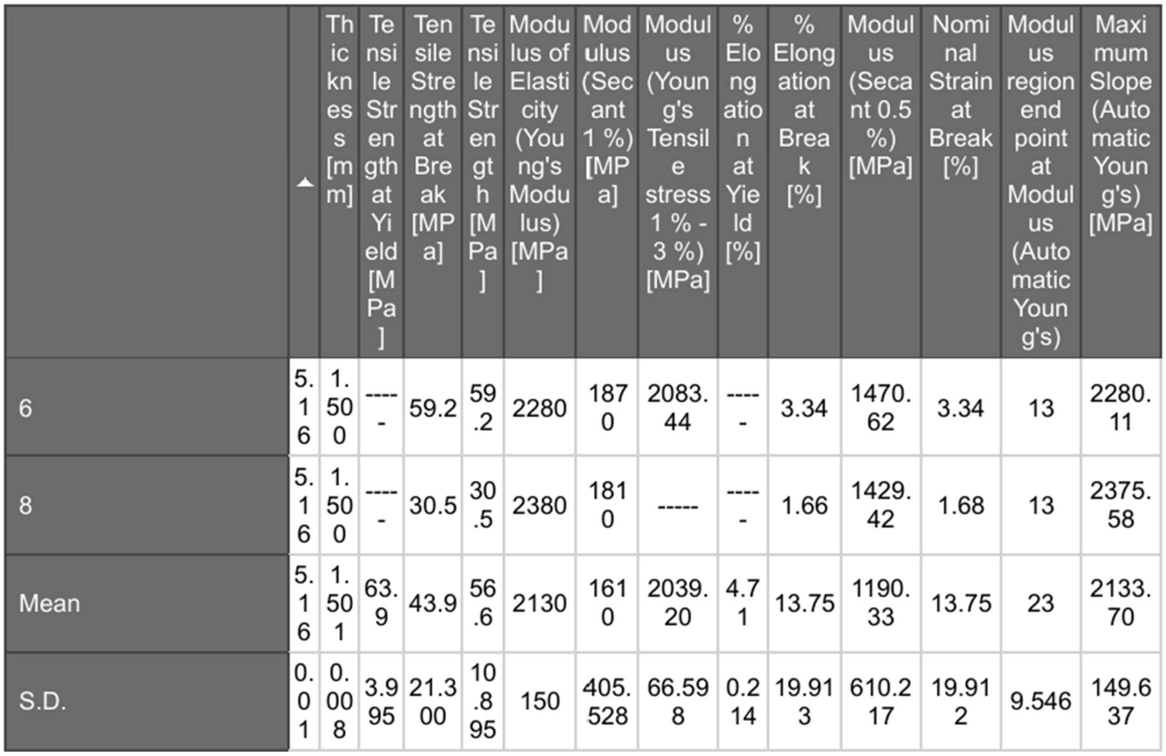

	▲	Thickness [mm]	Tensile Strength at Yield [MPa]	Tensile Strength at Break [MPa]	Tensile Strength [MPa]	Modulus of Elasticity (Young's Modulus) [MPa]	Modulus (Secant 1 %) [MPa]	Modulus (Young's Tensile stress 1 % - 3 %) [MPa]	% Elongation at Yield [%]	% Elongation at Break [%]	Modulus (Secant 0.5 %) [MPa]	Nominal Strain at Break [%]	Modulus region end point at Modulus (Automatic Young's)	Maximum Slope (Automatic Young's) [MPa]
6	5.16	1.500	-----	59.2	59.2	2280	1870	2083.44	-----	3.34	1470.62	3.34	13	2280.11
8	5.16	1.500	-----	30.5	30.5	2380	1810	-----	-----	1.66	1429.42	1.68	13	2375.58
Mean	5.16	1.501	63.9	43.9	56.6	2130	1610	2039.20	4.71	13.75	1190.33	13.75	23	2133.70
S.D.	0.001	0.008	3.995	21.300	10.895	150	405.528	66.598	0.214	19.913	610.217	19.912	9.546	149.637

Figure A.3: PET 90%/10% Thermoform

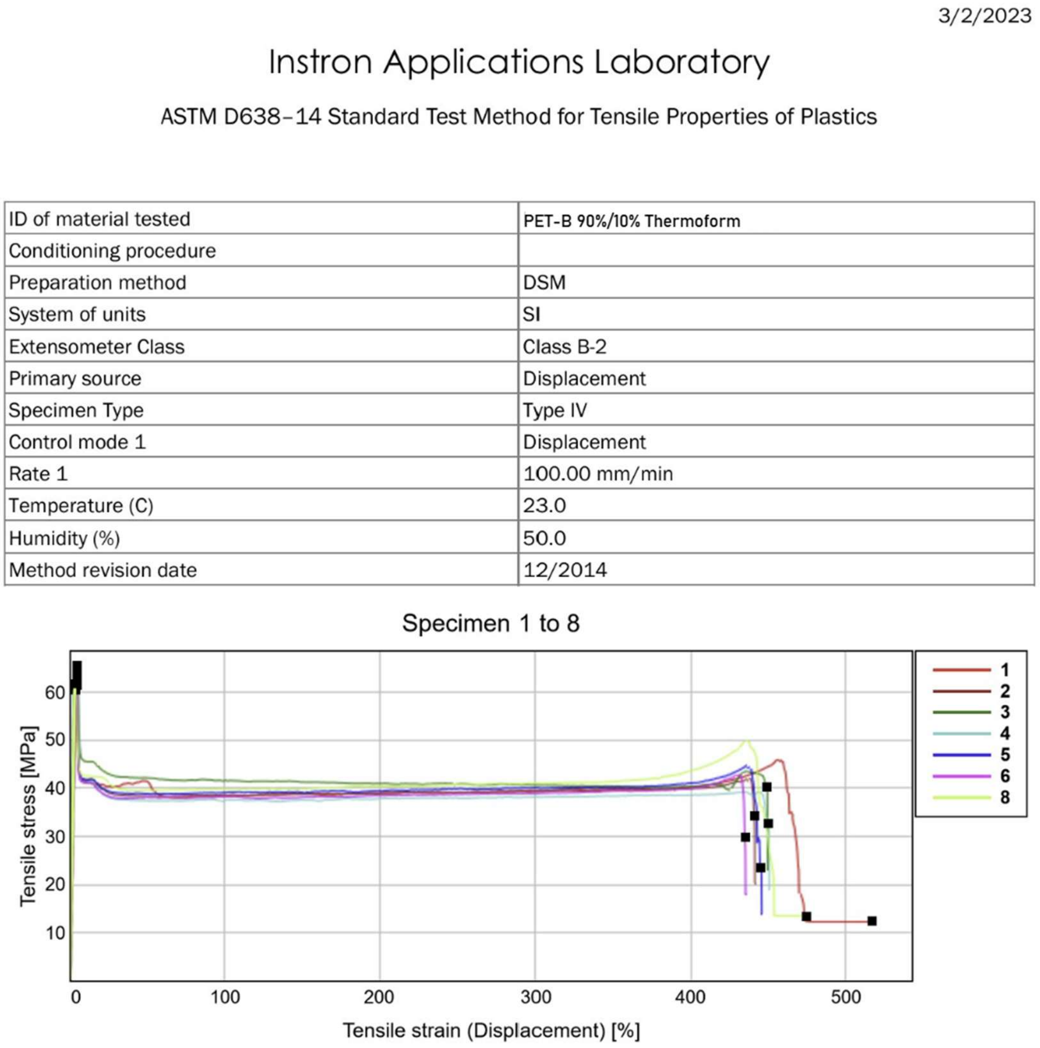

3/2/2023

Instron Applications Laboratory

ASTM D638–14 Standard Test Method for Tensile Properties of Plastics

ID of material tested	PET-B 90%/10% Thermoform
Conditioning procedure	
Preparation method	DSM
System of units	SI
Extensometer Class	Class B-2
Primary source	Displacement
Specimen Type	Type IV
Control mode 1	Displacement
Rate 1	100.00 mm/min
Temperature (C)	23.0
Humidity (%)	50.0
Method revision date	12/2014

Figure A.3: (cont’d)

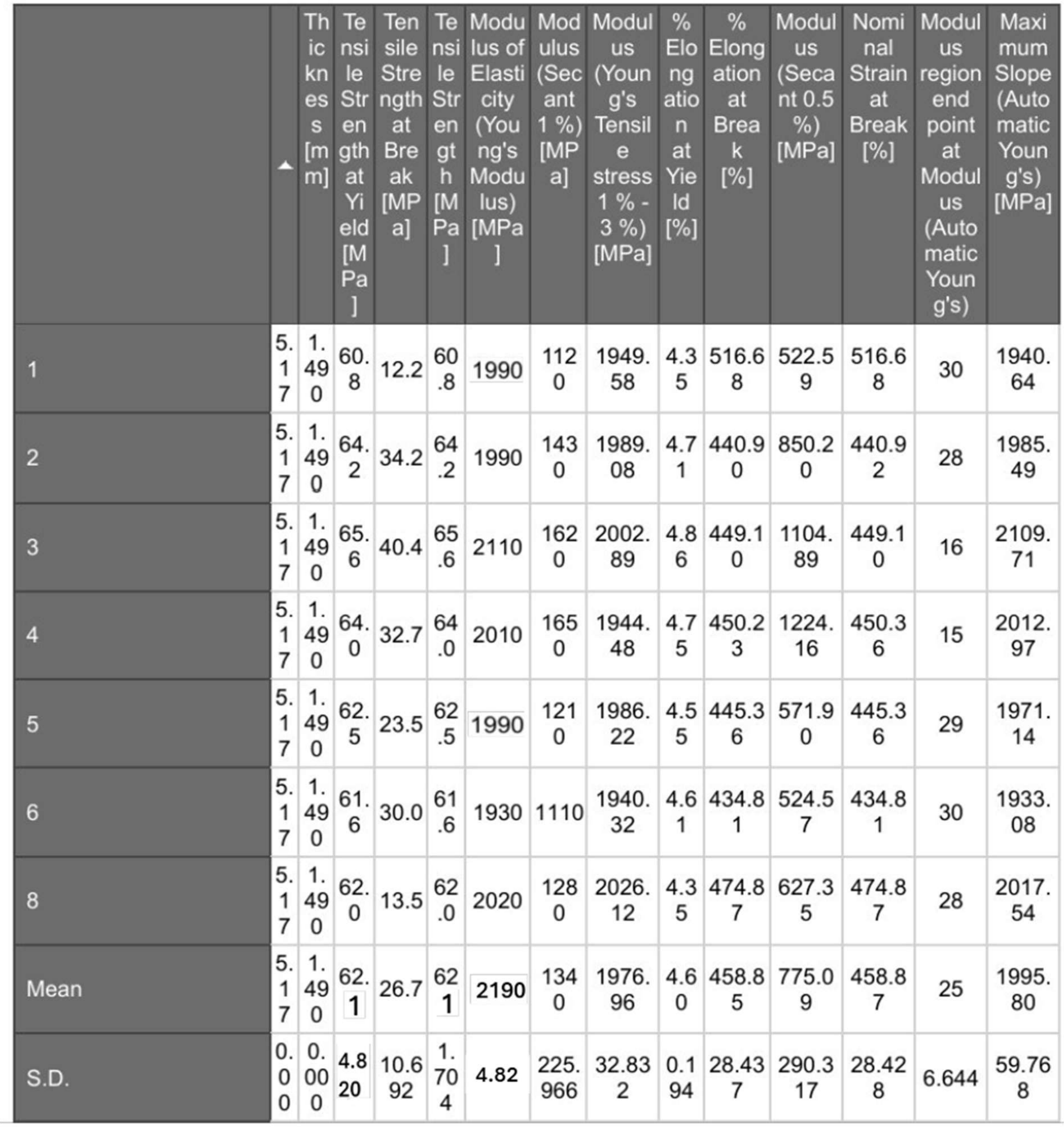

	▲	Thickness [mm]	Tensile Strength at Yield [MPa]	Tensile Strength at Break [MPa]	Tensile Strength [MPa]	Modulus of Elasticity (Young's Modulus) [MPa]	Modulus (Secant 1 %) [MPa]	Modulus (Young's Tensile stress 1 % - 3 %) [MPa]	% Elongation at Yield [%]	% Elongation at Break [%]	Modulus (Secant 0.5 %) [MPa]	Nominal Strain at Break [%]	Modulus region end point at Modulus (Automatic Young's)	Maximum Slope (Automatic Young's) [MPa]
1	5.177	1.490	60.8	12.2	60.8	1990	1120	1949.58	4.35	516.68	522.59	516.68	30	1940.64
2	5.177	1.490	64.2	34.2	64.2	1990	1430	1989.08	4.71	440.90	850.20	440.92	28	1985.49
3	5.177	1.490	65.6	40.4	65.6	2110	1620	2002.89	4.86	449.10	1104.89	449.10	16	2109.71
4	5.177	1.490	64.0	32.7	64.0	2010	1650	1944.48	4.75	450.23	1224.16	450.36	15	2012.97
5	5.177	1.490	62.5	23.5	62.5	1990	1210	1986.22	4.55	445.36	571.90	445.36	29	1971.14
6	5.177	1.490	61.6	30.0	61.6	1930	1110	1940.32	4.61	434.81	524.57	434.81	30	1933.08
8	5.177	1.490	62.0	13.5	62.0	2020	1280	2026.12	4.35	474.87	627.35	474.87	28	2017.54
Mean	5.177	1.490	62.1	26.7	621	2190	1340	1976.96	4.60	458.85	775.09	458.87	25	1995.80
S.D.	0.000	0.000	4.820	10.692	1.704	4.82	225.966	32.832	0.194	28.437	290.317	28.428	6.644	59.768

Figure A.4: PET 80%/20% Thermoform

INSTRON®

2/10/2023

Instron Applications Laboratory

ASTM D638-14 Standard Test Method for Tensile Properties of Plastics

ID of material tested	Neat PET 80 and T PET 20 _02.10.2023_1.5mm
Conditioning procedure	Pre conditioned for 48 Hours at 43%RH
Preparation method	DSM
System of units	SI
Extensometer Class	Class B-2
Primary source	Displacement
Specimen Type	Type IV
Control mode 1	Displacement
Rate 1	100.00 mm/min
Temperature (C)	23.0
Humidity (%)	50.0
Method revision date	12/2014

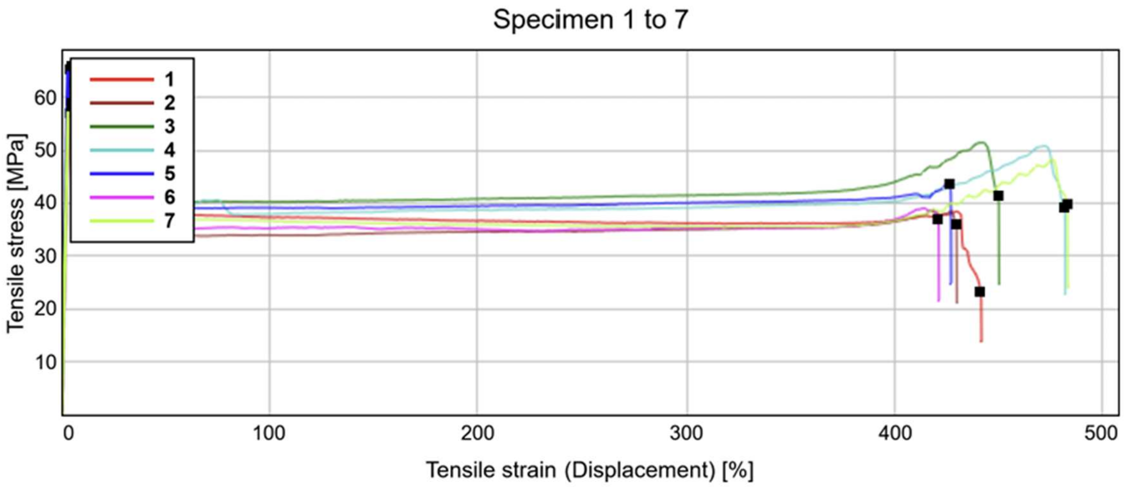

Figure A.4: (cont'd)

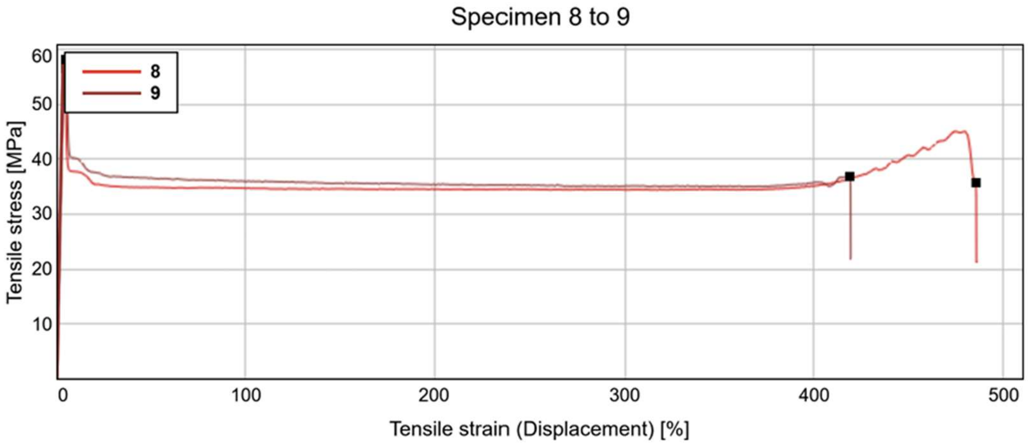

	▲	Thickness [mm]	Tensile Strength at Yield [MPa]	Tensile Strength at Break [MPa]	Tensile Strength [MPa]	Modulus of Elasticity (Young's Modulus) [MPa]	Modulus (Secant 1 %) [MPa]	Modulus (Young's Tensile stress 1 % - 3 %) [MPa]	% Elongation at Yield [%]	% Elongation at Break [%]	Modulus (Secant 0.5 %) [MPa]	Nominal Strain at Break [%]	Modulus region end point at Modulus (Automatic Young's)	Maximum Slope (Automatic Young's) [MPa]
3	5.200	1.500	65.2	41.4	65.2	2210	1690	2055.85	4.45	449.61	1162.21	449.61	16	2207.88
5	5.200	1.500	65.8	43.5	65.8	2210	1830	2011.27	4.76	426.61	1440.86	426.73	14	2210.41
1	5.400	1.600	62.8	23.3	62.8	2120	1750	1893.28	4.86	441.18	1396.17	441.37	14	2118.60
2	5.400	1.600	57.0	36.1	57.0	2010	1680	1804.82	4.35	429.31	1349.15	429.45	14	2010.50
6	5.400	1.600	58.8	37.0	58.8	1930	1500	1822.71	4.65	420.76	1027.38	420.87	16	1932.47
7	5.400	1.600	58.4	40.0	58.4	1960	1610	1817.91	4.55	482.72	1230.71	482.89	14	1963.45

Figure A.4: (cont'd)

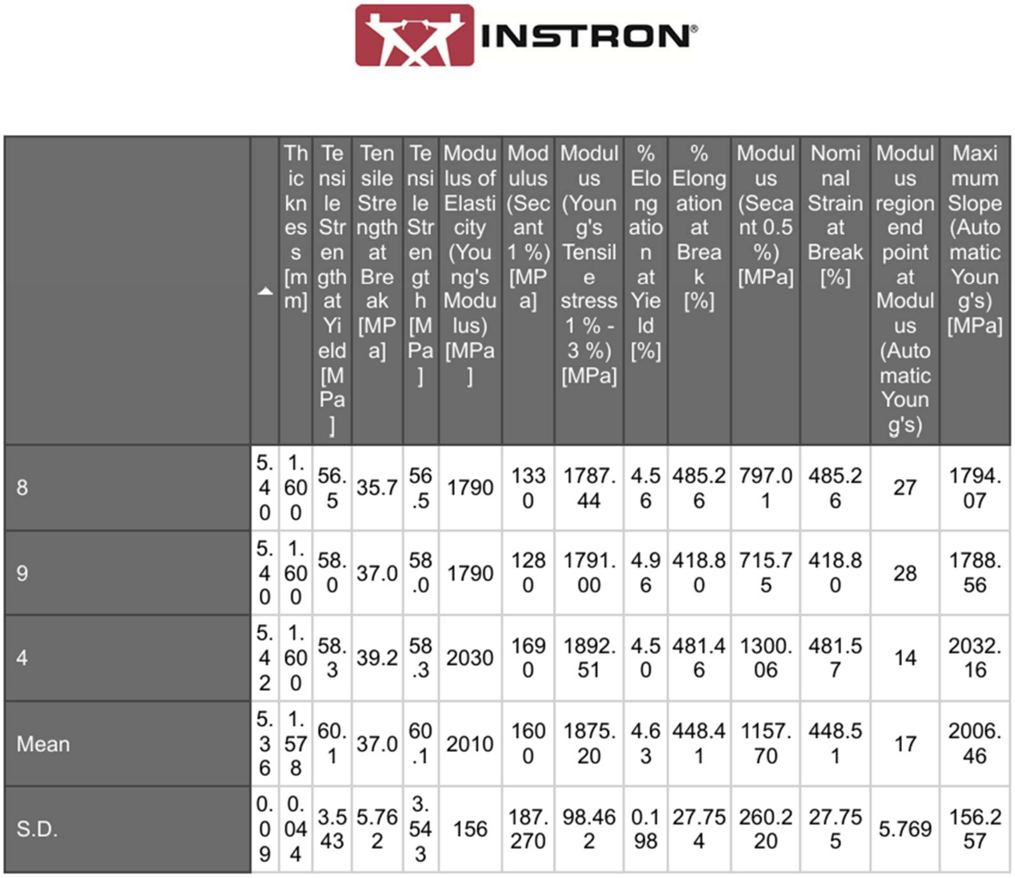

INSTRON

	▲	Thickness [mm]	Tensile Strength at Yield [MPa]	Tensile Strength at Break [MPa]	Tensile Strength [MPa]	Modulus of Elasticity (Young's Modulus) [MPa]	Modulus (Secant 1 %) [MPa]	Modulus (Young's Tensile stress 1 % - 3 %) [MPa]	% Elongation at Yield [%]	% Elongation at Break [%]	Modulus (Secant 0.5 %) [MPa]	Nominal Strain at Break [%]	Modulus region end point at Modulus (Automatic Young's)	Maximum Slope (Automatic Young's) [MPa]
8	5.40	1.600	56.5	35.7	56.5	1790	1330	1787.44	4.56	485.26	797.01	485.26	27	1794.07
9	5.40	1.600	58.0	37.0	58.0	1790	1280	1791.00	4.96	418.80	715.75	418.80	28	1788.56
4	5.42	1.600	58.3	39.2	58.3	2030	1690	1892.51	4.50	481.46	1300.06	481.57	14	2032.16
Mean	5.336	1.578	60.1	37.0	60.1	2010	1600	1875.20	4.63	448.41	1157.70	448.51	17	2006.46
S.D.	0.09	0.044	3.543	5.762	3.543	156	187.270	98.462	0.198	27.754	260.220	27.755	5.769	156.257

Figure A.5: PET 80%/20% Thermoform + 0.5 Phr JCR(B*)

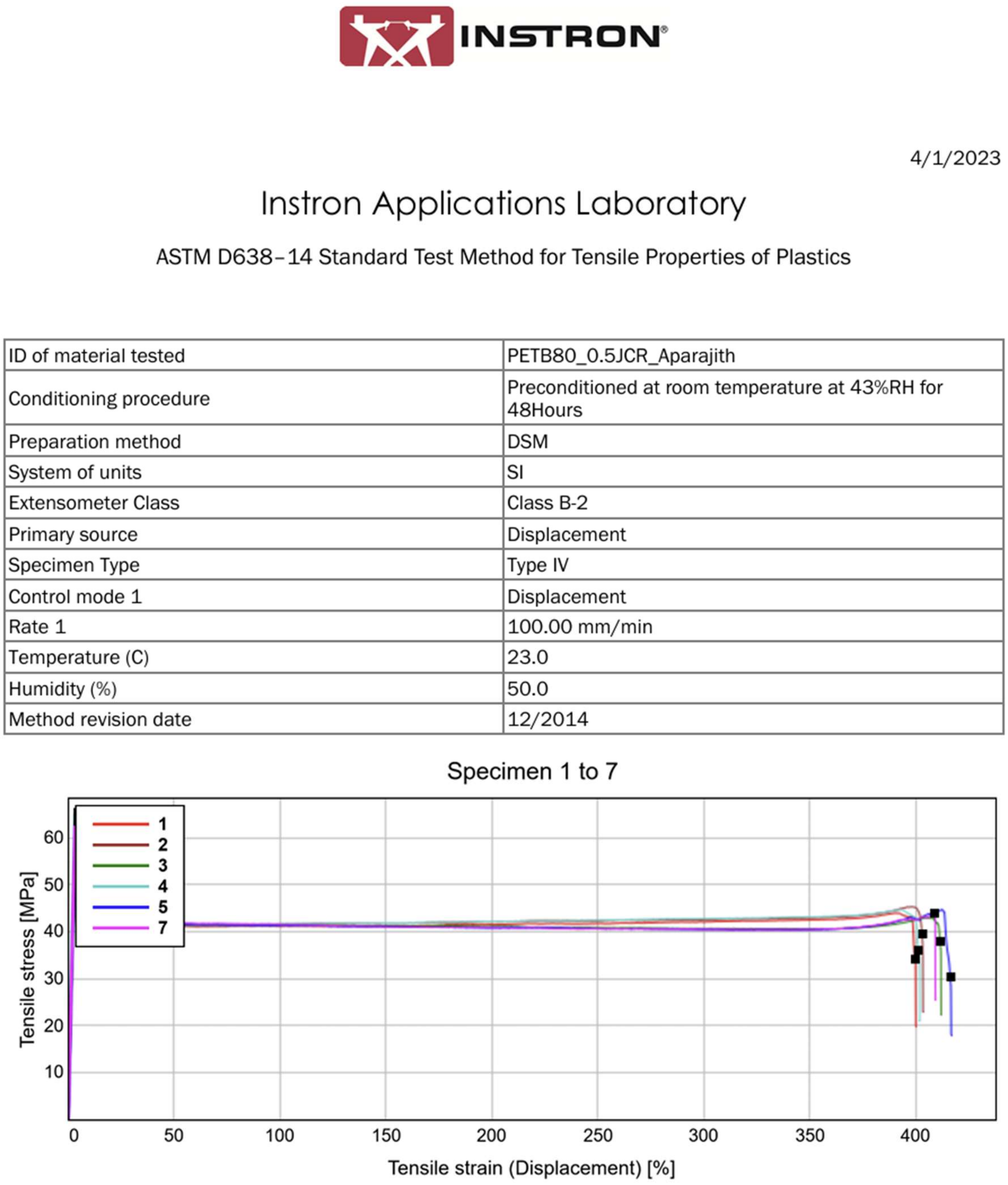

INSTRON

4/1/2023

Instron Applications Laboratory

ASTM D638-14 Standard Test Method for Tensile Properties of Plastics

ID of material tested	PETB80_0.5JCR_Aparajith
Conditioning procedure	Preconditioned at room temperature at 43%RH for 48Hours
Preparation method	DSM
System of units	SI
Extensometer Class	Class B-2
Primary source	Displacement
Specimen Type	Type IV
Control mode 1	Displacement
Rate 1	100.00 mm/min
Temperature (C)	23.0
Humidity (%)	50.0
Method revision date	12/2014

Specimen 1 to 7

Figure A.5: (cont'd)

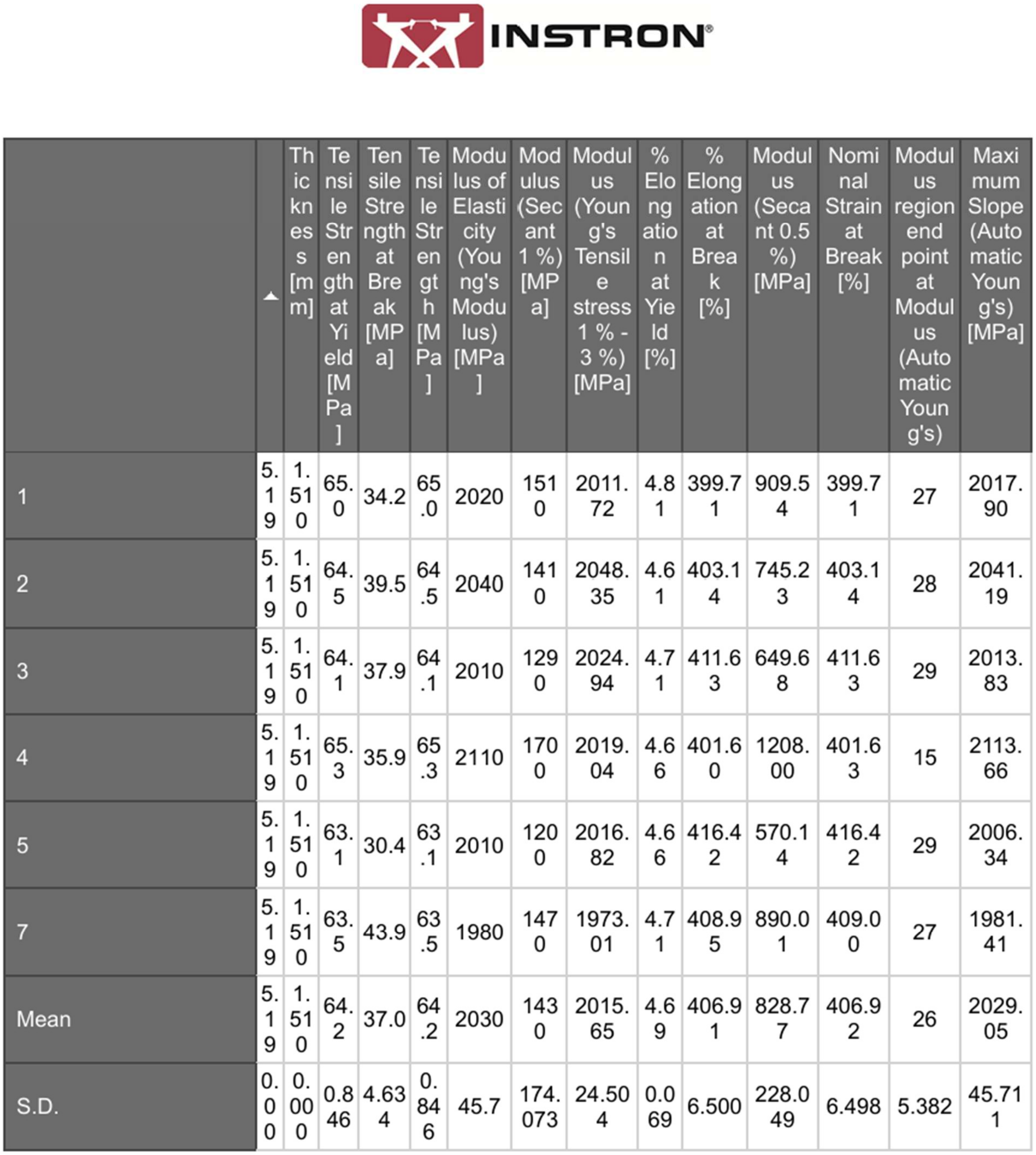

	▲	Thickness [mm]	Tensile Strength at Yield [MPa]	Tensile Strength at Break [MPa]	Tensile Strength [MPa]	Modulus of Elasticity (Young's Modulus) [MPa]	Modulus (Secant 1 %) [MPa]	Modulus (Young's Tensile stress 1 % - 3 %) [MPa]	% Elongation at Yield [%]	% Elongation at Break [%]	Modulus (Secant 0.5 %) [MPa]	Nominal Strain at Break [%]	Modulus region end point at Modulus (Automatic Young's)	Maximum Slope (Automatic Young's) [MPa]
1	5.19	1.510	65.0	34.2	65.0	2020	1510	2011.72	4.81	399.71	909.54	399.71	27	2017.90
2	5.19	1.510	64.5	39.5	64.5	2040	1410	2048.35	4.61	403.14	745.23	403.14	28	2041.19
3	5.19	1.510	64.1	37.9	64.1	2010	1290	2024.94	4.71	411.63	649.68	411.63	29	2013.83
4	5.19	1.510	65.3	35.9	65.3	2110	1700	2019.04	4.66	401.60	1208.00	401.63	15	2113.66
5	5.19	1.510	63.1	30.4	63.1	2010	1200	2016.82	4.66	416.42	570.14	416.42	29	2006.34
7	5.19	1.510	63.5	43.9	63.5	1980	1470	1973.01	4.71	408.95	890.01	409.00	27	1981.41
Mean	5.19	1.510	64.2	37.0	64.2	2030	1430	2015.65	4.69	406.91	828.77	406.92	26	2029.05
S.D.	0.000	0.000	0.846	4.634	0.846	45.7	174.073	24.504	0.069	6.500	228.049	6.498	5.382	45.711

Figure A.6: PET 80%/20% Thermoform + 1 Phr JCR

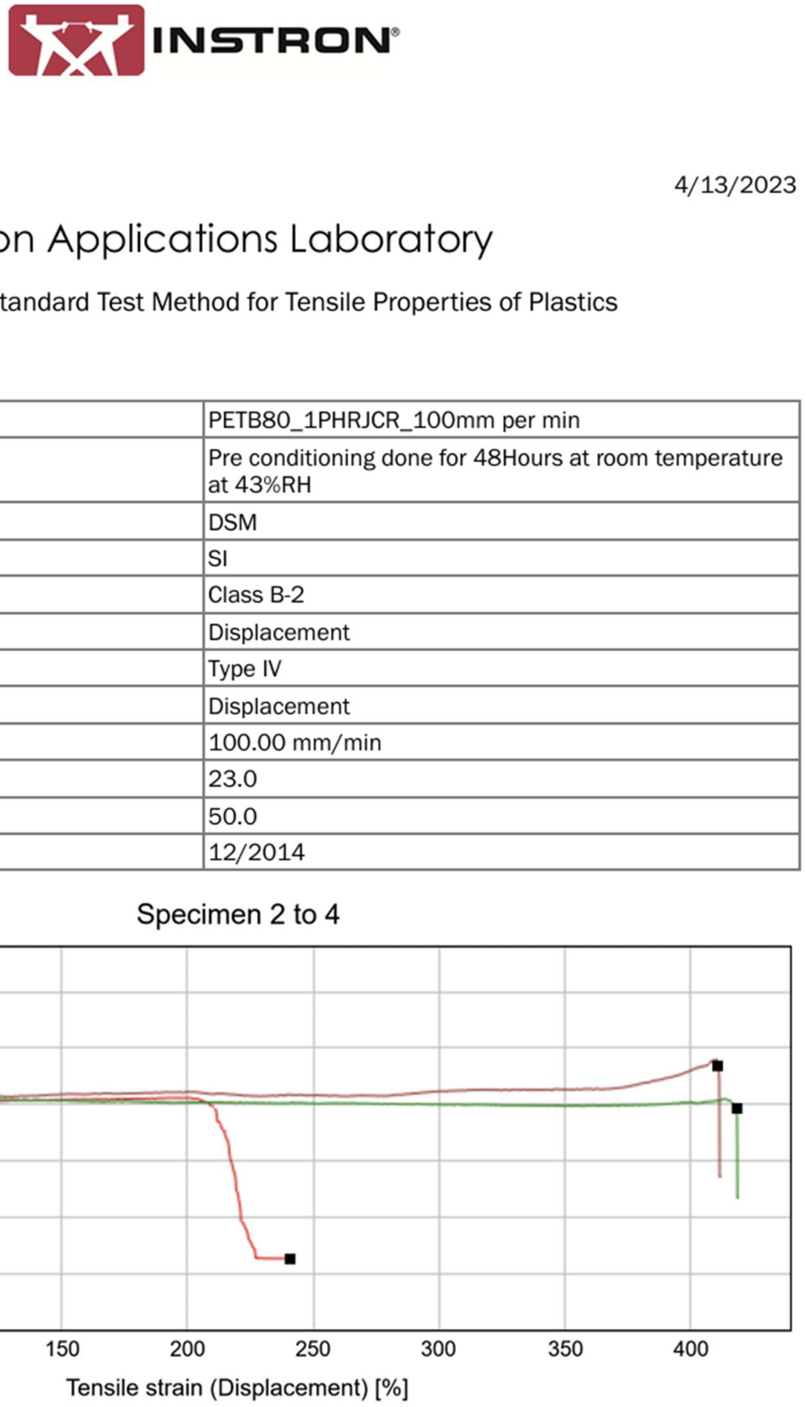

4/13/2023

Instron Applications Laboratory

ASTM D638–14 Standard Test Method for Tensile Properties of Plastics

ID of material tested	PETB80_1PHRJCR_100mm per min
Conditioning procedure	Pre conditioning done for 48Hours at room temperature at 43%RH
Preparation method	DSM
System of units	SI
Extensometer Class	Class B-2
Primary source	Displacement
Specimen Type	Type IV
Control mode 1	Displacement
Rate 1	100.00 mm/min
Temperature (C)	23.0
Humidity (%)	50.0
Method revision date	12/2014

Specimen 2 to 4

Figure A.6: (cont'd)

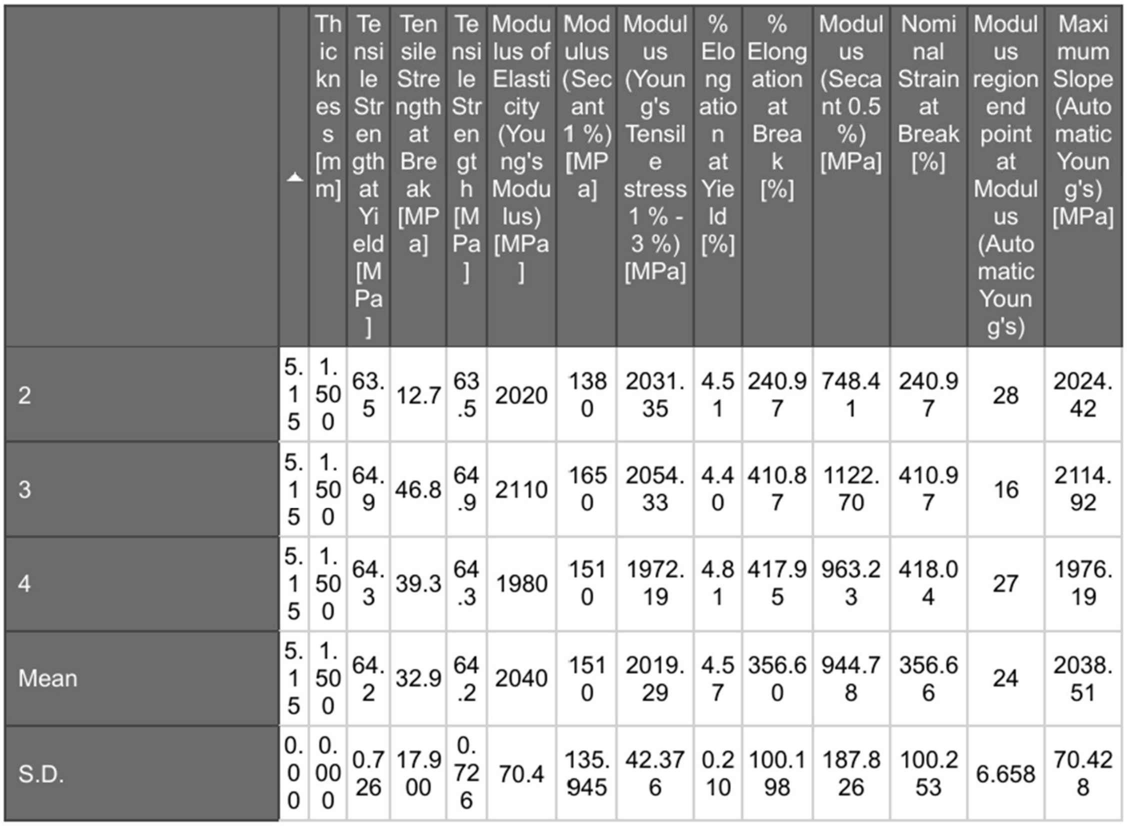

	▲	Thickness [mm]	Tensile Strength at Yield [MPa]	Tensile Strength at Break [MPa]	Tensile Strength [MPa]	Modulus of Elasticity (Young's Modulus) [MPa]	Modulus (Secant 1 %) [MPa]	Modulus (Young's Tensile stress 1 % - 3 %) [MPa]	% Elongation at Yield [%]	% Elongation at Break [%]	Modulus (Secant 0.5 %) [MPa]	Nominal Strain at Break [%]	Modulus region end point at Modulus (Automatic Young's)	Maximum Slope (Automatic Young's) [MPa]
2	5.15	1.500	63.5	12.7	63.5	2020	1380	2031.35	4.51	240.97	748.41	240.97	28	2024.42
3	5.15	1.500	64.9	46.8	64.9	2110	1650	2054.33	4.40	410.87	1122.70	410.97	16	2114.92
4	5.15	1.500	64.3	39.3	64.3	1980	1510	1972.19	4.81	417.95	963.23	418.04	27	1976.19
Mean	5.15	1.500	64.2	32.9	64.2	2040	1510	2019.29	4.57	356.60	944.78	356.66	24	2038.51
S.D.	0.000	0.000	0.726	17.900	0.726	70.4	135.945	42.376	0.210	100.198	187.826	100.253	6.658	70.428

Figure A.7: B*- 0.5in CF-1%

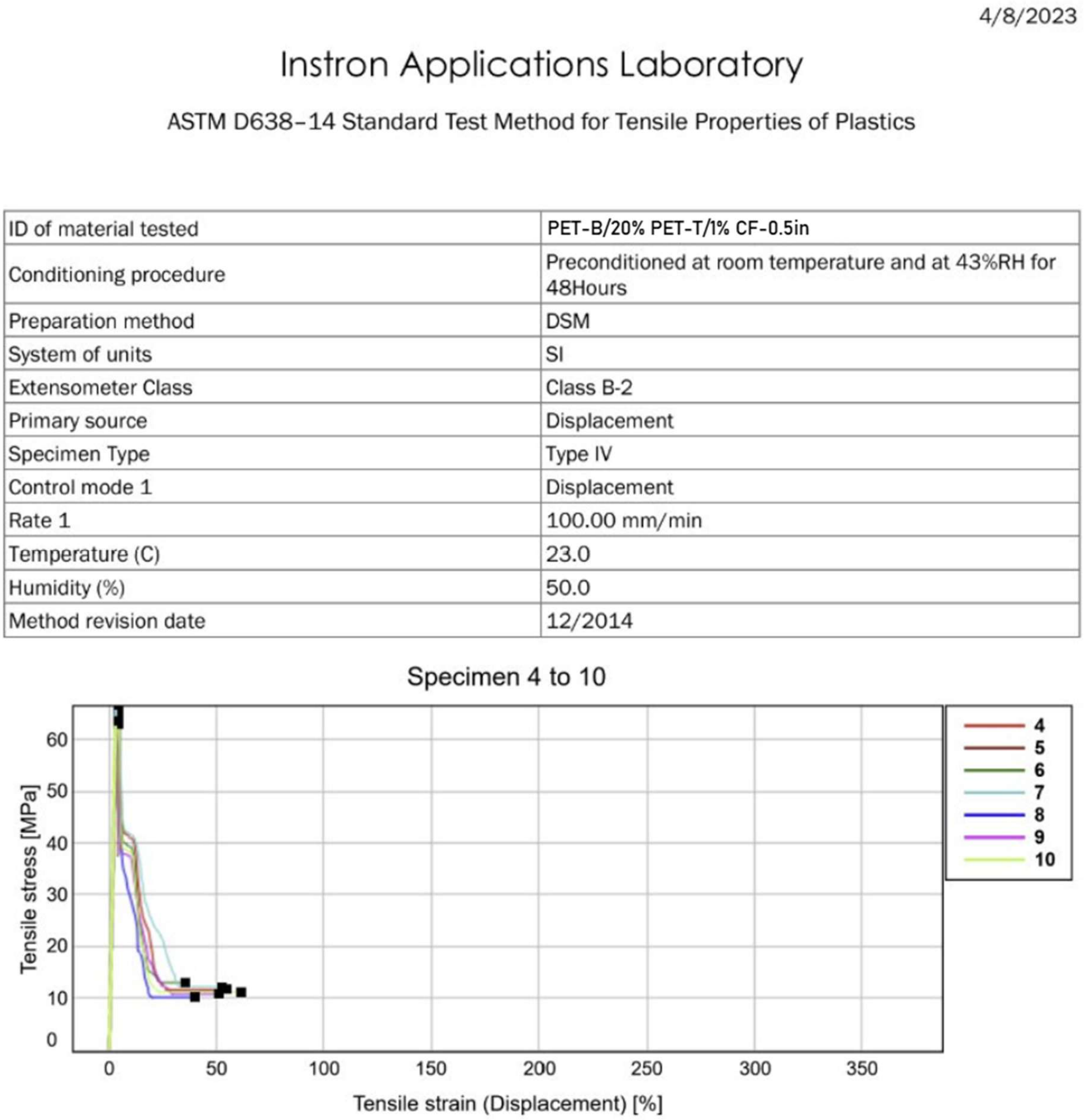

4/8/2023

Instron Applications Laboratory

ASTM D638–14 Standard Test Method for Tensile Properties of Plastics

ID of material tested	PET-B/20% PET-T/1% CF-0.5in
Conditioning procedure	Preconditioned at room temperature and at 43%RH for 48Hours
Preparation method	DSM
System of units	SI
Extensometer Class	Class B-2
Primary source	Displacement
Specimen Type	Type IV
Control mode 1	Displacement
Rate 1	100.00 mm/min
Temperature (C)	23.0
Humidity (%)	50.0
Method revision date	12/2014

Specimen 4 to 10

Figure A.7: (cont'd)

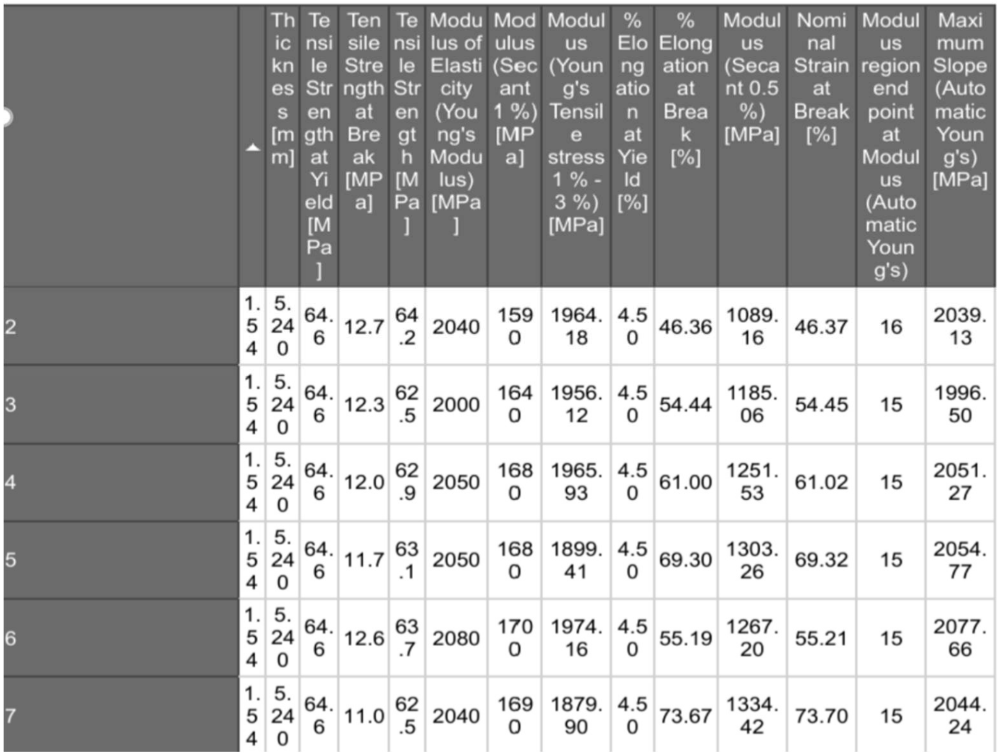

	▲	Thickness [mm]	Tensile Strength at Yield [MPa]	Tensile Strength at Break [MPa]	Tensile Strength [MPa]	Modulus of Elasticity (Young's Modulus) [MPa]	Modulus (Secant 1 %) [MPa]	Modulus (Young's Tensile stress 1 % - 3 %) [MPa]	% Elongation at Yield [%]	% Elongation at Break [%]	Modulus (Secant 0.5 %) [MPa]	Nominal Strain at Break [%]	Modulus region end point at Modulus (Automatic Young's)	Maximum Slope (Automatic Young's) [MPa]
2	1.54	5.240	64.6	12.7	64.2	2040	1590	1964.18	4.50	46.36	1089.16	46.37	16	2039.13
3	1.54	5.240	64.6	12.3	62.5	2000	1640	1956.12	4.50	54.44	1185.06	54.45	15	1996.50
4	1.54	5.240	64.6	12.0	62.9	2050	1680	1965.93	4.50	61.00	1251.53	61.02	15	2051.27
5	1.54	5.240	64.6	11.7	63.1	2050	1680	1899.41	4.50	69.30	1303.26	69.32	15	2054.77
6	1.54	5.240	64.6	12.6	63.7	2080	1700	1974.16	4.50	55.19	1267.20	55.21	15	2077.66
7	1.54	5.240	64.6	11.0	62.5	2040	1690	1879.90	4.50	73.67	1334.42	73.70	15	2044.24

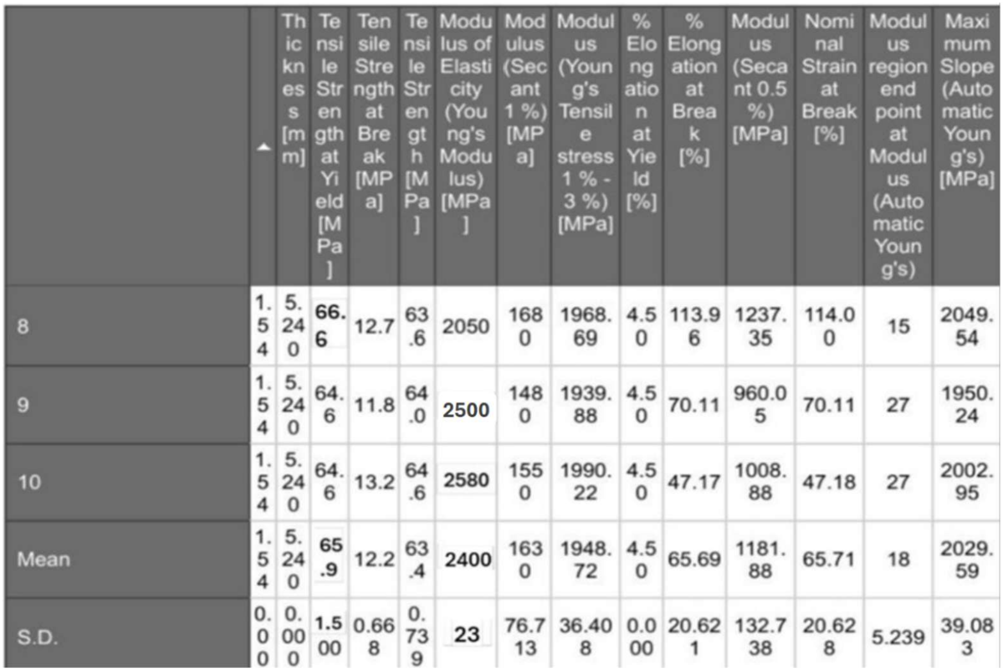

	▲	Thickness [mm]	Tensile Strength at Yield [MPa]	Tensile Strength at Break [MPa]	Tensile Strength [MPa]	Modulus of Elasticity (Young's Modulus) [MPa]	Modulus (Secant 1 %) [MPa]	Modulus (Young's Tensile stress 1 % - 3 %) [MPa]	% Elongation at Yield [%]	% Elongation at Break [%]	Modulus (Secant 0.5 %) [MPa]	Nominal Strain at Break [%]	Modulus region end point at Modulus (Automatic Young's)	Maximum Slope (Automatic Young's) [MPa]
8	1.54	5.240	66.6	12.7	63.6	2050	1680	1968.69	4.50	113.96	1237.35	114.00	15	2049.54
9	1.54	5.240	64.6	11.8	64.0	2500	1480	1939.88	4.50	70.11	960.05	70.11	27	1950.24
10	1.54	5.240	64.6	13.2	64.6	2580	1550	1990.22	4.50	47.17	1008.88	47.18	27	2002.95
Mean	1.54	5.240	65.9	12.2	63.4	2400	1630	1948.72	4.50	65.69	1181.88	65.71	18	2029.59
S.D.	0.000	0.000	1.500	0.668	0.739	23	76.713	36.408	0.000	20.621	132.738	20.628	5.239	39.083

Figure A.8: B*- 1in CF-1%

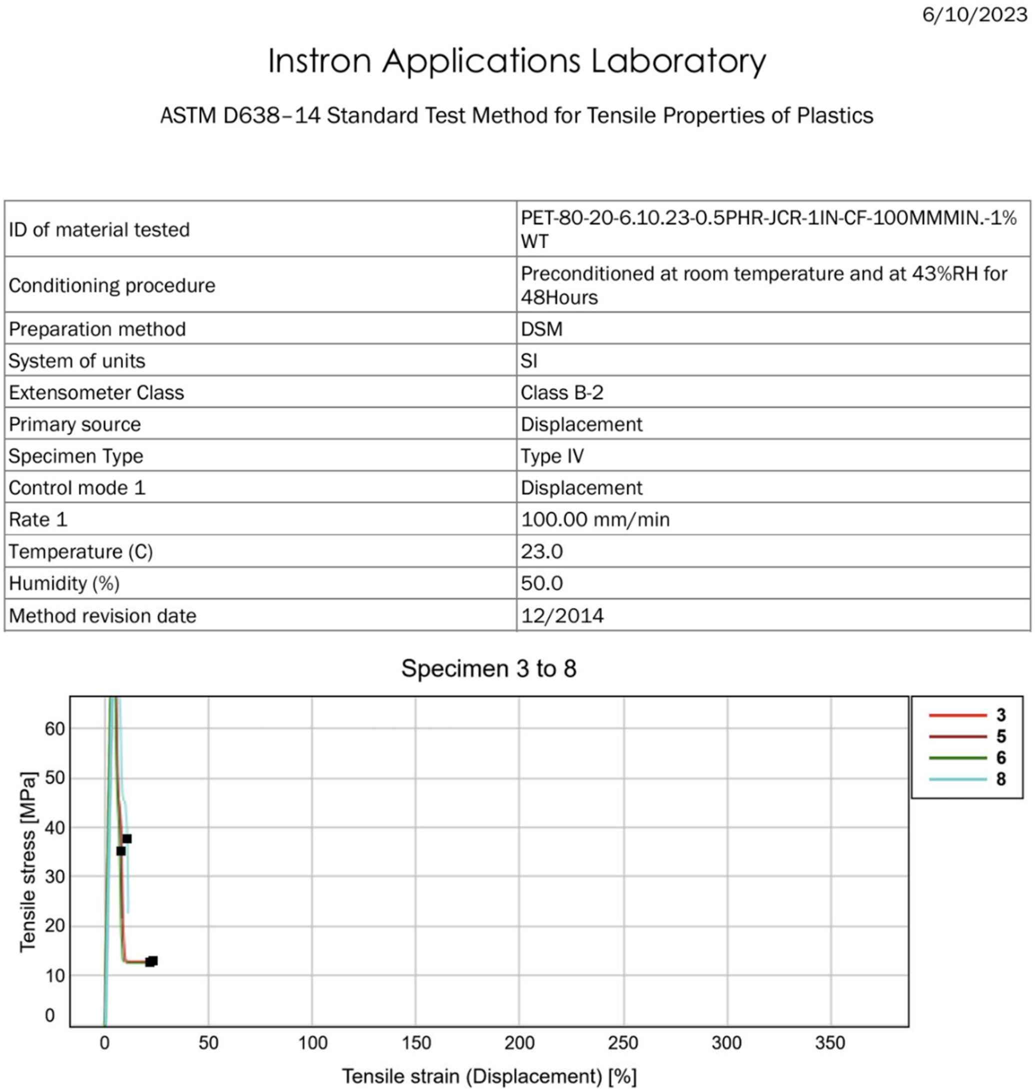

6/10/2023

Instron Applications Laboratory

ASTM D638–14 Standard Test Method for Tensile Properties of Plastics

ID of material tested	PET-80-20-6.10.23-0.5PHR-JCR-1IN-CF-100MMMIN.-1% WT
Conditioning procedure	Preconditioned at room temperature and at 43%RH for 48Hours
Preparation method	DSM
System of units	SI
Extensometer Class	Class B-2
Primary source	Displacement
Specimen Type	Type IV
Control mode 1	Displacement
Rate 1	100.00 mm/min
Temperature (C)	23.0
Humidity (%)	50.0
Method revision date	12/2014

Specimen 3 to 8

Figure A.8: (cont'd)

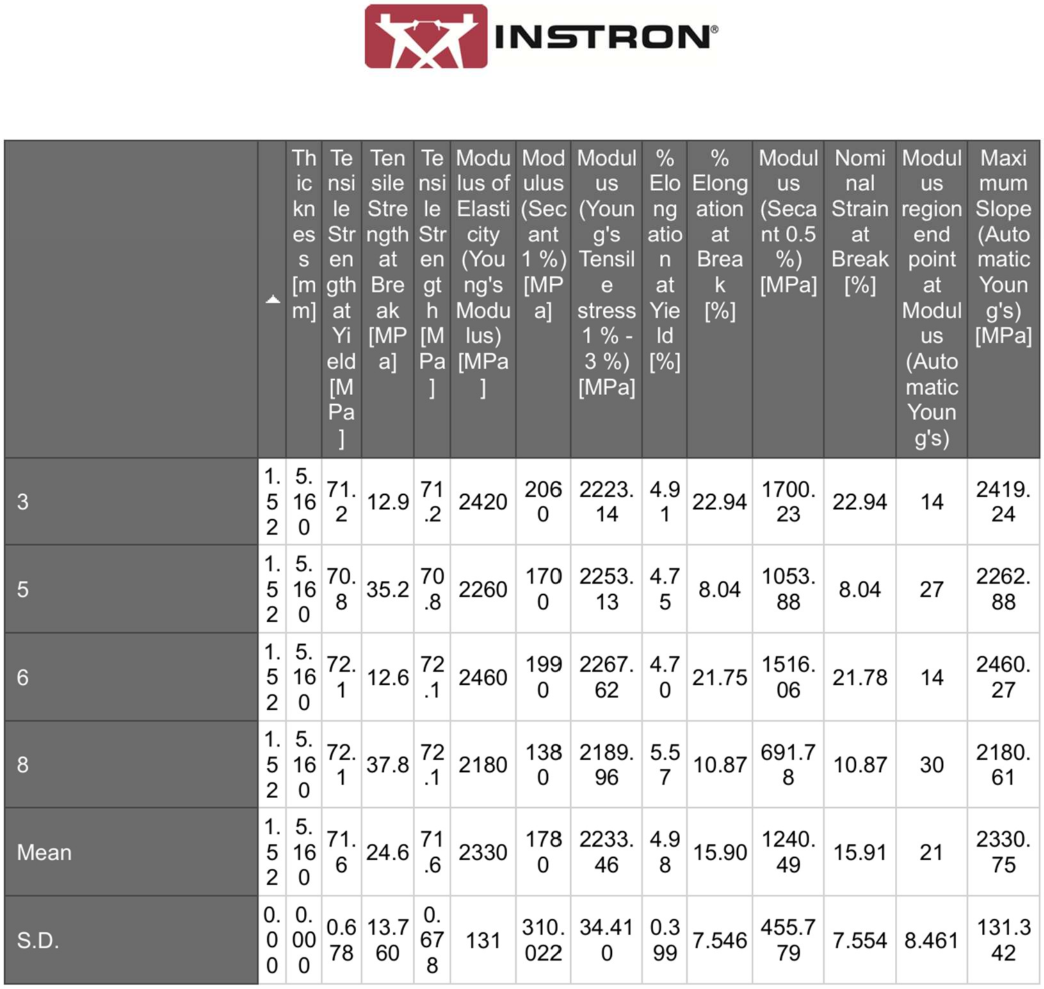

	▲	Thickness [mm]	Tensile Strength at Yield [MPa]	Tensile Strength at Break [MPa]	Tensile Strength [MPa]	Modulus of Elasticity (Young's Modulus) [MPa]	Modulus (Secant 1 %) [MPa]	Modulus (Young's Tensile stress 1 % - 3 %) [MPa]	% Elongation at Yield [%]	% Elongation at Break [%]	Modulus (Secant 0.5 %) [MPa]	Nominal Strain at Break [%]	Modulus region end point at Modulus (Automatic Young's)	Maximum Slope (Automatic Young's) [MPa]
3	1.52	5.160	71.2	12.9	71.2	2420	2060	2223.14	4.91	22.94	1700.23	22.94	14	2419.24
5	1.52	5.160	70.8	35.2	70.8	2260	1700	2253.13	4.75	8.04	1053.88	8.04	27	2262.88
6	1.52	5.160	72.1	12.6	72.1	2460	1990	2267.62	4.70	21.75	1516.06	21.78	14	2460.27
8	1.52	5.160	72.1	37.8	72.1	2180	1380	2189.96	5.57	10.87	691.78	10.87	30	2180.61
Mean	1.52	5.160	71.6	24.6	71.6	2330	1780	2233.46	4.98	15.90	1240.49	15.91	21	2330.75
S.D.	0.000	0.000	0.678	13.760	0.678	131	310.022	34.410	0.399	7.546	455.779	7.554	8.461	131.342

Figure A.9: B*- 2in CF-1%

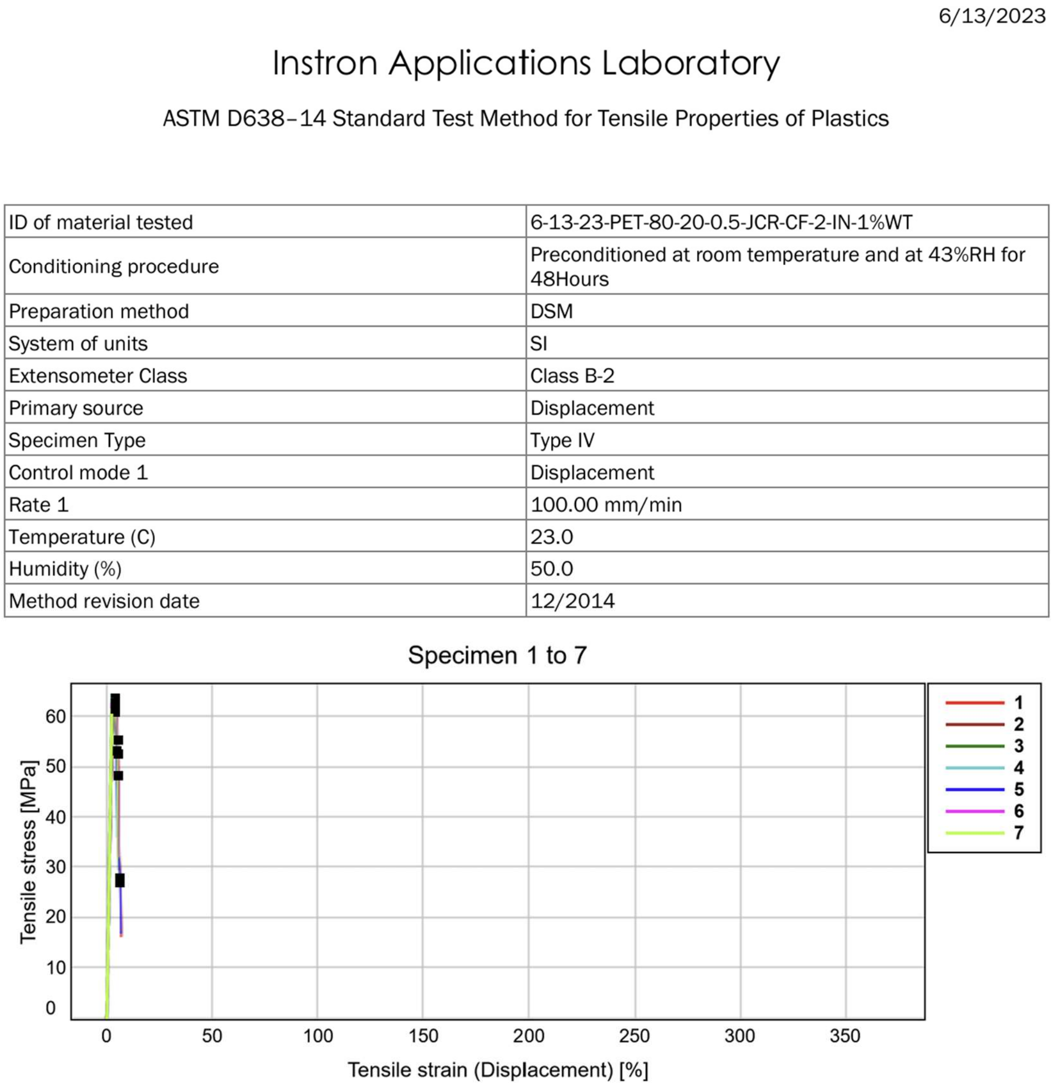

6/13/2023

Instron Applications Laboratory

ASTM D638–14 Standard Test Method for Tensile Properties of Plastics

ID of material tested	6-13-23-PET-80-20-0.5-JCR-CF-2-IN-1%WT
Conditioning procedure	Preconditioned at room temperature and at 43%RH for 48Hours
Preparation method	DSM
System of units	SI
Extensometer Class	Class B-2
Primary source	Displacement
Specimen Type	Type IV
Control mode 1	Displacement
Rate 1	100.00 mm/min
Temperature (C)	23.0
Humidity (%)	50.0
Method revision date	12/2014

Specimen 1 to 7

Figure A.9: (cont'd)

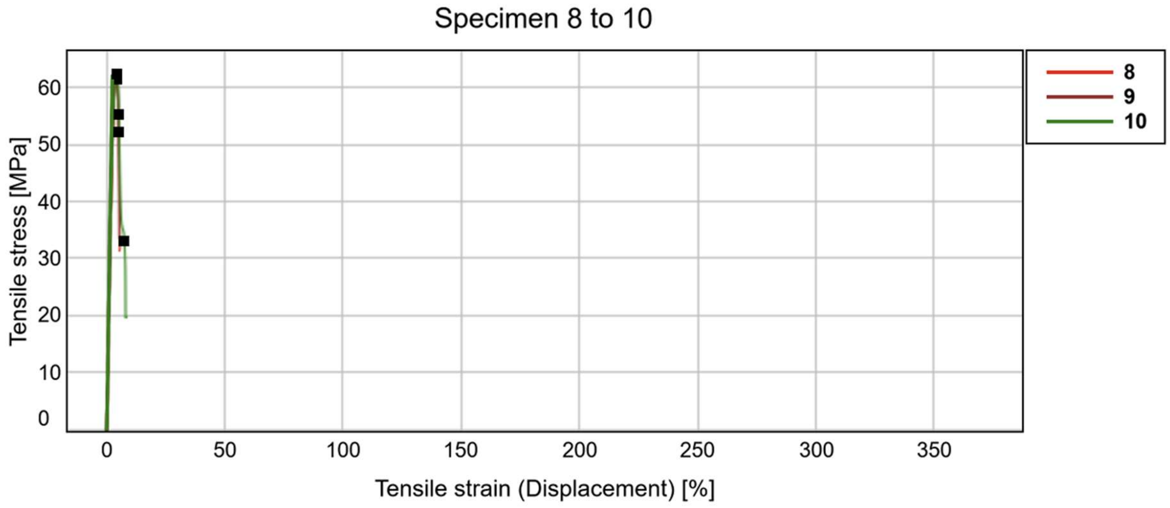

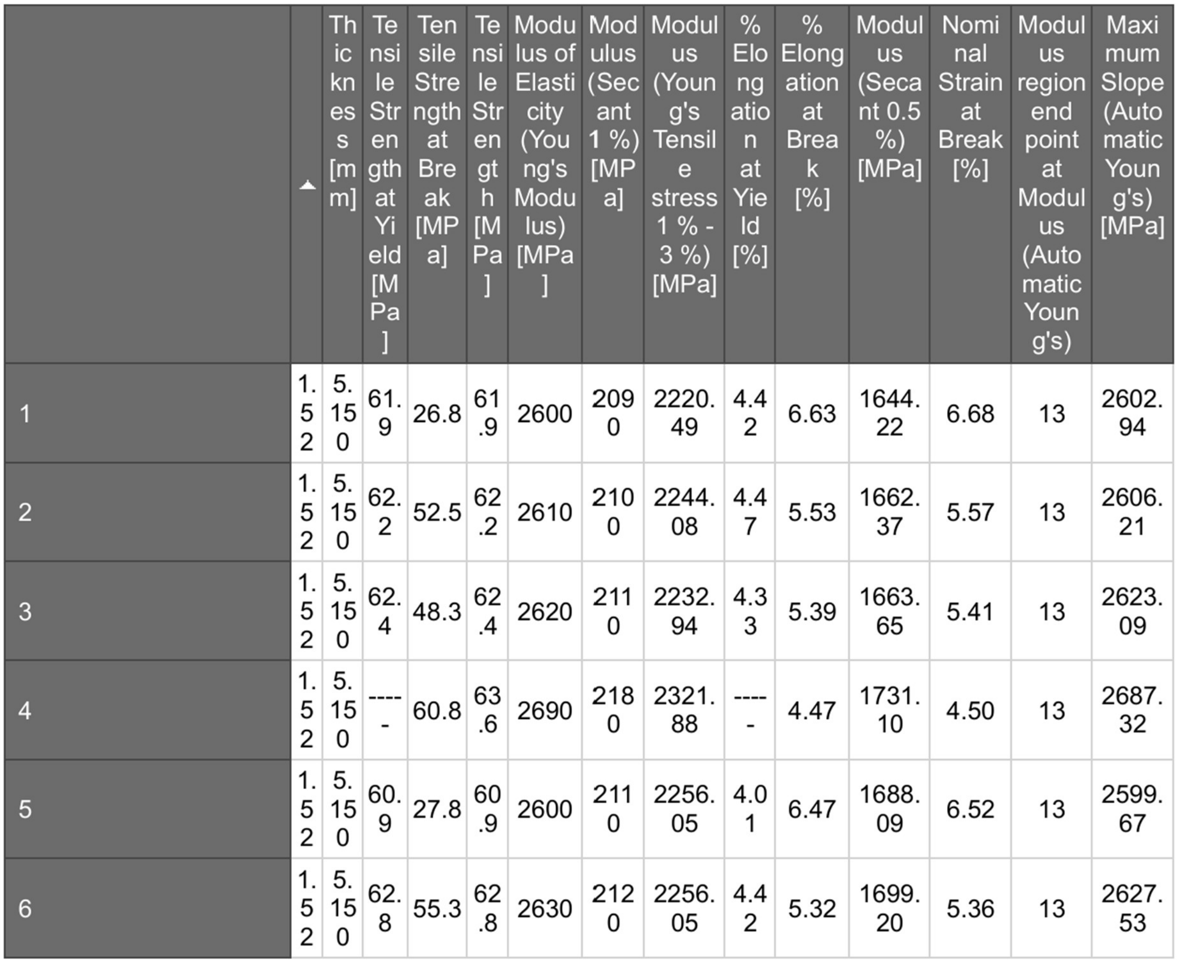

	▲	Thickness [mm]	Tensile Strength at Yield [MPa]	Tensile Stress at Break [MPa]	Tensile Strength [MPa]	Modulus of Elasticity (Young's Modulus) [MPa]	Modulus (Secant 1 %) [MPa]	Modulus (Young's Tensile stress 1 % - 3 %) [MPa]	% Elongation at Yield [%]	% Elongation at Break [%]	Modulus (Secant 0.5 %) [MPa]	Nominal Strain at Break [%]	Modulus region end point at Modulus (Automatic Young's)	Maximum Slope (Automatic Young's) [MPa]
1	1.52	5.150	61.9	26.8	61.9	2600	2090	2220.49	4.42	6.63	1644.22	6.68	13	2602.94
2	1.52	5.150	62.2	52.5	62.2	2610	2100	2244.08	4.47	5.53	1662.37	5.57	13	2606.21
3	1.52	5.150	62.4	48.3	62.4	2620	2110	2232.94	4.33	5.39	1663.65	5.41	13	2623.09
4	1.52	5.150	-----	60.8	63.6	2690	2180	2321.88	-----	4.47	1731.10	4.50	13	2687.32
5	1.52	5.150	60.9	27.8	60.9	2600	2110	2256.05	4.01	6.47	1688.09	6.52	13	2599.67
6	1.52	5.150	62.8	55.3	62.8	2630	2120	2256.05	4.42	5.32	1699.20	5.36	13	2627.53

Figure A.9: (cont'd)

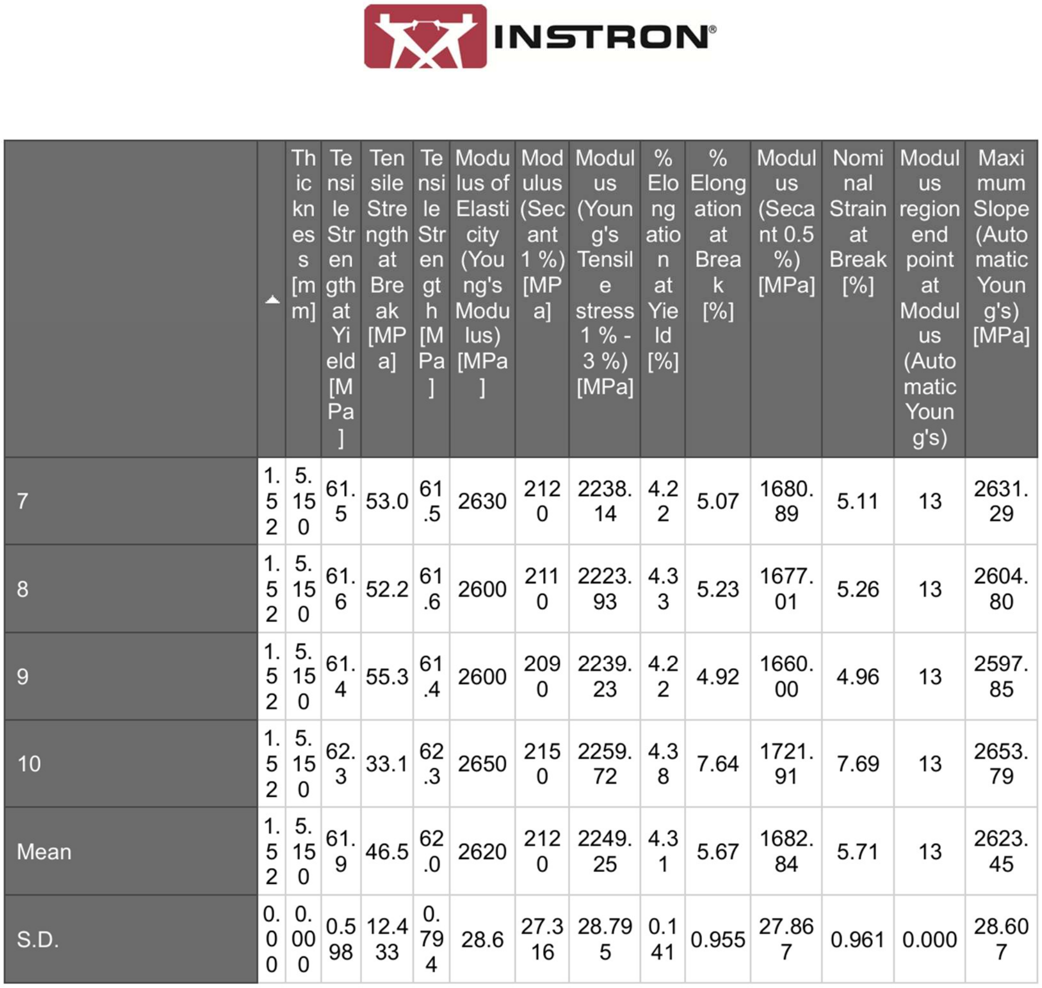
INSTRON

	▲	Thickness [mm]	Tensile Strength at Yield [MPa]	Tensile Strength at Break [MPa]	Tensile Strength [MPa]	Modulus of Elasticity (Young's Modulus) [MPa]	Modulus (Secant 1 %) [MPa]	Modulus (Young's Tensile stress 1 % - 3 %) [MPa]	% Elongation at Yield [%]	% Elongation at Break [%]	Modulus (Secant 0.5 %) [MPa]	Nominal Strain at Break [%]	Modulus region end point at Modulus (Automatic Young's)	Maximum Slope (Automatic Young's) [MPa]
7	1.52	5.150	61.5	53.0	61.5	2630	2120	2238.14	4.22	5.07	1680.89	5.11	13	2631.29
8	1.52	5.150	61.6	52.2	61.6	2600	2110	2223.93	4.33	5.23	1677.01	5.26	13	2604.80
9	1.52	5.150	61.4	55.3	61.4	2600	2090	2239.23	4.22	4.92	1660.00	4.96	13	2597.85
10	1.52	5.150	62.3	33.1	62.3	2650	2150	2259.72	4.38	7.64	1721.91	7.69	13	2653.79
Mean	1.52	5.150	61.9	46.5	62.0	2620	2120	2249.25	4.31	5.67	1682.84	5.71	13	2623.45
S.D.	0.000	0.000	0.598	12.433	0.794	28.6	27.316	28.795	0.141	0.955	27.867	0.961	0.000	28.607

Figure A.10: B*- 0.5in CF-3%

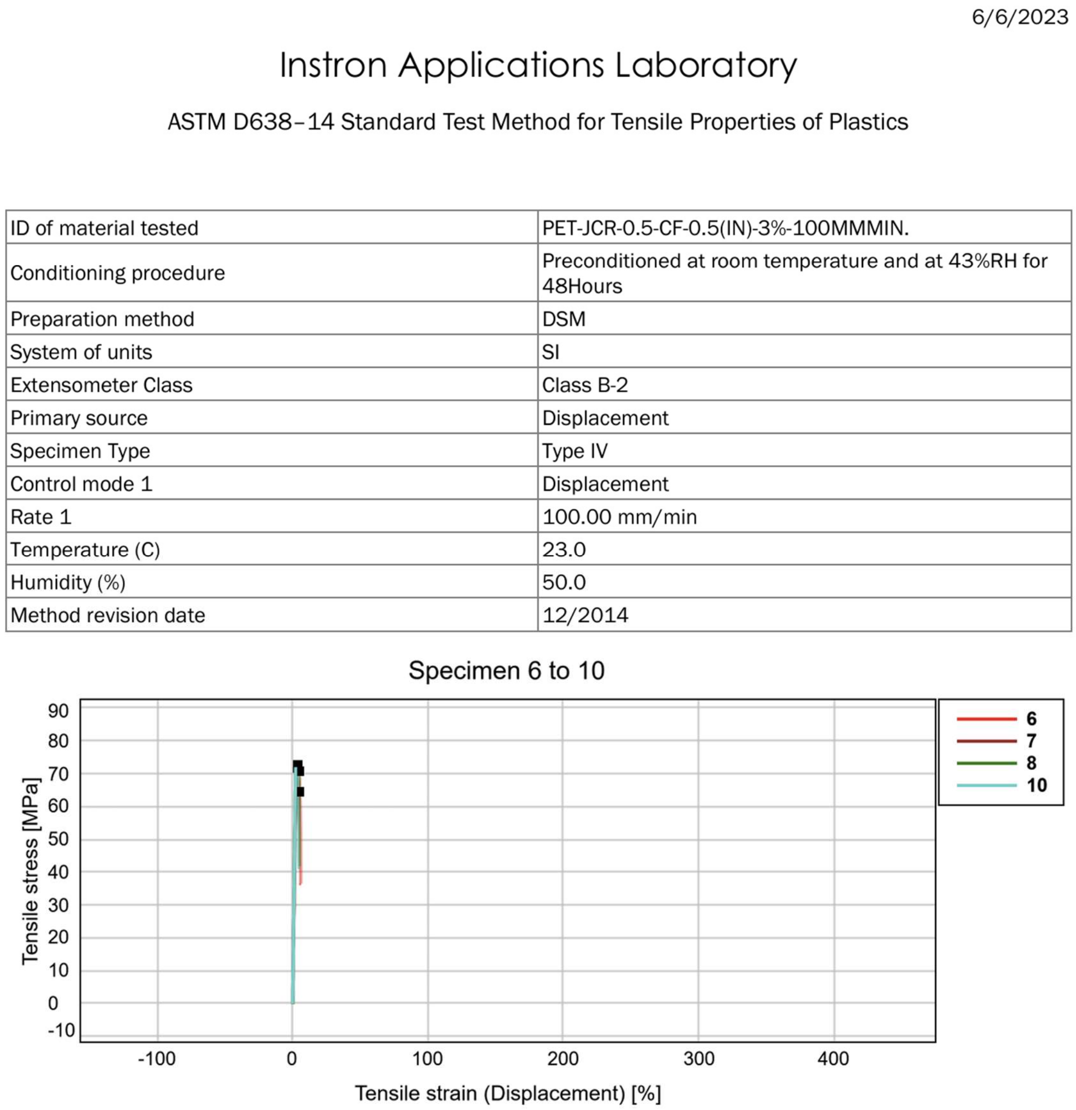

6/6/2023

Instron Applications Laboratory

ASTM D638–14 Standard Test Method for Tensile Properties of Plastics

ID of material tested	PET-JCR-0.5-CF-0.5(IN)-3%-100MMMIN.
Conditioning procedure	Preconditioned at room temperature and at 43%RH for 48Hours
Preparation method	DSM
System of units	SI
Extensometer Class	Class B-2
Primary source	Displacement
Specimen Type	Type IV
Control mode 1	Displacement
Rate 1	100.00 mm/min
Temperature (C)	23.0
Humidity (%)	50.0
Method revision date	12/2014

Specimen 6 to 10

Figure A.10: (cont'd)

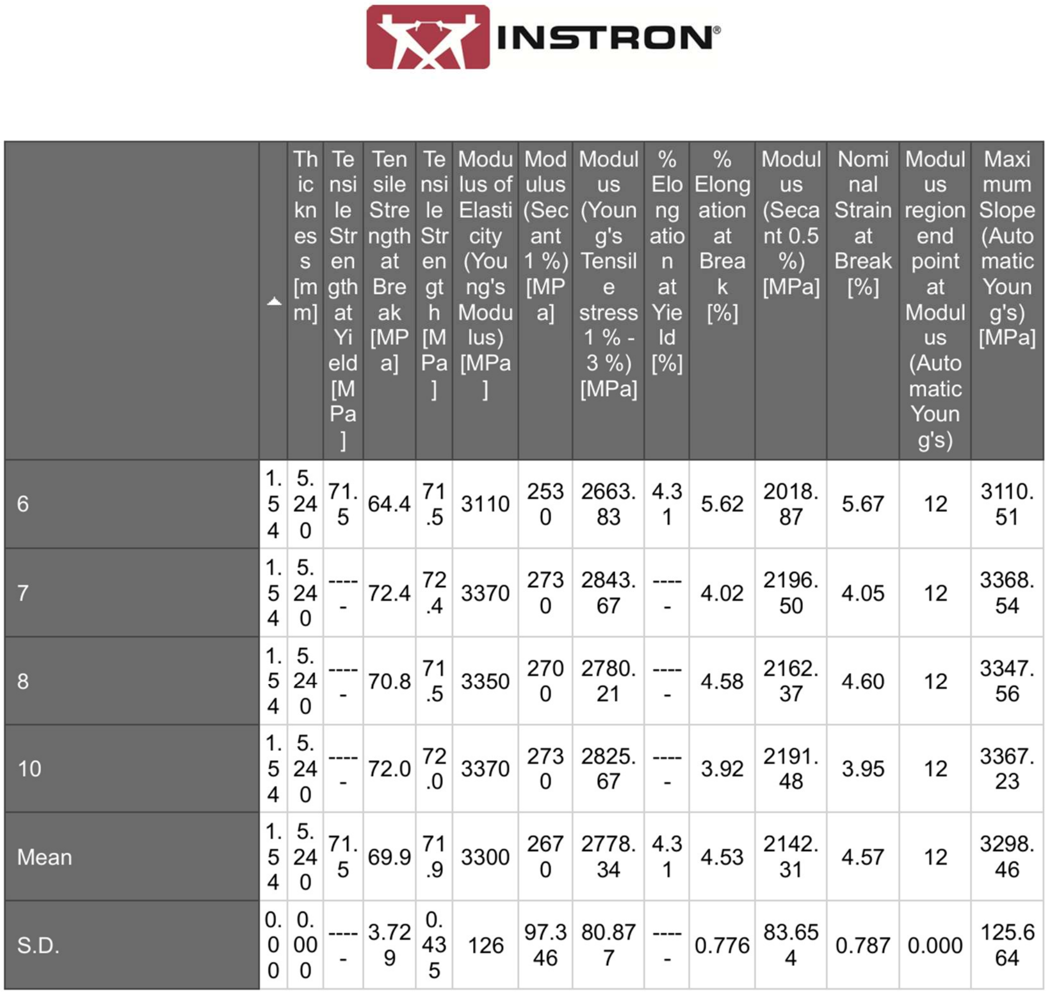

	▲	Thickness [mm]	Tensile Strength at Yield [MPa]	Tensile Strength at Break [MPa]	Tensile Strength [MPa]	Modulus of Elasticity (Young's Modulus) [MPa]	Modulus (Secant 1 %) [MPa]	Modulus (Young's Tensile stress 1 % - 3 %) [MPa]	% Elongation at Yield [%]	% Elongation at Break [%]	Modulus (Secant 0.5 %) [MPa]	Nominal Strain at Break [%]	Modulus region end point at Modulus (Automatic Young's)	Maximum Slope (Automatic Young's) [MPa]
6	1.54	5.240	71.5	64.4	71.5	3110	2530	2663.83	4.31	5.62	2018.87	5.67	12	3110.51
7	1.54	5.240	-----	72.4	72.4	3370	2730	2843.67	-----	4.02	2196.50	4.05	12	3368.54
8	1.54	5.240	-----	70.8	71.5	3350	2700	2780.21	-----	4.58	2162.37	4.60	12	3347.56
10	1.54	5.240	-----	72.0	72.0	3370	2730	2825.67	-----	3.92	2191.48	3.95	12	3367.23
Mean	1.54	5.240	71.5	69.9	71.9	3300	2670	2778.34	4.31	4.53	2142.31	4.57	12	3298.46
S.D.	0.000	0.000	-----	3.729	0.435	126	97.346	80.877	-----	0.776	83.654	0.787	0.000	125.664

Figure A.11: B*- 1in CF-3%

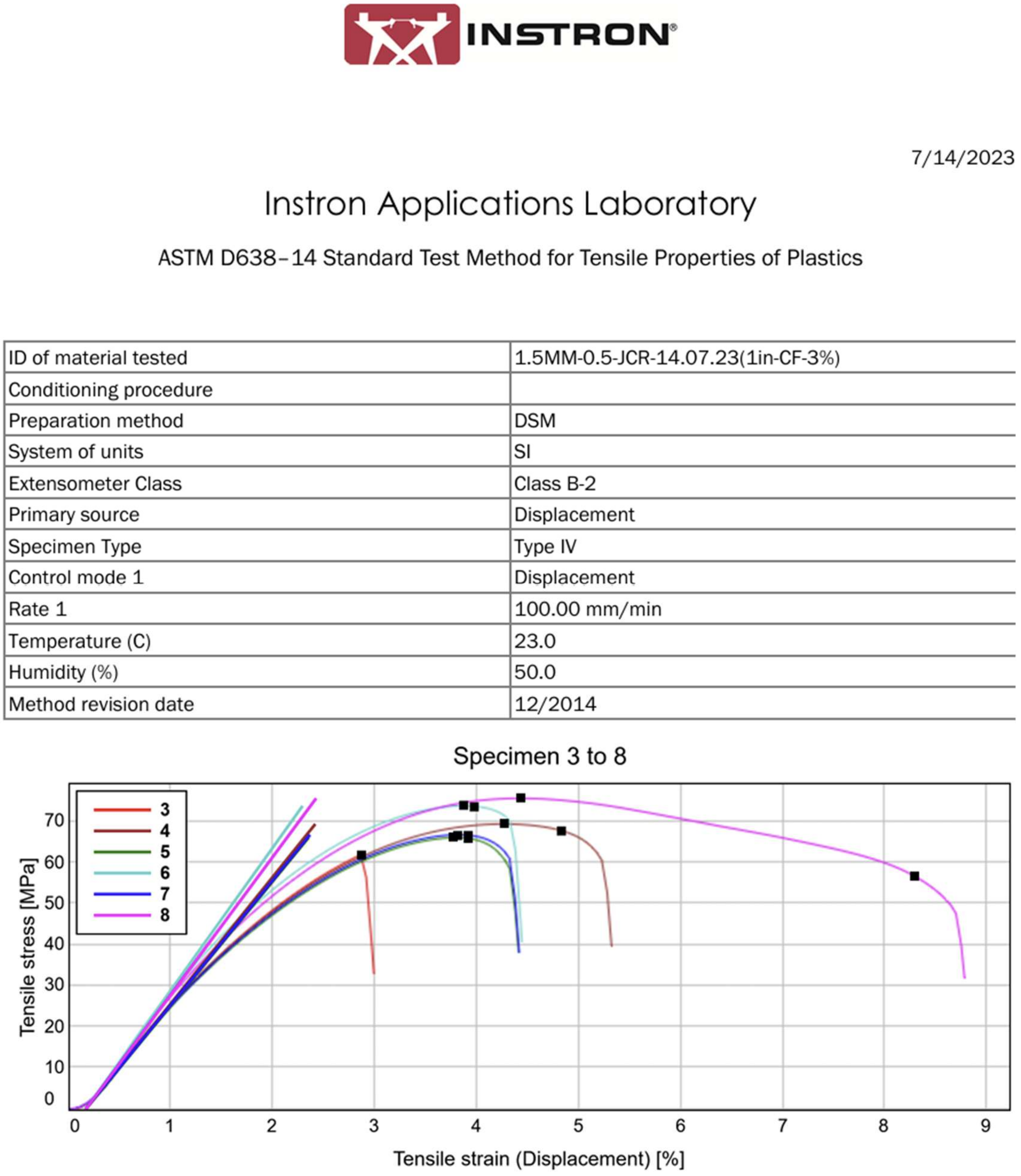

7/14/2023

Instron Applications Laboratory

ASTM D638–14 Standard Test Method for Tensile Properties of Plastics

ID of material tested	1.5MM-0.5-JCR-14.07.23(1in-CF-3%)
Conditioning procedure	
Preparation method	DSM
System of units	SI
Extensometer Class	Class B-2
Primary source	Displacement
Specimen Type	Type IV
Control mode 1	Displacement
Rate 1	100.00 mm/min
Temperature (C)	23.0
Humidity (%)	50.0
Method revision date	12/2014

Specimen 3 to 8

Figure A.11: (cont'd)

INSTRON

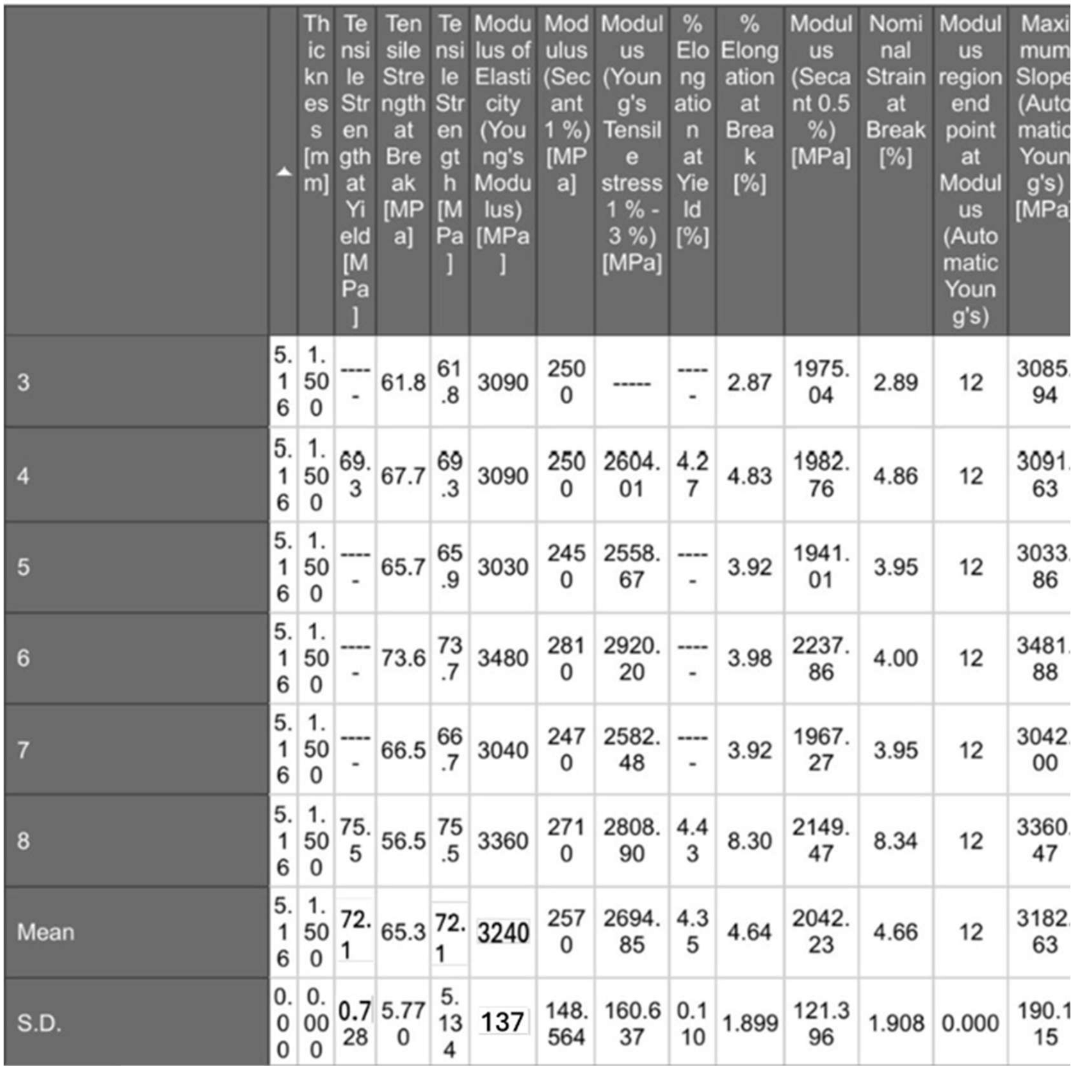

	▲	Thickness [mm]	Tensile Strength at Yield [MPa]	Tensile Strength at Break [MPa]	Tensile Strength [MPa]	Modulus of Elasticity (Young's Modulus) [MPa]	Modulus (Secant 1 %) [MPa]	Modulus (Young's Tensile stress 1 % - 3 %) [MPa]	% Elongation at Yield [%]	% Elongation at Break [%]	Modulus (Secant 0.5 %) [MPa]	Nominal Strain at Break [%]	Modulus region end point at Modulus (Automatic Young's)	Maximum Slope (Automatic Young's) [MPa
3	5.16	1.500	-----	61.8	61.8	3090	2500	-----	-----	2.87	1975.04	2.89	12	3085.94
4	5.16	1.500	69.3	67.7	69.3	3090	2500	2604.01	4.27	4.83	1982.76	4.86	12	3091.63
5	5.16	1.500	-----	65.7	65.9	3030	2450	2558.67	-----	3.92	1941.01	3.95	12	3033.86
6	5.16	1.500	-----	73.6	73.7	3480	2810	2920.20	-----	3.98	2237.86	4.00	12	3481.88
7	5.16	1.500	-----	66.5	66.7	3040	2470	2582.48	-----	3.92	1967.27	3.95	12	3042.00
8	5.16	1.500	75.5	56.5	75.5	3360	2710	2808.90	4.43	8.30	2149.47	8.34	12	3360.47
Mean	5.16	1.500	72.1	65.3	72.1	3240	2570	2694.85	4.35	4.64	2042.23	4.66	12	3182.63
S.D.	0.000	0.000	0.728	5.770	5.134	137	148.564	160.637	0.110	1.899	121.396	1.908	0.000	190.115

Figure A.12: B*- 2in CF-3%

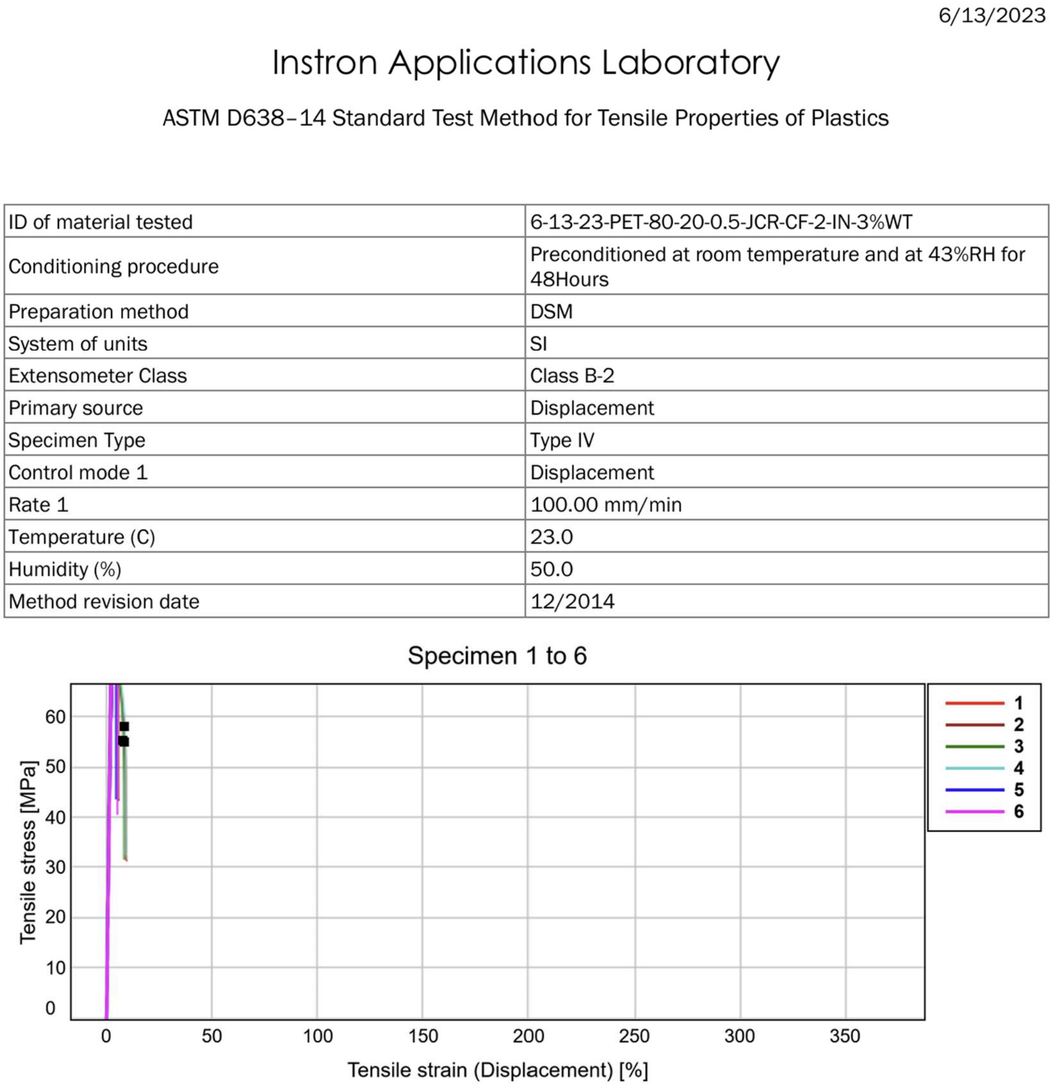

6/13/2023

Instron Applications Laboratory

ASTM D638–14 Standard Test Method for Tensile Properties of Plastics

ID of material tested	6-13-23-PET-80-20-0.5-JCR-CF-2-IN-3%WT
Conditioning procedure	Preconditioned at room temperature and at 43%RH for 48Hours
Preparation method	DSM
System of units	SI
Extensometer Class	Class B-2
Primary source	Displacement
Specimen Type	Type IV
Control mode 1	Displacement
Rate 1	100.00 mm/min
Temperature (C)	23.0
Humidity (%)	50.0
Method revision date	12/2014

Specimen 1 to 6

Figure A.12:(cont'd)

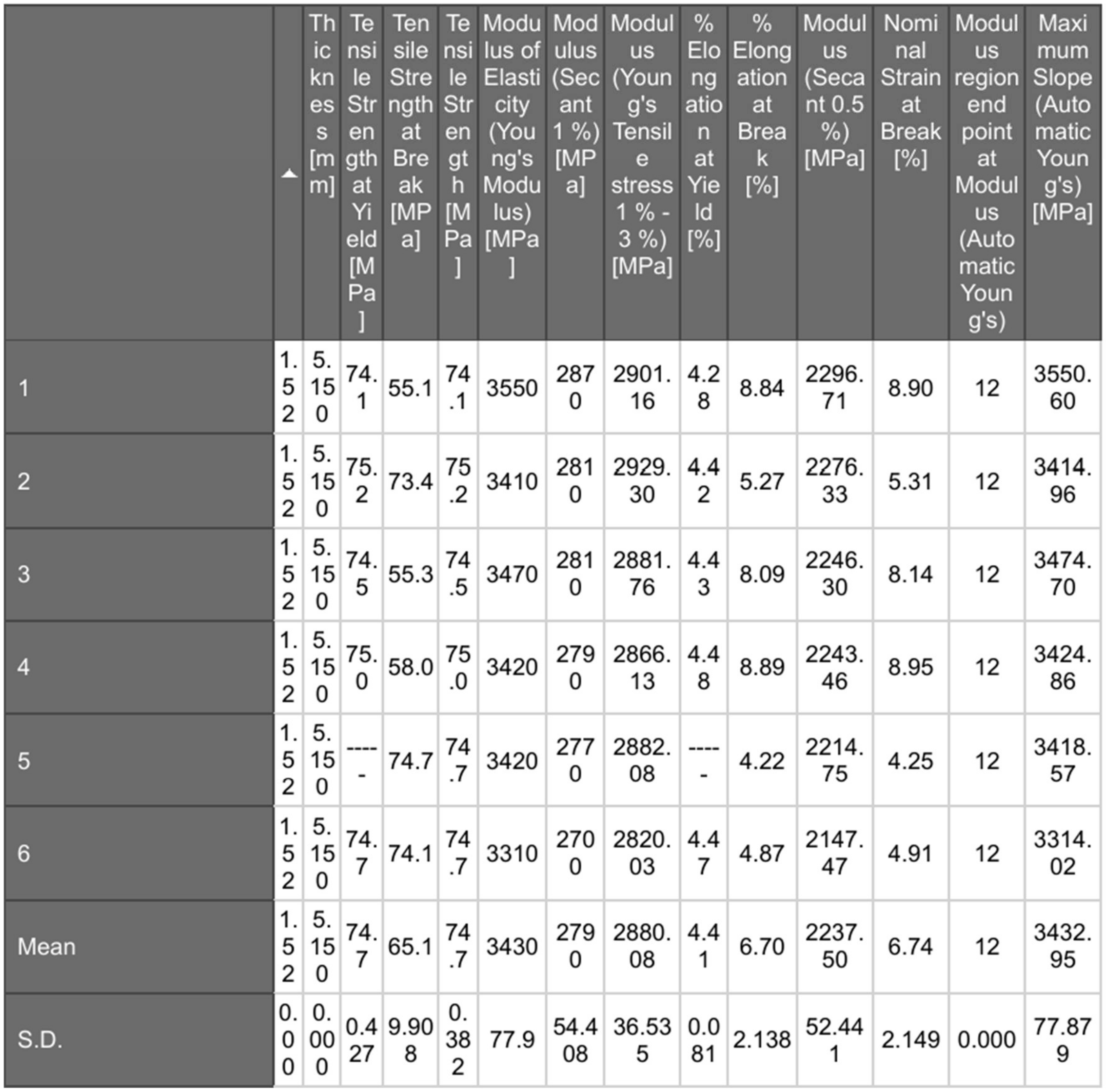

	▲	Thickness [mm]	Tensile Strength at Yield [MPa]	Tensile Strength at Break [MPa]	Tensile Strength [MPa]	Modulus of Elasticity (Young's Modulus) [MPa]	Modulus (Secant 1 %) [MPa]	Modulus (Young's Tensile stress 1 % - 3 %) [MPa]	% Elongation at Yield [%]	% Elongation at Break [%]	Modulus (Secant 0.5 %) [MPa]	Nominal Strain at Break [%]	Modulus region end point at Modulus (Automatic Young's)	Maximum Slope (Automatic Young's) [MPa]
1	1.52	5.150	74.1	55.1	74.1	3550	2870	2901.16	4.28	8.84	2296.71	8.90	12	3550.60
2	1.52	5.150	75.2	73.4	75.2	3410	2810	2929.30	4.42	5.27	2276.33	5.31	12	3414.96
3	1.52	5.150	74.5	55.3	74.5	3470	2810	2881.76	4.43	8.09	2246.30	8.14	12	3474.70
4	1.52	5.150	75.0	58.0	75.0	3420	2790	2866.13	4.48	8.89	2243.46	8.95	12	3424.86
5	1.52	5.150	-----	74.7	74.7	3420	2770	2882.08	-----	4.22	2214.75	4.25	12	3418.57
6	1.52	5.150	74.7	74.1	74.7	3310	2700	2820.03	4.47	4.87	2147.47	4.91	12	3314.02
Mean	1.52	5.150	74.7	65.1	74.7	3430	2790	2880.08	4.41	6.70	2237.50	6.74	12	3432.95
S.D.	0.000	0.000	0.427	9.908	0.382	77.9	54.408	36.535	0.081	2.138	52.441	2.149	0.000	77.879

Thermal Stability Raw Data:

Figure A.13: The DSC graph represented shows about the thermal data of Neat, Blends and CE enhanced blend (B*)

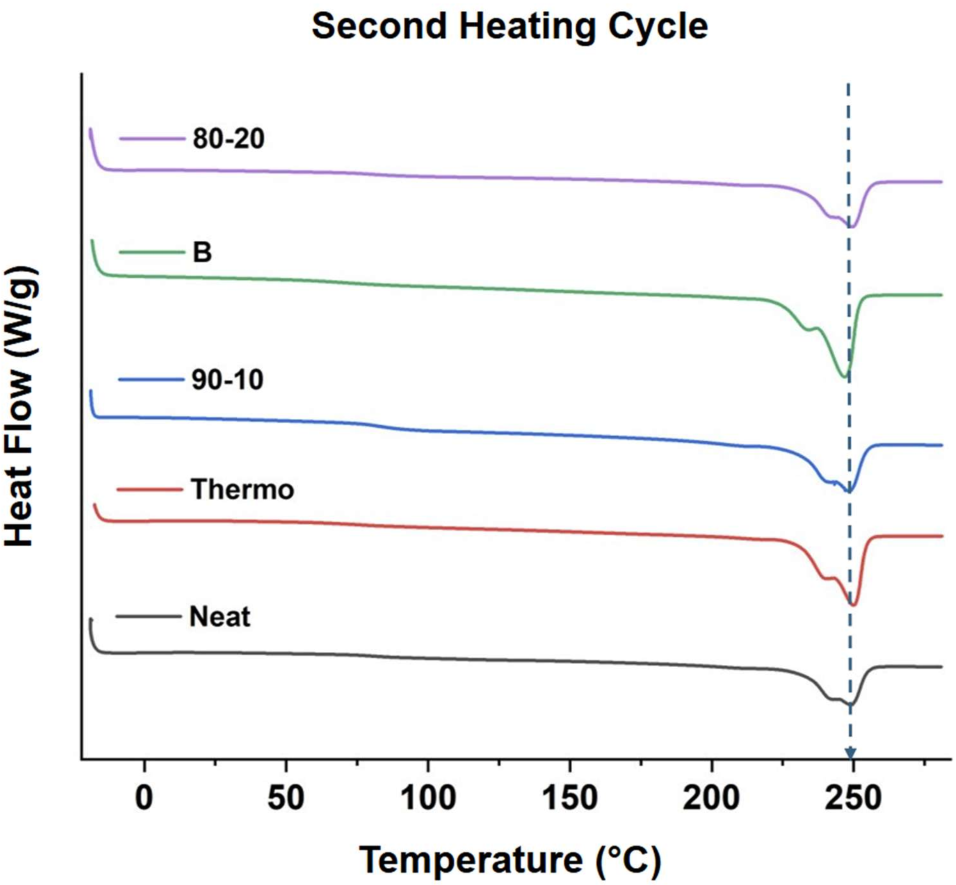

Figure A.14: The figure shows the graph comparing the carbon fiber reinforced blends with different lengths of fiber at 1wt. %.

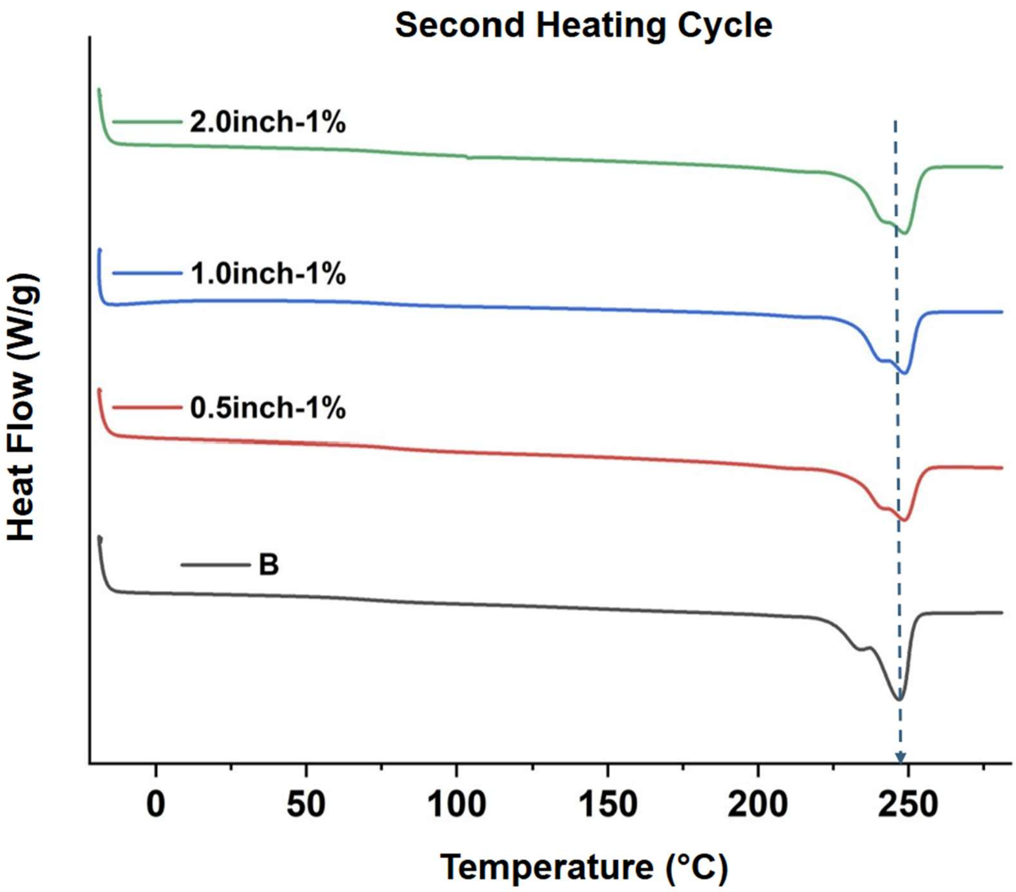

Figure A.15: The figure shows the graph comparing the carbon fiber reinforced blends with different lengths of fiber at 3 wt. %.

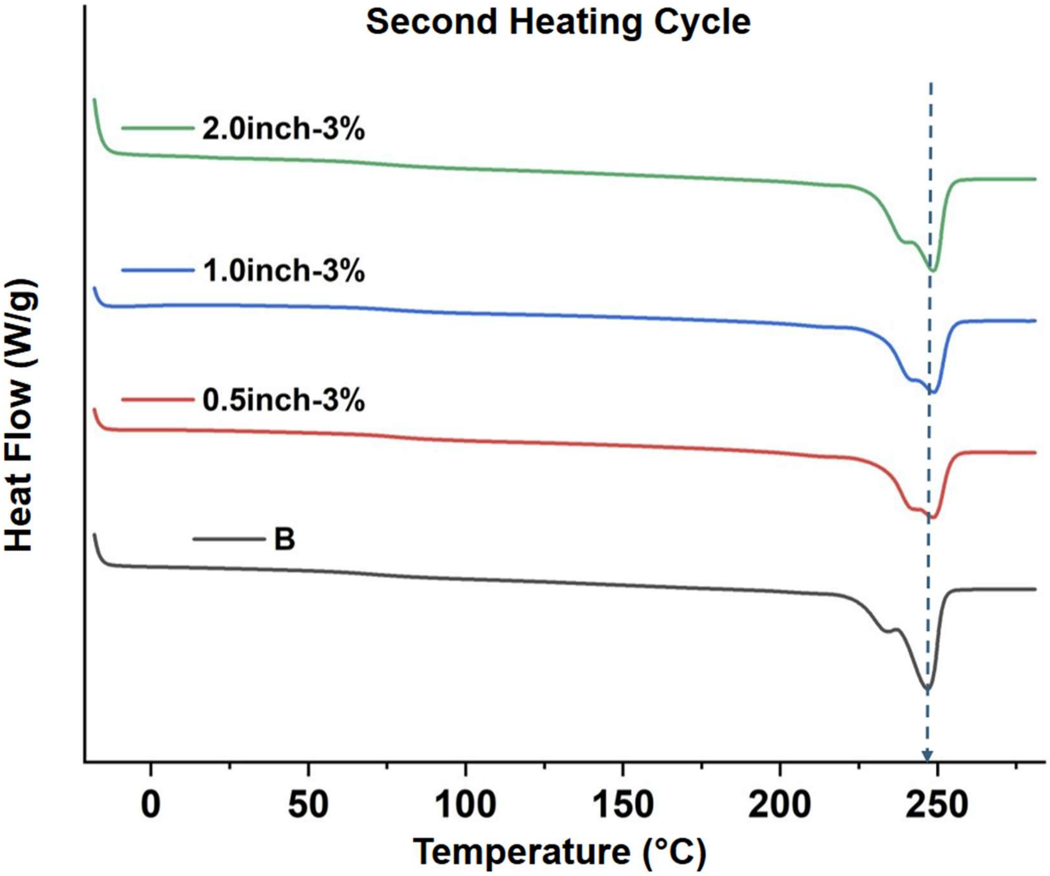

Table A.1: The table below represents the raw DSC data.

Cycle	**1st Cycle**				**2nd Cycle**	**3rd Cycle**				**%Xc**
Name	Tc (°C)	Tg(°C)	Tm1 (°C)	ΔHm (J/g)	T cold crystallization (°C)	Tg(°C)	Tm1 (°C)	Tm2 (°C)	ΔHm (J/g)	Crystallinity%
Neat PET-B	73.09±4.03	126.54±0.01	249.365±0.43	32.66±0.91	204.53±0.83	80.77±0.32	241.35±0.17	249.25±0.01	35.41±1.73	25.29
Neat PET-T	74.39±39	115±0.34	254.95±0.04	45.43±0.12	211.82±0.414	87.22±0.3	251.75±1.01	250.535±0.51	41.58±3.16	29.7
PET-B/10% PET-T	54.18±45	——	251.01±9.24	45.21±23.4	201.88±2.4	81.745±3.04	241.7±1.41	249.085±0.49	36.16±2.1	25.82
PET-B/20%PET-T	58.37±4.3	——	251.80±32	47.85±4.8	206.89±1.34	72.18 ± 4.34	241.70±1.45	250.20±1.043	37.23±2.11	26.59
PET-B/20% PET-T + 0.5 phr Joncryl (B*)	72.95±0.81	122.86±0.04	250.36±0.25	37.8±2.78	204.34±3.17	79.92±0.35	236.75±2.49	247.695±0.76	38.10±8.44	27.21
PET-B/20% PET-T + 1 phr Joncryl	67.07±2.4	118.53±88	251.56±7.34	37.31±5.4	208.45±0.32	75.09±0.24	240.64±.48	249.02±0.21	39.87±0.23	28.47
B*-1%CF (0.5 in)	76.305±2.62	119.72±6.34	253.48±6.13	39.44±1.11	208.08±0.76	76±0.96	240.29±1.56	251.69±0.23	41.25±0.55	29.46

Table A.1:(cont’d)

Cycle	1st Cycle				2nd Cycle	3rd Cycle				%Xc
B*-1%CF (1 in)	73.87±1.29	121.48±0.25	252.07±0.8	41.28±2.72	208.59±1.29	77.73±0.25	240.465±0.17	248.925±0.15	39.17±0.18	27.97
B*-1%CF (2 in)	64.31±0.07	118.50±0.05	245.62±4.96	42.78±0.38	209.25±0.61	73.26±3.50	240.335±0.93	248.75±0.01	40.08±1.35	31.36
B*-3%CF (0.5 in)	68.90±3.56	118.525±1.24	251.74±0.47	41.36±1.37	209.33±0.804	74.65±3.89	240.685±2.16	248.525±0.275	40.76±1.56	28.40
B*-3%CF (1 in)	73.03±8.96	121.94±2.45	253.37±6.33	42.33±7.05	209.08±4.98	77.44±9.24	240.29±2.05	249±0.75	40.17±0.68	27.98
B*-3%CF (2 in)	76.70±6.12	125.75±4.65	262.80±2.45	42.83±0.86	209.78±0.726	76.18±3.24	240.28±2.65	249.73±0.93	40.37±0.24	28.35

Table A.2: The Table Below represents the TGA raw data.

Name	Temp at 2%	Temp at 5%	Temp at 10%	Peak P	Residue
Neat PET-B	390.475±1.14	402.64±1.37	412.18±1.07	439.76±0.66	1.18±0.03
Neat PET-T	363.11±1.05	386.11±0.38	402.53±0.27	436.66±3.49	0.7525±0.12
PET-B /10% PET-T	385.655±1.94	399.34±1.91	410.695±1.69	441.905±0.8	1.206±0.15
PET-B /20%PET-T	385.945±0.64	399.115±0.94	410.185±0.93	443.33±0.04	1.152±0.4
PET-B/20% PET-T + 0.5 phr Joncryl	384.565±0.66	399.005±0.47	409.255±0.22	441.035±1.39	1.242±0.08
PET-B/20% PET-T + 1 phr Joncryl	384.045±0.27	394.045±0.39	409.68±0.34	443.06±2.4	1.209±0.73
B*-1%CF (0.5 in)	381.275±2.53	396.82±3.36	408.17±3.63	442.18±0.06	1.418±2.2
B*- 1%CF (1 in)	389.781±4.32	398.23±1.11	409.58±2	435.59±7.4	1.553±3.22
B*- 1%CF (2 in)	389.92±4.23	398.16±1.23	409.66±2.14	441.21±2.67	2.611±1.245
B*- 3%CF (0.5 in)	389.69±0.23	398.92±0.76	410.34±0.23	443.18±0.79	1.83±0.23
B*- 3%CF (1 in)	390.455±0.93	395.425±1.12	411.22±0.88	442.03±0.004	2.475±0.041
B*- 3%CF (2 in)	380.105±0.67	395.315±0.11	412.855±0.17	442.535±1.03	2.839±0.02